CASS BUSINESS SCHOOL

DOCTORAL THESIS

Asset Pricing across Asset Classes and Microstructure Analysis in Equity and Cryptocurrency Market

---

Author:
Lulu Feng

Supervisor:
Prof. Richard Payne
Prof. Ian Marsh

A thesis submitted in fulfilment of the requirements for the degree of Doctor of Philosophy

to the

Department of Finance
Cass Business School
City, University of London

June, 2021

Contents

List of Figures

List of Tables

Acknowledgements

First I would like to express my sincere gratitude to my supervisors Professor Richard Payne and Professor Ian Marsh. They have guided me all the way through my Ph.D path and I have learned a lot from them, not only research method but also rigorous attitude towards research and passion for work.

Second I would like to thank my family, especially my husband who has tried his best to support my research. My family is the reason that I thrive to fulfil my value and get the most out of my life.

And finally, last but not least, I am grateful for all the staff at Cass Business School who have helped me during my studies. Their support helps me to gain many resources provided by the school.

Declaration

I grant powers of discretion to the University Librarian to allow the thesis to be copied in whole or part without further reference to me. This permission covers only single copies made for study purposes, subject to normal conditions of acknowledgement.

I, Lulu Feng, declare that this thesis titled, Asset Pricing across Asset Classes and Microstructure Analysis in Equity and Cryptocurrency Market and the work presented in it is my own. I confirm that:

- This work is done wholly or mainly while in candidature for a research degree at Cass Business School.
- Based on the results of the thesis, research papers have been developed with Professor Richard Payne and Professor Ian Marsh.

Abstract

In Chapter 1, I form a single cross-section from the USD returns on international equity indices, international sovereign bonds, and currencies; I then sort the entire cross-section according to (standardised) value, momentum, and carry measures. In these international, multi-asset-class portfolios, there are large, significant returns available to carry investors and significant – though somewhat smaller – returns to momentum and value investors. The premiums are not much larger than a simple average of within-asset-class premiums for all three strategies. Asset pricing tests show that volatility risk can explain currency carry returns, but bond and equity carry returns have a different source. Value, carry, and momentum returns of across-asset-class portfolios – including all three asset classes – are difficult to explain using an equilibrium asset pricing model.

In Chapter 2 and 3, I decompose prices into two unobserved processes: fundamental value and pricing error. The former is influenced by private information contained in order flows, while the latter depends on liquidity providers' inventory control. Analysis of UK equity data during the 2008 financial crisis shows that order flows had a more significant impact on pricing errors during the crisis, indicating that strained inventory absorption capacity of liquidity providers was the main factor in the decline of equity market liquidity. The results also reveal that liquidity provision is reduced in volatile markets due to inventory control, while changes in information asymmetry only affect equities with small market capitalisation and trading volume. The Bitcoin and Ethereum results on two leading exchanges (Bitfinex and Kraken), between January 2017 and January 2018, demonstrate that cryptocurrency price change is determined by order flows through information asymmetry and inventory control. Additionally, when the emerging cryptocurrency market saw a boom and then crashed, the impacts of order flows on fundamental value and pricing errors were greater at the beginning of both the boom and the crash. Cross-cryptocurrency and cross-exchange results indicate that orders of one cryptocurrency on one exchange can also influence the price of another cryptocurrency on another exchange through information.

Introduction

This thesis comprises three chapters. Chapter 1 is an asset pricing paper that presents common risk factors to explain cross-sectional returns of multi-asset classes, including currencies, international sovereign bonds, and equity indices in 43 countries. I put all the assets into a single investment pool and sort them into portfolios by value, carry, and momentum signals, which Asness et al. (2013) and Koijen et al. (2013) have found to generate significant excess returns within each asset class. Through this multi-asset-class investment, an international investor based in the US could further benefit from the predictive power of these signals, if value, carry, and momentum are caused by the same set of systematic risk factors across different asset classes. In addition, I test whether these across-asset-class value, carry, and momentum returns can be explained by a unified equilibrium asset pricing model. My results indicate that all the multi-asset-class value, carry, and momentum portfolios generate a large high-minus-low (HML) return and Sharpe ratio (SR), but the returns are no larger than a simple average of HML returns within each asset class. In addition, the returns cannot be fully explained by an asset pricing model including a market return factor, a market volatility factor, and a liquidity factor. I also find that the return cross-section of carry portfolios with only currencies can be explained by market volatility; however, when bonds and equities are added to the portfolio, the volatility factor no longer applies. This suggests that although value, carry, and momentum portfolios can generate excess returns in different asset classes, the returns may come from different sources, and they are thus exposed to different asset-specific risk factors. However, investors can still benefit from diversification by investing internationally in multiple asset classes.

Chapters 2 and 3 are microstructure papers that study how order flow – the most important variable in microstructure finance according to Evans and Lyons (2002a)

– drives price change. Previous studies have proven that order flows influence price primarily through price discovery (Hasbrouck (1991a); Hasbrouck (1991b); Evans and Lyons (2002a); Brandt and Kavajecz (2004); etc.) and price pressure (Hendershott and Seasholes (2007); Reiss and Werner (1998); Naik and Yadav (2003); etc.). Inspired by Hendershott and Menkveld (2014), I use State Space Form (SSF) to decompose the observed prices into two unobserved processes: a random walk process influenced by private information contained in order flows (price discovery), and a mean-reversion process influenced by liquidity providers' inventory control (price pressure). Then I use the Kalman Filter to estimate parameters in SSF, and apply the method to high-frequency trading data on UK equities and cryptocurrencies to explore the reason for the market crashes. The results for the UK equity market indicate that the market crash during the financial crisis was primarily due to the liquidity providers' increased inventory control costs, such as funding constraints or greater risk aversion during the financial crisis, rather than the amplified adverse selection problem. The results are consistent with those of Nagel (2012) concerning the US equity market during the crisis. My results for the emerging cryptocurrency market indicate that Bitcoin and Ethereum prices on Bitfinex and Kraken are also driven by information in orders through price discovery and liquidity providers' inventory control through price pressure. The market boom in May 2017 was caused by uninformed liquidity providers' larger quote adjustment in response to buy orders than in response to sell orders, likely due to a belief that buy orders were more informative than sell orders. The market crash that began in January 2018 was caused by the larger impact of orders through both channels. In addition, my cross-cryptocurrency results confirm that some information on the fundamental values of Bitcoin and Ethereum is market-wide. Therefore, the price of one cryptocurrency is primarily influenced by the order flow of itself, but is also influenced by the order flow of the other cryptocurrency. My cross-exchange results conclude that prices of Bitcoin and Ethereum on one exchange are influenced by order flows on the other exchange only through price discovery.

Chapter 1

Common risks across asset classes

1.1 Introduction

Previous studies have described significant excess returns generated by value, carry, and momentum signals in different asset classes (Asness et al. (2013); Koijen et al. (2013)). However, the literature discusses return predictability by value, carry, and momentum signals within each asset class. Therefore, my research aims to find out whether an international investor based in the US can obtain the cross-sectional difference in returns if all these assets are put into one investment pool, regardless of their asset classes, and sorted into portfolios according to value, carry, and momentum signals. If these signals are across-asset-class phenomena caused by common factors, the multi-asset-class portfolios – sorted only by these signals, regardless of their asset classes – should generate significant and potentially larger excess returns than a portfolio combined by value, carry, and momentum portfolios within each asset class. In addition, previous studies have proposed theories of risk factors that could explain the excess returns of value, carry, and momentum portfolios. For example, Brunnermeier and Pedersen (2009) argue that funding constraints can explain the risk premia of popular trades. Shleifer and Vishny (1997) propose an agency model of limited arbitrage that may explain excess returns that are difficult to understand in terms of the conventional model. Menkhoff et al. (2014) show that carry returns in the currency market are driven by market volatility. Therefore, in this chapter, I test whether the returns of my across-asset-class portfolios are exposed to some standard systematic risk factors that successfully explain these excess returns within asset classes in the existing literature. For investors who want to invest across asset classes, when they benefit from diversification, they should also bear in mind of any systematic risk factors if multiple asset classes are integrated and part of the returns are caused by common risk factors, and thus adjust their strategies accordingly based on their risk-bearing capacity and liquidity needs.

I combine currencies and bonds first because, in my research, currency excess returns are equal to currency appreciation plus short-term interest rates, while bond returns are equal to currency appreciation plus long-term interest rates. The results indicate that all three strategies are profitable, generating a positive HML return over time. I then investigate whether one could explain the differences in mean returns of my value, carry, and momentum portfolios using simple risk factors. In addition to a simple 'market' portfolio return (computed as the cross-sectional average of all of our individual asset returns), I consider a volatility factor similar to that employed in Menkhoff et al. (2014) and Cenedese et al. (2014). The asset pricing test indicates that carry returns can be partly explained by market mean returns and volatility risk factors. However, pricing errors suggest that my volatility factor cannot explain bond carry returns. Although value and momentum signals can predict both currency and bond returns within each asset class, they are caused by different factors in the currency and bond markets and should be studied separately within each market.

I put all currencies, bonds, and equities together and sort them into portfolios by value, carry and momentum signals. My key finding is that an international investor can generate significant excess returns from investing in value, carry, and momentum, as applied to the aggregate cross-section. The HML portfolio for my carry signal has a mean return of around 9.4% per annum, with a Sharpe ratio (SR) over 1. The value and momentum signals generate HML portfolios with mean returns around 4.7% and 6.5%, respectively. As a benchmark, the US value-weighted stock market generate a mean excess return of 6% over my sample period, with an SR of 0.41. Therefore, value, carry, and momentum appear to be across-asset-class phenomena. However, my sorting strategy do not outperform an equally-weighted portfolio combined by value, carry, and momentum portfolios from each asset class. In addition, a unified asset pricing model with a set of market-wide systematic risk factors across asset classes – including mean return, volatility and liquidity – cannot explain the across-asset-class return cross-section. Therefore, my results suggest that value, carry and momentum returns across asset classes are not caused by a common set of systematic risk factors. Investors cannot purposely tilt to systematic risk factors associated with value, carry and momentum signals across asset classes to earn a bigger excess return than simply combining value, carry and momentum portfolios within each asset class. In addition, currencies, bonds and equities are segmented from the perspective of asset pricing. One limitation of my research is that my systematic risk factors may not be able to capture the international time variations of the real volatility or liquidity across asset classes. However, my results could convince investors of the diversification benefits provided by value, carry, and momentum portfolios across asset classes.

The remainder of this chapter is organised as follows. Section 1.2 presents a review of the theories in the existing literature and provides evidence for both information asymmetry and inventory control channels. Sections 1.3 and 1.4 describe the data and methodology used in this paper, respectively. The empirical results of the research are presented in Section 1.5, and Section 1.6 concludes the paper.

1.2 Related literature

Many recent asset pricing papers have explored the determination of cross-sectional difference in mean returns within asset classes. While many of these papers have identified risk factors explain cross-sectional difference within specific asset classes – and some authors have argued that the same risk factors work in different asset classes – there have been no studies on an aggregated cross-section of assets drawn from different asset classes.

Fama and French (2012) have found value and momentum premia in international stock returns in four regions, with all the premia decreasing with firm size. Asness et al. (2013) assert that value and momentum phenomena exist in eight asset classes globally and that liquidity risk does a better job than macroeconomic factors of explaining the value and momentum excess returns. Koijen et al. (2013) suggest that carry strategies applied to various individual asset classes can generate excess returns, but carry portfolios do poorly in global recessions. All previous research has indicated a cross-sectional difference in returns if assets within each asset class are sorted by value, carry, and momentum internationally.

My research is also inspired by a strand of literature that aims to explain risk premia in international investments using standard asset pricing techniques. Lustig et al. (2013) propose a downward-sloping term structure of currency premia and demonstrate that currency carry trade premia can be explained by common innovations to the pricing kernel and a large fraction of risk priced in securities markets is shared between countries. Menkhoff et al. (2014) find that the cross-section of currency returns can be priced by global currency volatility. Their findings are similar to those of Ang et al. (2006) on the stock market. Ang et al. (2006) conclude that stocks with higher sensitivities to innovation in aggregate volatility have smaller average returns. In international equity markets, the positive returns obtained by Cenedese et al. (2014) adopting strategies that take advantage of Uncovered Equity Parity violations, mirror the carry trade profits in currency markets. They find that international equity excess returns can be partly explained by systematic risk factors.

The studies described above hint at commonality in asset pricing across asset classes, with their reliance on similar risk factors (e.g., volatility and liquidity) and their demonstration that similar sorting rules work in a variety of individual asset classes. However, each examines one asset class at a time. Although Asness et al. (2013) and Koijen et al. (2013) explore the across-asset-class phenomena, both have sorted the portfolios by the value, carry, or momentum signals within each asset class first and then combined them across asset classes. Some studies have attempted to apply a unified asset pricing model to different asset classes. For example, Bansal and Shaliastovich (2012) show that a long-run risk set-up is critical for solving market anomalies across asset classes, such as violation of the expectation hypothesis in the bond market and violation of uncovered interest parity in the foreign exchange market. Lettau et al. (2014) find evidence that the downside-risk capital asset pricing model (DR-CAPM) can reconcile the cross-sectional dispersion in returns across multiple asset classes. The key contribution of my research is that it sorts assets into portfolios solely by signals and regardless of asset classes from the beginning, thereby identifying whether the strategies provide better risk-adjusted returns than returns within each asset class. In addition, I test whether any standard systematic risk factors across asset classes can explain the excess returns.

My research also sheds light on market integration, as my asset pricing test relies heavily on a financial market integrated both internationally and across-asset-class. Bekaert and Harvey (1995) propose that the market is fully integrated if assets exposed to the same risks have the same expected returns, irrespective of their market. The authors examine a number of countries and conclude that some are not becoming more closely integrated into the global financial market. Griffin (2002) concludes that country-specific risk factors are more useful than global factors for explaining time variation in portfolio and individual stock returns in the Fama/ French three-factor setting. Fama and French (2012) provide mixed evidence, but their test results across four regions demonstrate that global asset pricing models do poorly in explaining global and regional returns. All previous literature on market integration through asset pricing tests faces the 'bad model' problem. My research focuses on whether patterns in returns across asset classes can be captured by across-asset-class risk factors. In my case, if the asset pricing test across asset classes fails, this could be attributed to either a bad model with poor risk factors or to a segmented market. However, if within-asset-class asset pricing tests work, while across-asset-class asset pricing tests fail, I can conclude that the three asset classes are not fully integrated.

My research has dual focuses. On one hand, it is a natural extension of Asness et al. (2013) and Koijen et al. (2013).They find that value, carry and momentum are everywhere in different asset classes and claim that those excess returns might be caused by the same factors. Therefore, I go further to test whether these across-asset-classes excess returns are caused by the same factors and what are the factors. Both Asness et al. (2013) and Koijen et al. (2013) still sort assets into portfolios by those signals within each asset classes first and combine them. While I sort assets of different asset classes altogether first and sort them into portfolios only by value, carry and momentum signals. If value, carry and momentum returns across asset classes are caused by the same risk factors, my portfolios should generate bigger expected returns than those in Asness et al. (2013) and Koijen et al. (2013) because my across-asset-class strategy creates a bigger cross-sectional difference in signals and thus further tilts portfolios to those risk factors. On the other hand, my research is trying to find out some common systematic risk factors that can price assets across different asset classes. Since value, carry and momentum are ubiquitous across asset classes, they provide me with a good way to sort assets into portfolios to minimise randomness in returns before standard asset pricing tests. If different asset classes can be priced by the same risk factors, markets are integrated across asset classes. Therefore, my research contributes by using the common phenomena of value, carry and momentum to study multi-asset-class pricing and integration.

1.3 Data

All asset returns used in this paper including exchange rates, government bonds and equity indices are measured in US dollars. I choose exchange rates, government bonds and equity indices because they are similar in nature. Apart from currency appreciation, these assets are short-term interest rates, long-term interest rates and equities, respectively. They are also the most frequently traded and most accessible international assets to US investors. In addition, according to previous literature, they are exposed to similar risk factors such as volatility risk and liquidity risk, while for other asset classes such as credit assets, credit risk or counterparty risks are more prominent. Therefore, testing whether currencies, bonds and equities are integrated is the first step of multi-asset-classes integration test. If those asset returns can be explained by common risk factors, I can further include more asset classes such as commodities and credits in my future research.

The equity performance for each country is measured by MSCI equity index data obtained from Thomson Datastream. I also obtain dividend yields and BE/ME ratios from MSCI. Exchange rates are obtained from Barclays Bank International (BBI) and Reuters via Thomson Datastream. I measure total returns to currency investments (ie. interest rate differentials plus depreciation rates) by assuming that Covered Interest Parity (CIP) holds, and using spot and one month forward exchange rates. To measure long-term bond returns, I use the percentage changes in the total return index on the 10-year government bonds of each country. I obtain bond returns and 10-year yields from Global Financial Data. The sample covers November 1983 to September 2011, but the number of currencies, government bonds and equity indices for which data are available varies over time. The sample consists of the following 43 countries: Australia, Austria, Belgium, Brazil, Bulgaria, Canada, Czech Republic, Denmark, Egypt, euro area, Finland, France, Germany, Greece, Hong Kong, Hungary, India, Indonesia, Ireland, Israel, Italy, Japan, Kuwait, Malaysia, Mexico, Netherlands, New Zealand, Norway, Philippines, Poland, Portugal, Russia, Singapore, South Africa, South Korea, Spain, Sweden, Switzerland, Taiwan, Thailand, Ukraine, the United Kingdom, and the United States[1].

1.4 Methodology

1.4.1 Predicative variables

The predictors I employ for all assets are value, carry, and momentum. I measure value by similar methods of Asness et al. (2013) across asset classes. The value measure for currencies is five-year change in purchasing power parity, which is the negative five year return minus CPI change relative to US during the same period. It is measured as the log of average exchange rate of a certain country from 4.5 to 5.5 years ago divided by the spot exchange rate of that country today minus log difference in CPI relative to US during the same period. For government bonds, value is measured as five-year change in the yields of the 10-year government bonds. For equity indices, value is measured as previous month's BE/ME ratio. I measure carry by methods proposed by Koijen et al. (2013). For currencies, carry is measured by

[1] Since the United states is the home country, I do not have currency return data for the United States. Therefore, I only have exchange rates for 42 countries.

one-month interest rate differentials against US rates. For bonds, I use 10-year yield to maturity to measure carry, and use dividend yields (adjusted by log) for equity indices. Momentum measures are more straightforward than value and carry, but the indicators are still slightly different for different asset classes according to previous literature. Currency momentum is measured as return over the past three months, same as Menkhoff et al. (2012); bond momentum is return over the past 12 months, and equity momentum is return over the past 12 months skipping the most recent month as suggested by Jegadeesh and Titman (2001).

1.4.2 Portfolio formation

To maximise cross-sectional difference of returns, I sort all assets into non-segmented portfolios regardless of their asset classes and hold the portfolios for one month, mimicking an international investor who manages three asset classes as if they formed a single pool of investments. Every month, I sort all assets into portfolios regardless of their asset classes by a particular predictor variable. Therefore, I first sort the assets into 15 non-segmented portfolios based on each asset's value, carry, or momentum predictor, and then the one fifteenth of assets with the smallest predictors are allocated to Portfolio 1 (P1) while the one fifteenth of assets with the biggest predictors are allocated to Portfolio 15 (P15). All assets in each portfolio are equally weighted. Portfolios are held for one month and reconstructed every month using re-estimated predictors and the asset pricing tests use these monthly portfolio return data. The monthly holding period return is excess return for all assets and I denote the excess return of asset or portfolio i by rx^i_{t+1}. Excess returns for currencies are equal to depreciation rates plus interest rate differentials, which by CIP are equal to $rx^i_{t+1} = f^i_t - s^i_{t+1}$. Excess returns for bonds and equities are proxied by holding the assets while shorting the risk free asset, which is US T-bills in this paper. The excess return for bond and equity is thus calculated as $rx^i_{t+1} = r^i_{t+1} - r^f_{t+1}$.

As the mean and variance of indicators of three asset classes are quite different, I standardise the indicators by cross-sectional mean and variance within each asset class before sorting assets into non-segmented portfolios. For example, every month, value predictors are standardised by synchronous value measures within each asset class to generate a predictor as follows:

$$s_{t,i} = \frac{I_{t,i} - \mu_t}{\sigma_t} \tag{1.1}$$

where $I_{t,i}$ is value measure for asset i at time t, μ_t is average of value measures of all assets within the same asset class of i at time t, σ_t is standard deviation of value measures of all assets within the same asset class of i at time t.

I then sort all assets into non-segmented portfolios by a standardised score s_t. Standardised scores for carry and momentum are calculated in the same way.

1.4.3 Asset pricing test

I adopt two-step Ordinary Least Squares Fama-Macbeth (OLS-FMB) estimations to uncover risk factors that can price the excess returns of all assets. The excess return of any asset should satisfy the Euler equation:

$$E_t\left(rx^i_{t+1}m^h_{t+1}\right) = 0 \tag{1.2}$$

and I assume a linear stochastic discount factor (SDF) $m_t = 1 - b'(h_{t+1} - \mu_h)$, where h_{t+1} denotes a vector of risk factors and μ_h denote a vector of factor means. This specification is equivalent to an expected return-beta representation

$$E(rx^i) = \lambda'\beta_i \tag{1.3}$$

Under the ICAPM framework, the factors are state variables that represent investment opportunities in the market.

I use two-step OLS-FMB to estimate parameters in equation (1.3) by running time-series regressions to estimate β_i and then running cross-sectional regressions of mean returns on β_i.

In the asset pricing tests, I employ three risk factors – mean return factor, volatility factor and liquidity factor, all of which reflect market status that represent investment opportunities. Mean return factor is the global market risk constructed by averaging monthly returns of all assets. The factor thus mimics holding an equally-weighted portfolio of all assets, which can be regarded as 'market return'. I construct volatility proxies for currencies and equities by the method in Menkhoff et al. (2014). The measure is realised volatility, which is averaging absolute daily return of all available assets on any given day and then averaging daily values to the monthly frequency. The Equity VOL/FX VOL in month t is given by

$$\sigma_t^{FX} = \frac{1}{T_t} \sum_{\tau \in T_t} \left[\sum_{k \in K_\tau} \left(\frac{|r_\tau^k|}{K_\tau} \right) \right], \tag{1.4}$$

where $|r_\tau^k|$ denotes absolute daily return for currency k on day τ, K_τ denotes the number of available currencies on day τ and T_t denotes the total number of trading days in month t. In empirical analysis, I use volatility innovation, which is residuals of AR(1) as the volatility risk factor. I use constructed equity volatility to replace bond volatility because I do not have daily bond data to construct the bond volatility. The liquidity factor is the Pastor-Stambaugh Liquidity series, which covers only the US data.

1.5 Empirical results

Table 1.1 presents the results of separately applying the three sorting rules to the three asset classes. In each of the nine experiments, the HML portfolios have positive mean returns, with the FX carry and the equity carry and momentum having the largest HML returns. However, from the perspective of SR, the FX carry and the equity carry perform best, with SR larger than 0.7, while the large HML return of the equity momentum is compensated for by its large standard deviation, with an SR of just 0.35. The results in Table 1.1 are similar to those reported in previous studies (e.g., Asness et al. (2013); Lustig et al. (2013); Cenedese et al. (2014); Koijen et al. (2013); Menkhoff et al. (2012)), although their sample periods and countries differ from mine. Asness et al. (2013) cite an HML return for value portfolios on global indices of 0.06, while my result is 0.0625; a momentum HML return on global indices of 0.087, compared to my 0.0737; a currency value HML return of 0.033, while my own is 0.0589; and a currency momentum HML return of 0.035, while my result is 0.0579. Koijen et al. (2013) cite results for currency, bond, and equity carry HML returns of 0.0529, 0.0385, and 0.09140, respectively, while my own are 0899, 0.0472, and 0.1147. The final panel of the table summarises the returns and standard deviations of the combined portfolios, composed of equally weighted assets in each asset class, sorted by each strategy (e.g., the value portfolio is composed of 1/3 currencies sorted by value, 1/3 bonds, and 1/3 equity indices). Asness et al. (2013) and Koijen et al. (2013) also constructed their across-asset-class portfolios in this way. We can see from Panel D that were investors to adopt the carry strategy and invest equally in the three asset classes, they would earn a 8.68% return and an SR of more than 1, while both the value and momentum strategies would generate HML returns of around 0.5 and an SR of slightly above 0.5.

Table 1.2 summarises the results of a regression of within-asset-class portfolio returns on market return and volatility risk factors. The findings demonstrate that the currency carry returns can be explained by the currency mean return and the volatility risk, which is consistent with previous studies, such as Menkhoff et al. (2012). The loading of the carry portfolio on the volatility risk factor is negative and significant. The market mean return and the volatility risk can explain more than 90% of the cross-sectional difference in portfolio returns. The equity carry and momentum returns can be partly explained by the equity mean return and volatility risk, which is consistent with the conclusions of Cenedese et al. (2014). The risk factor loadings are significant, meaning that assets with greater exposure to market risk and market volatility risk yield higher expected returns. In addition, equity volatility has a significant impact on cross-sectional difference in bond momentum returns and a slightly significant impact on bond carry returns. Bond momentum returns can be largely explained by bond mean return and equity volatility risk factors. Therefore, I find that, within each asset class, all three signals have predictive power, and

TABLE 1.1: Value, carry, momentum returns within different asset classes

This table presents means and standard deviations of value, carry and momentum predictors and portfolio returns for currencies, bonds and equities respectively. In each asset classes, assets are sorted into five portfolios by value, carry and momentum predictors. The predictors (s) and returns (r) of P1 to P5 and HML portfolio(P5-P1) for each asset class and each sorting method are summarised separately in the table. The combined value/carry/momentum portfolio is constructed by holding 1/3 within-asset-class value/carry/momentum portfolio of each asset class respectively.

Panel A: Currency

	Value				Carry				MOM			
	s	σ_s	r	σ_r	s	σ_s	r	σ_r	s	σ_s	r	σ_r
P1	-0.3286	0.1688	0.0050	0.0877	-0.0079	0.0062	-0.0129	0.0795	-0.0378	0.0374	0.0123	0.0967
P2	-0.2160	0.1738	0.0298	0.0862	-0.0024	0.0015	0.0194	0.0762	-0.0096	0.0319	0.0160	0.0870
P3	-0.1055	0.1780	0.0202	0.0726	-0.0008	0.0014	0.0351	0.0808	0.0047	0.0329	0.0392	0.0836
P4	0.0213	0.1835	0.0321	0.0743	0.0006	0.0015	0.0465	0.0875	0.0194	0.0317	0.0407	0.0843
P5	0.3511	0.3203	0.0640	0.0909	0.0028	0.0047	0.0770	0.1135	0.0446	0.0360	0.0703	0.0907
HML			0.0589	0.0910			0.0899	0.1004			0.0579	0.1059

Panel B: Bond

	Value				Carry				MOM			
	s	σ_s	r	σ_r	s	σ_s	r	σ_r	s	σ_s	r	σ_r
P1	-0.5107	0.2175	0.0457	0.0958	4.6877	1.6794	0.0366	0.0968	-0.0362	0.0935	0.0472	0.1013
P2	-0.2931	0.1792	0.0543	0.1005	6.1927	2.2205	0.0435	0.1046	0.0653	0.1002	0.0555	0.0966
P3	-0.1885	0.1720	0.0641	0.1038	6.9729	2.8112	0.0738	0.0958	0.1197	0.1166	0.0715	0.1056
P4	-0.0849	0.1721	0.0830	0.1019	8.1950	3.2748	0.0660	0.1010	0.1661	0.1229	0.0729	0.0989
P5	0.1251	0.1990	0.0544	0.1079	12.0002	3.3755	0.0838	0.1157	0.2818	0.1404	0.0909	0.0934
HML			0.0088	0.0953			0.0472	0.1068			0.0437	0.0997

Panel C: Equity

	Value				Carry				MOM			
	s	σ_s	r	σ_r	s	σ_s	r	σ_r	s	σ_s	r	σ_r
P1	-1.0219	0.2671	0.0670	0.1961	-4.3919	0.3640	0.0382	0.2341	-0.1197	0.2259	0.0788	0.2371
P2	-0.7700	0.2420	0.0770	0.1828	-3.8651	0.2701	0.1173	0.2089	0.0546	0.2201	0.0803	0.1942
P3	-0.6192	0.2320	0.1021	0.1938	-3.6320	0.2567	0.1085	0.1950	0.1595	0.2430	0.1140	0.1913
P4	-0.4601	0.2091	0.1072	0.1974	-3.3652	0.2254	0.1486	0.1952	0.2826	0.2915	0.1387	0.1979
P5	-0.1345	0.2684	0.1294	0.2372	-3.0202	0.2133	0.1529	0.2055	0.6156	0.4405	0.1525	0.2343
HML			0.0625	0.1778			0.1147	0.1635			0.0737	0.2077

Panel D: Combined Portfolio

	Value		Carry		MOM	
	r	σ_r	r	σ_r	r	σ_r
P1	0.0315	0.0951	0.0248	0.1041	0.0469	0.1199
P2	0.0458	0.1004	0.0643	0.1044	0.0526	0.1032
P3	0.0571	0.1014	0.0768	0.0994	0.0775	0.1026
P4	0.0584	0.1012	0.0899	0.1066	0.0874	0.1025
P5	0.0765	0.1227	0.1116	0.1173	0.1064	0.1104
HML	0.0450	0.0846	0.0868	0.0756	0.0595	0.0995

the excess returns generated by the signals can be explained by the systematic risk factors.

TABLE 1.2: Two Factor OLS-FMB of Segmented Portfolios – Volatility Risk

Panel A reports OLS-FMB test results of currency portfolios sorted by value, carry and momentum signals, Panel B reports results of bonds and Panel C reports results of equities. The risk factors are market risk ('Globe') and market volatility risk ('Volatility').

Panel A: Currency

	value	carry	mom
Globe	0.0026	0.0025	0.0026
t-stats	1.5854	8.2738	4.2219
Volatility	-0.0474	-0.0717	0.0965
t-stats	-0.6274	-6.0178	2.0669
r-squared	0.0688	0.9567	0.6432
adjusted-r	-0.8623	0.9135	0.2864

Panel B: Bond

	value	carry	mom
Globe	0.0053	0.0050	0.0056
t-stats	8.8442	7.2937	11.9814
Volatility	-0.2987	-0.1148	-0.5599
t-stats	-1.2788	-1.9137	-3.1450
r-squared	0.5059	0.5154	0.7544
adjusted-r	0.0118	0.0309	0.5088

Panel C: Equity

	value	carry	mom
Globe	0.0084	0.0091	0.0093
t-stats	10.0832	6.7815	11.3697
Volatility	0.0774	-0.3618	-0.1551
t-stats	0.7860	-2.7267	-3.2893
r-squared	0.6424	0.6962	0.7834
adjusted-r	0.2847	0.3923	0.5669

To further test whether value, carry, and momentum are across-asset-class phenomena, rather than investing equally in each asset class, I adopt another measure to diversify across asset classes. Specifically, I put all assets into a single investment pool at the beginning, then sort them into portfolios by their signals, regardless of asset class. However, as demonstrated in Table 1.1, the signals of the portfolios (labelled 's' in the columns) varied dramatically across asset classes. For example, equity value portfolios have signals of between -1.02 and -0.13, from P1 to P5. The distribution of the bond value signals across portfolios is, however, very different, with average values from -0.51 to 0.12. This implies that, when sorting the aggregated cross-section, equities will ultimately reach the low-value portfolios and bonds the high-value portfolios; thus, there is little or no mixing across asset classes. Similarly, equity carry signals are very small, while bond carry signals are large. This problem of clear heterogeneity in signal distributions across asset classes is least pronounced for momentum, simply because momentum is measured as a cumulative historical return for all asset classes. My solution to this problem is to standardise the predictors within asset classes by subtracting a within-asset-class cross-sectional mean and scaling by a within-asset-class cross-sectional variance (thus, there is no look-ahead bias in these computations). This removes the across-asset-class heterogeneity in signal distributions and thus provides the sorting schemes with more consistent data across assets.

Since currency excess returns are equal to currency appreciation plus the short-term interest rate, while bond excess returns are equal to currency appreciation plus the long-term interest rate, and both currency and bond returns are exposed to market mean return and volatility risk factors, I begin by putting currencies and bonds into a single investment pool. Tables 1.3, 1.4, and 1.5 present the summary statistics of 10 portfolios when currencies and bonds are put into a single investment pool and the assets sorted according to their standardised value, carry, and momentum signals. All three strategies generate significant cross-sectional differences in returns from P1 to P10. The SRs of across-asset-class value and carry HML portfolios are slightly smaller than those of the currency value and carry HML portfolios in the previous table, but much larger than those of bond and equity portfolios mainly due to a smaller standard deviation. The momentum HML portfolio performs very well, with SR larger than those of all within-asset-class momentum portfolios and a positive skewness. All HML portfolios have kurtosis larger than normal and a positive autocorrelation. Figure 1.1 indicates that the value portfolio experienced a significant slump in 1998, when the global currency and bond markets together went through a liquidity crisis. The value strategy performed well between 2002 and 2010. Its performance was particularly positive during the 2008 financial crisis. However, after 2008, when the whole market recovered from the crisis, the value portfolio had negative returns. Its performance after 2005 seems to have provided a good hedge for the global currency and bond markets. Figure 1.2 suggests that, after 1998, when the carry HML portfolio went through a downturn, together with the market portfolio, carry generated much larger cumulative HML returns than an equally-weighted market portfolio. However, carry investors suffered a significant loss during the financial crisis. In addition, the large carry draw-downs all began abruptly. Figure 1.3 demonstrates that the momentum portfolio performed badly in the mid-1990s, and then generated positive returns year-on-year, but after 2005, its cumulative returns did not change much.

TABLE 1.3: Summary Statistics of Non-segmented Value Portfolios – Currency and Bond

This table presents summary statistics of 10 non-segmented portfolios sorted by standardised value measure. Value measure for currencies is negative five-year change in purchasing power parity (relative to US); for bonds, it is negative five-year change in 10-year yield. Every month, value measures are standardised by cross-sectional value measures to generate a predictor as follows:

$$s_t = \frac{I_{t,i} - \mu_t}{\sigma_t} \quad (1.5)$$

where $I_{t,i}$ is value measure for asset i at time t, μ_t is mean value measure of all assets within the same asset class as i at time t, σ_t is standard deviation of value measures of all assets within the same asset class as i.
All assets are put in one investment pool regardless their asset classes and sorted into 10 portfolios by the predictor. P1 include assets with smallest value measure. HML return is calculated by average return of P8 to P10 minus average return of P1 to P3.

P	P1	P2	P3	P4	P5	P6	P7	P8	P9	P10	HML
mean	0.0330	0.0242	0.0300	0.0202	0.0354	0.0672	0.0524	0.0705	0.0421	0.0947	0.0400
std	0.0843	0.0831	0.0871	0.0857	0.0888	0.0931	0.0930	0.0889	0.0886	0.1129	0.0642
SR	0.3913	0.2909	0.3438	0.2356	0.3987	0.7214	0.5629	0.7927	0.4747	0.8391	0.6236
skew	-0.1264	-0.4737	-0.3014	-0.4785	-0.2744	-0.0081	-0.0484	-0.0909	0.1651	0.4422	-0.1960
kurtosis	3.9537	4.2466	4.0937	4.4025	4.5440	4.0268	4.5476	4.3204	4.5495	6.4200	4.2197
autocorr.	0.1279	0.0754	0.1110	0.0647	0.1084	0.0595	0.1317	0.0726	0.1098	0.2216	0.1986

TABLE 1.4: Summary Statistics of Non-segmented Carry Portfolios – Currency and Bond

This table presents summary statistics of 10 non-segmented portfolios sorted by standardised carry measure. Carry measure for currencies is one-month interest rate differentials against US rates; for bonds, it is 10-year yield to maturity. Every month, carry measures are standardised by cross-sectional carry measures to generate a predictor as follows:

$$s_t = \frac{I_{t,i} - \mu_t}{\sigma_t} \tag{1.6}$$

where $I_{t,i}$ is carry measure for asset i at time t, μ_t is mean carry measure of all assets within the same asset class as i at time t, σ_t is standard deviation of carry measures of all assets within the same asset class as i.
All assets are put in one investment pool regardless their asset classes and sorted into 10 portfolios by the predictor. P1 include assets with smallest carry measure. HML return is calculated by average return of P8 to P10 minus average return of P1 to P3.

P	P1	P2	P3	P4	P5	P6	P7	P8	P9	P10	HML
mean	0.0128	0.0146	0.0259	0.0316	0.0660	0.0570	0.0577	0.0470	0.0522	0.1309	0.0589
std	0.0970	0.0843	0.0859	0.0977	0.0895	0.0871	0.0919	0.0991	0.1014	0.1214	0.0718
SR	0.1315	0.1730	0.3017	0.3229	0.7372	0.6550	0.6273	0.4739	0.5143	1.0788	0.8203
skew	0.4129	0.2470	-0.0084	-0.1058	-0.1617	0.1033	-0.3219	-0.6810	-0.5065	0.1454	-0.4030
kurtosis	4.1585	3.5514	3.0919	4.1780	4.0546	4.0842	4.6914	5.5719	5.3013	5.2803	4.3629
autocorr.	0.0588	0.0302	0.1034	0.0771	0.0753	0.1004	0.0284	0.0392	0.0899	0.2087	0.1598

TABLE 1.5: Summary Statistics of Non-segmented Momentum Portfolios – Currency and Bond

This table presents summary statistics of 10 non-segmented portfolios sorted by standardised momentum measure. Momentum measure for currencies is cumulative return over the past three months; for bonds, it is cumulative return over previous 12 months. Every month, momentum measures are standardised by cross-sectional momentum measures to generate a predictor as follows:

$$s_t = \frac{I_{t,i} - \mu_t}{\sigma_t} \tag{1.7}$$

where $I_{t,i}$ is momentum measure for asset i at time t, μ_t is mean momentum measure of all assets within the same asset class as i at time t, σ_t is standard deviation of momentum measures of all assets within the same asset class as i.
All assets are put in one investment pool regardless their asset classes and sorted into 10 portfolios by the predictor. P1 include assets with smallest momentum measure. HML return is calculated by average return of P8 to P10 minus average return of P1 to P3.

P	P1	P2	P3	P4	P5	P6	P7	P8	P9	P10	HML
mean	0.0375	0.0335	0.0372	0.0447	0.0553	0.0556	0.0589	0.0744	0.0768	0.0930	0.0453
std	0.1087	0.0905	0.0878	0.0892	0.0952	0.0947	0.0917	0.0915	0.0913	0.0970	0.0696
SR	0.3452	0.3699	0.4230	0.5014	0.5807	0.5871	0.6423	0.8129	0.8411	0.9585	0.6507
skew	-0.5356	-0.1577	0.0193	-0.1388	0.0559	0.0006	0.1223	-0.0746	0.3428	-0.1481	0.0550
kurtosis	8.4713	5.4592	4.4788	3.9185	4.4675	4.6406	4.3997	4.4704	4.5212	4.4154	4.2952
autocorr.	0.0778	0.0619	0.1040	0.1025	0.0463	0.0653	0.0258	0.0102	0.0771	0.1399	0.0569

FIGURE 1.1: Cumulative HML Return of Non-segmented Value Portfolio – Currency and Bond

I plot cumulative HML returns of the non-segmented value portfolio together with cumulative excess returns of an equally-weighted portfolio from 1990 to 2011. Both portfolios are composed of currencies and government bonds.

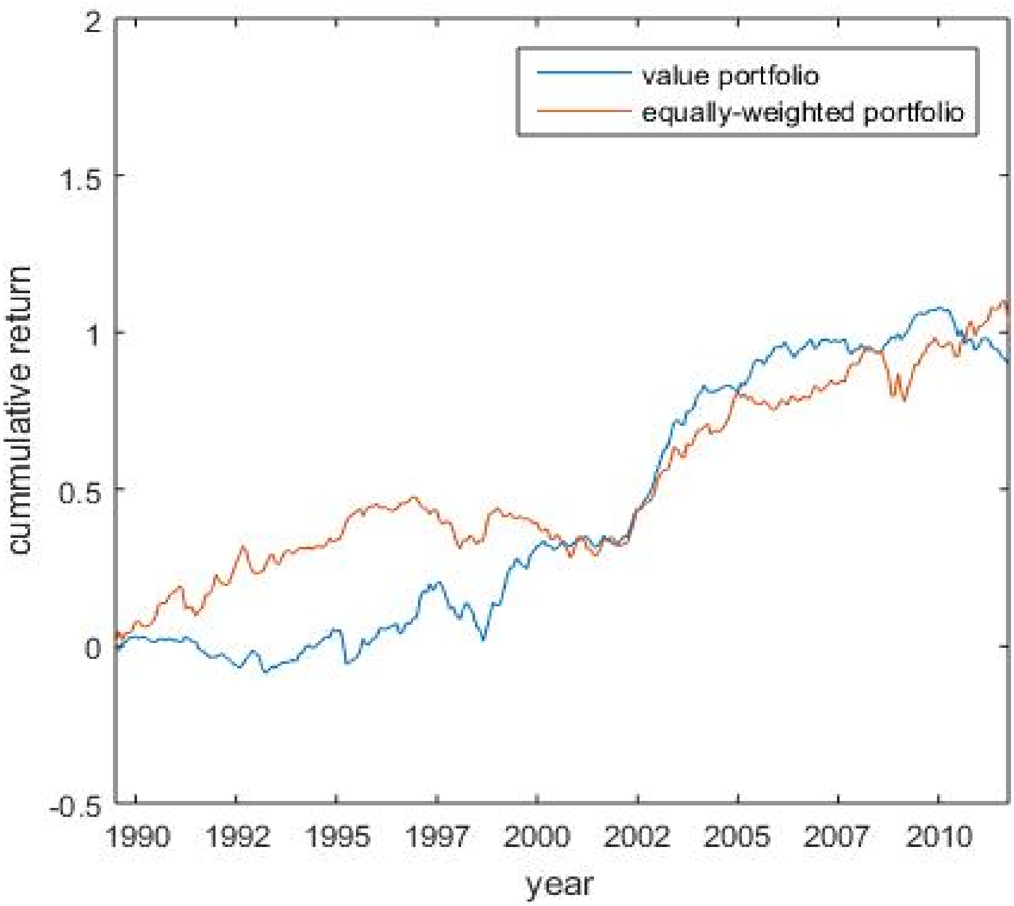

FIGURE 1.2: Cumulative HML Return of Non-segmented Carry Portfolio – Currency and Bond

I plot cumulative HML returns of the non-segmented carry portfolio together with cumulative excess returns of an equally-weighted portfolio from 1983 to 2011. Both portfolios are composed of currencies and government bonds.

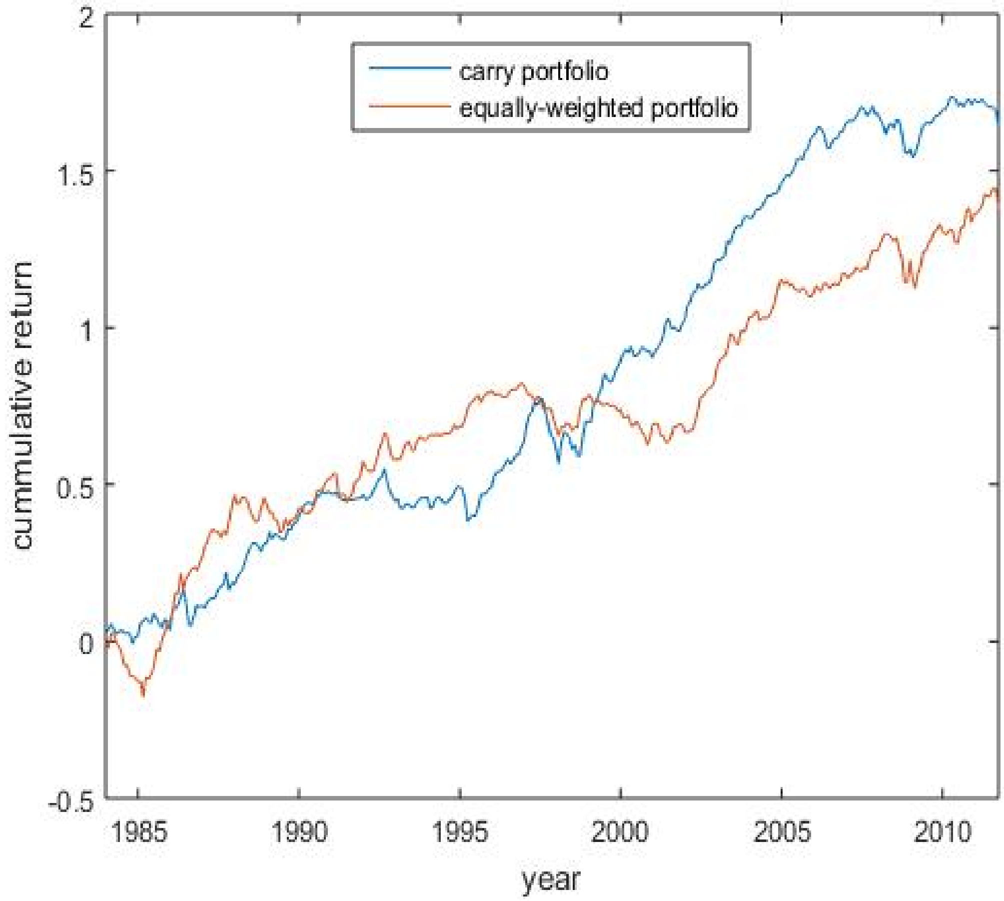

FIGURE 1.3: Cumulative HML Return of Non-segmented MOM Portfolio – Currency and Bond

I plot cumulative HML returns of the non-segmented momentum portfolio together with cumulative excess returns of an equally-weighted portfolio from 1983 to 2011. Both portfolios are composed of currencies and government bonds.

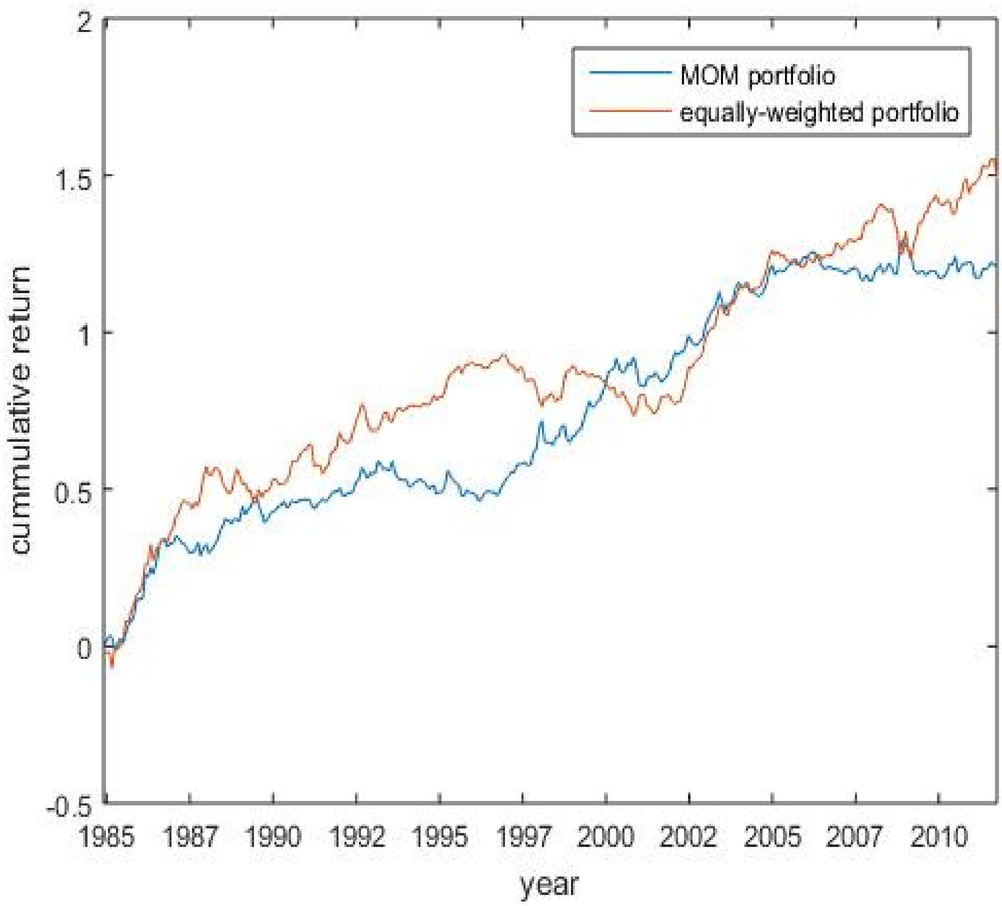

I have further attempted to determine a common set of systematic risk factors to explain the cross-sectional difference between returns of portfolios composed of currencies and bonds. Table 1.6 indicates that carry returns can be partly explained by market mean return and market volatility factors, and both factors have a significant impact on the return cross-section. Therefore, the results suggest that assets with larger 'carry' are cheaper and can generate larger expected returns, as the returns of those assets are negatively correlated with market volatility. However, as shown in Figure 1.4, while the upward trending of returns from P1 to P10 can be partly explained by the risk factors, pricing errors of some portfolios are far from zero. It cast doubt upon the previous asset pricing test results, because the portfolios with large pricing errors might be primarily composed of bonds. The table also shows that volatility risk does not work to explain non-segmented value and momentum returns.

TABLE 1.6: Two Factor OLS-FMB of 10 Non-segmented Portfolios – Currency and Bond

This table reports OLS-FMB test results of non-segmented portfolios composed of currencies and bonds sorted by value, carry and momentum signals. The risk factors are market risk ('Globe') and market volatility risk ('Volatility').

	value	carry	mom
Globe	0.0041	0.0041	0.0047
t-stats	4.8397	6.0576	7.4054
Volatility	-0.0484	-0.0994	0.0058
t-stats	-0.4921	-2.9779	0.0710
r-squared	0.1575	0.5469	-0.1531
adjusted-r	-0.0832	0.4174	-0.4826

FIGURE 1.4: Carry Pricing Errors

I plot mean returns of 10 non-segmented standardised carry portfolios composed of currencies and bonds, and their pricing errors after conducting two-factor (market mean return and volatility risk) OLS-FMB asset pricing test.

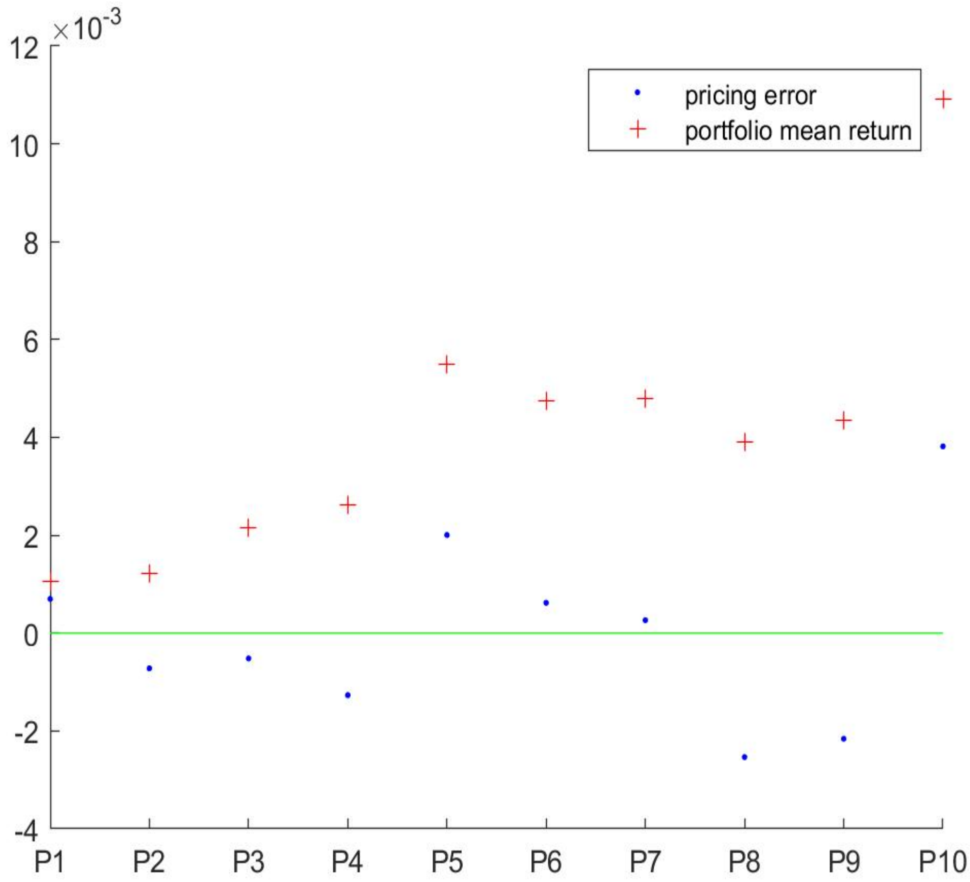

I put all currency, bond, and equity excess returns together to study the cross-section of value, carry, and momentum returns. Table 1.7 indicates that value generates a slightly larger HML return when my non-segmented standardised sorting method is adopted, rather than a simple combination of value portfolios for each asset class, as demonstrated in Table 1.1. The HML portfolio generates a moderate Sharpe ratio of around 0.5, but its skewness is very positive, from which investors can benefit through small extreme loss but large extreme profit. Therefore, assets sorted solely by value signals, regardless of their asset classes, can slightly outperform the equally-weighted portfolio composed of value portfolios from each asset class. Figure 1.5 indicates how returns of value portfolios accumulate over time, demonstrating that the value portfolio provides a good hedge for the market risk (represented by the return of a market portfolio composed of all currencies, bonds, and equities) from 2006 to 2011, but its return strongly correlates with the market mean return before 2006.

FIGURE 1.5: Cumulative HML Return of Non-segmented Value Portfolio

I plot cumulative HML returns of the non-segmented standardised value portfolio together with cumulative excess returns of an equally-weighted portfolio of all assets from 1990 to 2011.

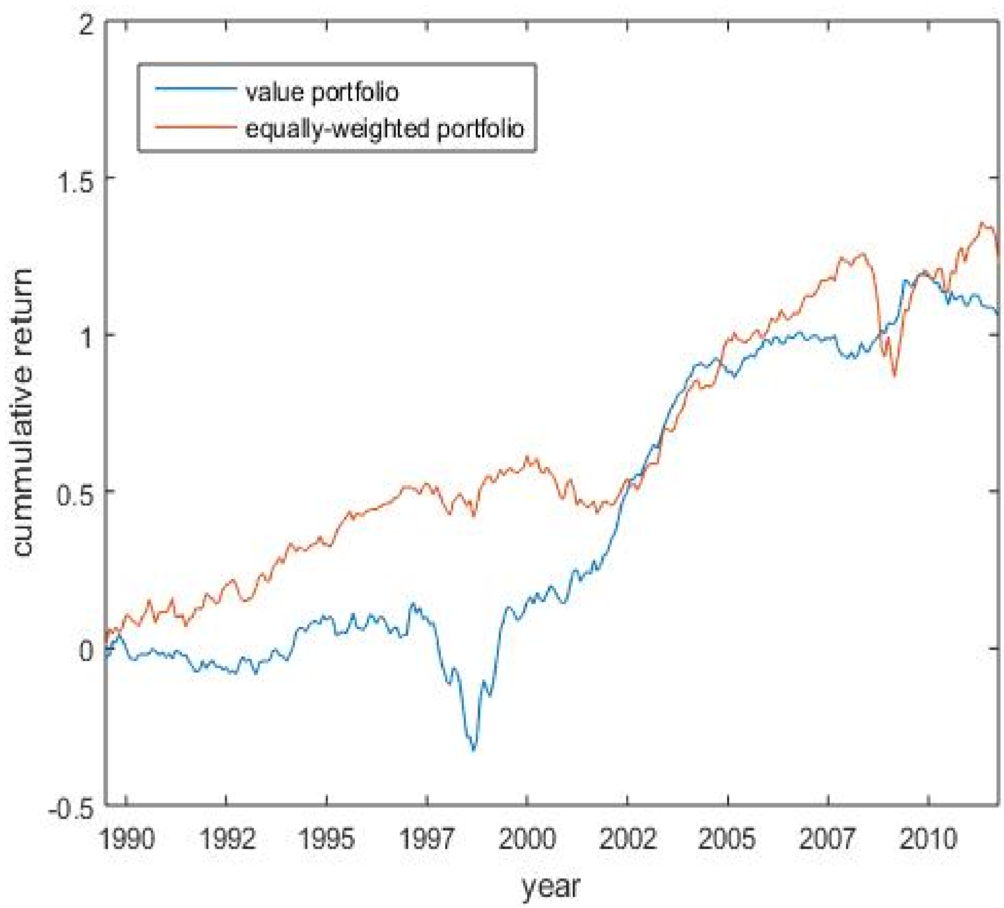

TABLE 1.7: Summary Statistics of 15 Non-segmented Value Portfolios – Currency, Bond and Equity

This table presents summary statistics of 15 non-segmented portfolios sorted by standardised value measure. Value measure for currencies is negative five-year change in purchasing power parity (relative to US); for bonds, it is negative five-year change in 10-year yield; for equities, it is log of previous month's BE/ME ratio. Every month, value measures are standardised by cross-sectional value measures to generate a predictor as follows:

$$s_t = \frac{I_{t,i} - \mu_t}{\sigma_t} \tag{1.8}$$

where $I_{t,i}$ is value measure for asset i at time t, μ_t is mean value measure of all assets within the same asset class as i at time t, σ_t is standard deviation of value measures of all assets within the same asset class as i.
All assets are put in one investment pool regardless their asset classes and sorted into 15 portfolios by the predictor. P1 include assets with smallest value measure. HML return is calculated by average return of P13 to P15 minus average return of P1 to P3.

P	P1	P2	P3	P4	P5	P6	P7	P8	P9	P10	P11	P12	P13	P14	P15	HML
mean	0.0319	0.0444	0.0302	0.0146	0.0643	0.0639	0.0370	0.0589	0.0842	0.0543	0.0435	0.0759	0.0503	0.1015	0.0959	0.0471
std	0.1208	0.1176	0.1201	0.1150	0.1140	0.1162	0.1169	0.1124	0.1211	0.1184	0.1209	0.1251	0.1319	0.1554	0.1764	0.0920
SR	0.2637	0.3777	0.2512	0.1272	0.5639	0.5503	0.3165	0.5242	0.6951	0.4585	0.3594	0.6066	0.3809	0.6530	0.5435	0.5115
skew	-0.5144	-0.4551	-0.9787	-0.5184	-0.0605	-1.0382	-1.6827	-0.3228	-0.0067	-0.6542	-0.3284	-0.8546	0.2438	0.4525	-0.2325	0.4396
kurtosis	4.6416	4.6599	7.6731	4.1844	4.0415	10.2997	12.8965	4.0682	3.6941	4.9038	4.1293	6.9357	6.0062	4.7080	7.8059	5.6150
autocorr.	0.0586	0.1307	0.1067	0.0989	0.0492	0.0727	0.1471	0.0959	0.0656	0.1039	0.0519	0.0855	0.1497	0.1960	0.2202	0.2438

Table 1.8 indicates that mean returns of carry portfolios increase from 4.60% per year for P1 to 17.11% per year for P15. The annual HML for the value sort is 9.38%. Table 1.8 also demonstrates that standard deviations do not change in any monotonic fashion between P1 and P15. Thus, the carry HML portfolio has a mean return of over 9%, a Sharpe ratio larger than 1, and *negative* skewness. Figure 1.6 confirms that investors can accumulate large returns over time by adopting this across-asset-class carry strategy. However, although the HML return of my strategy is slightly larger than that of the combined portfolio in Table 1.1, my SR is smaller.

TABLE 1.8: Summary Statistics of 15 Non-segmented Carry Portfolios – Currency, Bond and Equity

This table presents summary statistics of 15 non-segmented portfolios sorted by standardised carry measure. Carry measure for currencies is one-month interest rate differentials against US rates; for bonds, it is 10-year yield to maturity; for equities, it is log of previous month's dividend yields. Every month, carry measures are standardised by cross-sectional carry measures to generate a predictor as follows:

$$s_t = \frac{I_{t,i} - \mu_t}{\sigma_t} \quad (1.9)$$

where $I_{t,i}$ is carry measure for asset i at time t, μ_t is mean carry measure of all assets within the same asset class as i at time t, σ_t is standard deviation of carry measures of all assets within the same asset class as i.
All assets are put in one investment pool regardless their asset classes and sorted into 15 portfolios by the predictor. P1 include assets with smallest carry measure. HML return is calculated by average return of P13 to P15 minus average return of P1 to P3.

P	P1	P2	P3	P4	P5	P6	P7	P8	P9	P10	P11	P12	P13	P14	P15	HML
mean	0.0460	0.0157	0.0168	0.0364	0.0535	0.0912	0.0916	0.0823	0.0571	0.0888	0.1078	0.1057	0.1031	0.0857	0.1711	0.0938
std	0.1839	0.1336	0.1075	0.1049	0.1135	0.1181	0.1141	0.1217	0.1319	0.1343	0.1539	0.1475	0.1669	0.1482	0.1476	0.0856
SR	0.2501	0.1175	0.1566	0.3465	0.4714	0.7717	0.8031	0.6766	0.4327	0.6608	0.7004	0.7165	0.6178	0.5784	1.1595	1.0960
skew	0.6205	-0.1227	-0.3783	-0.7213	-0.2569	0.1144	-0.3332	-0.4097	-0.6308	-0.5014	-0.9740	-0.6515	-1.3902	-0.1121	0.6853	-0.8596
kurtosis	8.9462	3.8125	3.9039	5.7495	6.0677	4.2008	5.0072	4.8863	6.8766	5.7539	8.1719	5.2587	8.4544	4.4086	5.8795	12.6133
autocorr.	0.2209	-0.0180	0.0067	0.0252	0.0412	0.1066	0.1201	0.1321	0.1084	0.1326	0.1047	0.0900	0.1212	0.1437	0.2436	0.1271

FIGURE 1.6: Cumulative HML Return of Non-segmented Carry Portfolio

I plot cumulative HML returns of the non-segmented standardised carry portfolio together with cumulative excess returns of an equally-weighted portfolio of all assets from 1983 to 2011.

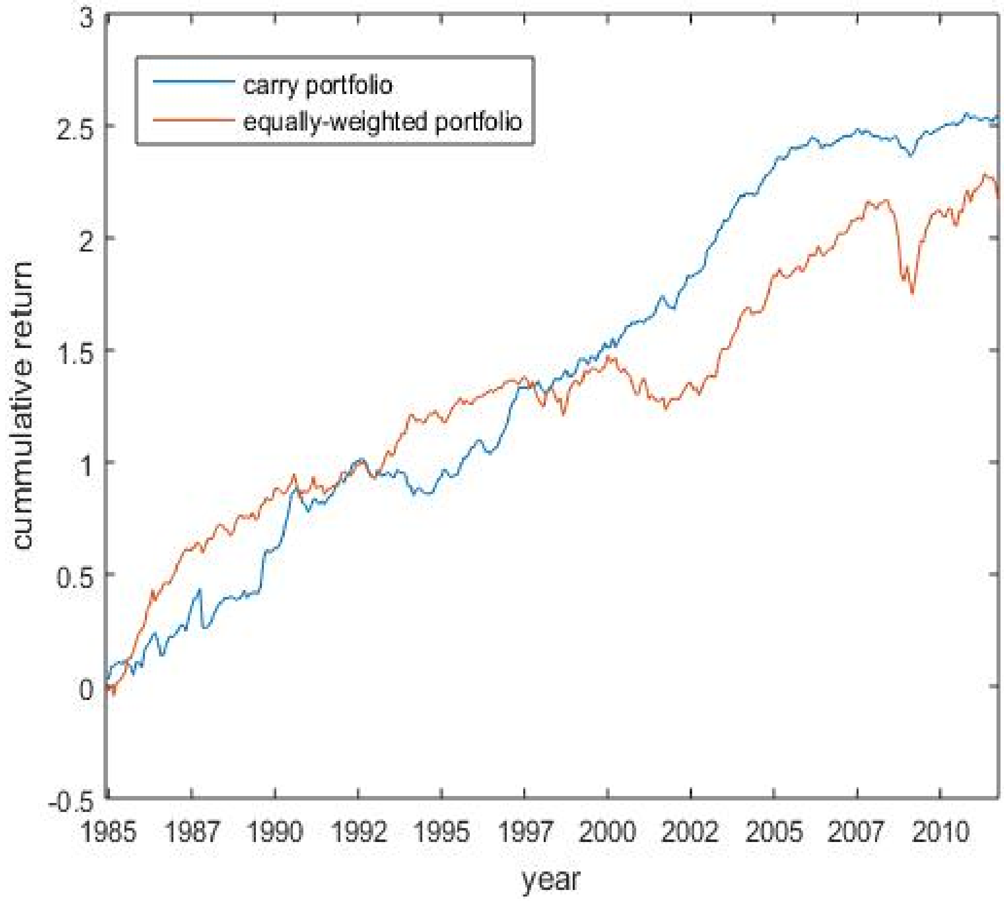

Like carry, sorting on momentum generated large differences in portfolio returns in my aggregated cross-section. The momentum portfolio returns are presented in Table 1.9. The annual return increase from 6.79% for P1 to roughly 15.41% for P15. As illustrated in Figure 1.7, the cumulative HML momentum return in my strategy increased over time and performed poorly, together with the market portfolio, during the market downturns after 2000. As with my across-asset-class value and carry portfolios, my momentum portfolio had a slightly larger HML return than the combined momentum portfolio in Table 1.1.

FIGURE 1.7: Cumulative HML Return of Non-segmented Momentum Portfolio

I plot cumulative HML returns of the non-segmented standardised momentum portfolios and cumulative excess returns of an equally-weighted portfolio of all assets from 1983 to 2011.

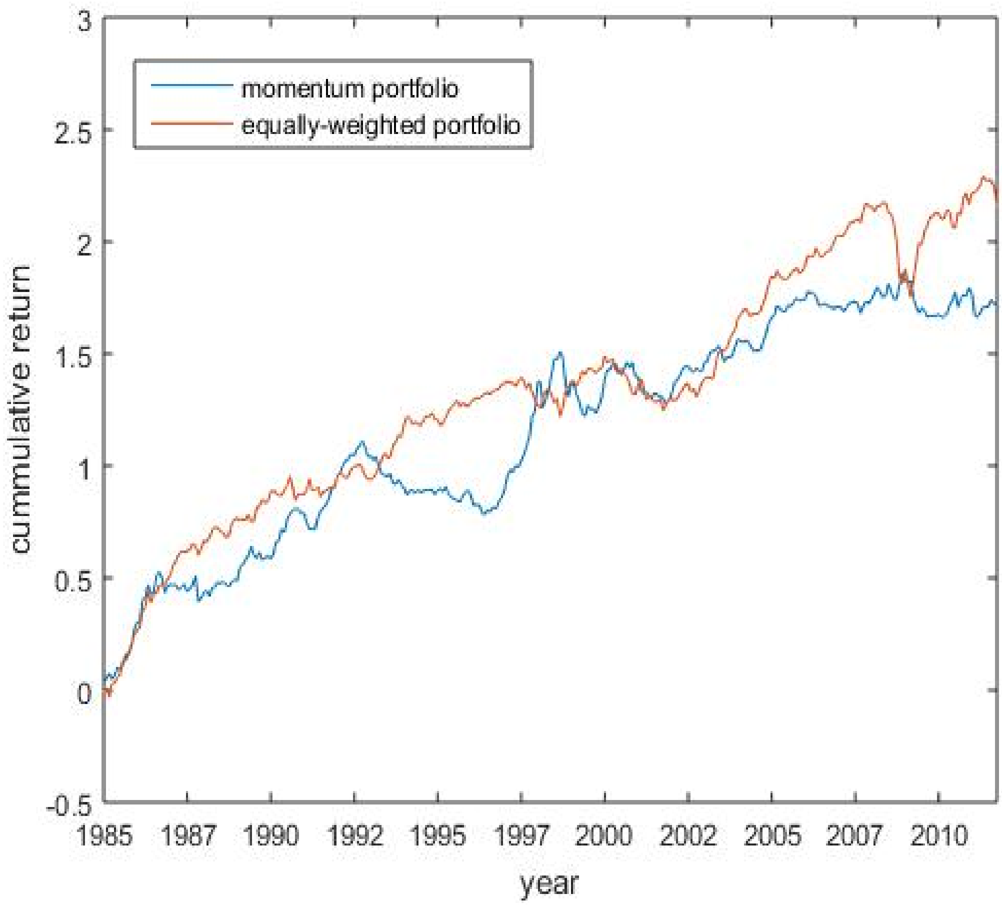

Table 1.10 presents the correlation coefficients between across-asset-class value, carry, and momentum HML returns. The negative correlation coefficient between value and momentum is similar to that reported by Asness et al. (2013) because, intuitively, value and momentum are 'opposite' strategies. In addition, my results suggest that carry is slightly positively correlated with both value and momentum.

TABLE 1.9: Summary Statistics of 15 Non-segmented Momentum Portfolios – Currency, Bond and Equity

This table presents summary statistics of 15 non-segmented portfolios sorted by standardised momentum measure. Momentum measure for currencies is cumulative return over the past three months; for bonds, it is cumulative return over previous 12 months; for equities, it is cumulative return over previous 12 months skipping the most recent month. Every month, momentum measures are standardised by cross-sectional momentum measures to generate a predictor as follows:

$$s_t = \frac{I_{t,i} - \mu_t}{\sigma_t} \quad (1.10)$$

where $I_{t,i}$ is momentum measure for asset i at time t, μ_t is mean momentum measure of all assets within the same asset class as i at time t, σ_t is standard deviation of momentum measures of all assets within the same asset class as i.
All assets are put in one investment pool regardless their asset classes and sorted into 15 portfolios by the predictor. P1 include assets with smallest momentum measure. HML return is calculated by average return of P13 to P15 minus average return of P1 to P3.

P	P1	P2	P3	P4	P5	P6	P7	P8	P9	P10	P11	P12	P13	P14	P15	HML
mean	0.0679	0.0444	0.0452	0.0506	0.0625	0.0469	0.0699	0.0873	0.0852	0.0728	0.0955	0.0891	0.0931	0.1033	0.1541	0.0644
std	0.1653	0.1584	0.1331	0.1382	0.1270	0.1298	0.1278	0.1212	0.1263	0.1221	0.1186	0.1193	0.1187	0.1413	0.1728	0.1100
SR	0.4106	0.2802	0.3394	0.3660	0.4919	0.3609	0.5474	0.7206	0.6749	0.5966	0.8050	0.7467	0.7848	0.7313	0.8920	0.5851
skew	1.0524	-0.8239	-0.3308	-0.7125	-0.3194	-0.5622	-0.4586	-1.0898	-0.0962	-0.3583	-0.1311	-0.2897	-0.3064	-0.5394	-0.0803	-0.2901
kurtosis	7.8571	8.1345	4.9614	6.5411	4.6236	5.3094	6.1741	9.7556	4.6930	5.0904	4.7865	4.3483	4.4070	7.2210	5.0046	5.2912
autocorr.	0.1442	0.1595	0.1167	0.1190	0.0932	0.0799	0.0551	0.0988	0.0286	0.0368	0.0919	0.0204	0.0490	0.1094	0.0625	0.1331

These small correlations suggest that if investors simply combine value, carry, and momentum portfolios, they can expand their efficient frontier and achieve portfolios with greater Sharpe ratios. Therefore, my results suggest that investors can further diversify among those three strategies. Asness et al. (2013) have combined value and momentum portfolios because of their negative correlation. They could generate a portfolio with a bigger SR by constructing a 1:1 value and momentum portfolio. No previous research has tried to put all three strategies together to take advantage of the diversification benefits. However, as mentioned by Cenedese et al. (2014), portfolios sorted by different signals are exposed to different systematic risk factors. It is important for investors to understand what systematic risk factors they are exposed to when they adopt these strategies. Although investing in multiple asset classes by multiple strategies might provide diversification benefits, part of the excess returns may be caused by systematic risk factors.

TABLE 1.10: Correlation Coefficient Matrix

This table presents time-series correlation coefficient matrix of non-segmented standardised HML portfolios sorted by value, carry and momentum predictors.

P	value	carry	mom
value	1.0000	0.1322	-0.4061
carry	0.1322	1.0000	0.1370
mom	-0.4061	0.1370	1.0000

Figures 1.8, 1.9, and 1.10 indicate the probability of an asset in portfolio P_m being allocated to portfolio P_n in the following month, thus indicating whether the standardisation procedure helps to 'mix' assets in different asset classes. For example, in the value sorting, there is a 63% probability of an asset in P2 remaining there the following month and a 17% probability of it moving to P3. The figures demonstrate that there is moderate movement of assets between portfolios. The probabilities of high and low portfolios are around 0.6 for value and carry and 0.4 for momentum, implying that investors do not suffer significant transaction costs. Previous literature has provided sufficient evidence that taking transaction cost into account, value, carry

and momentum signals can still generate significant cross-sectional difference in returns. In addition, the focus of my research is whether returns across different asset classes can be explained by common risk factors, even if transaction costs decrease returns, they decrease returns for all assets at the same time, which will not influence my asset pricing test results.[2]

FIGURE 1.8: Transition Matrix of Non-segmented Value Portfolio

The number in *ith* column and *jth* row of the transition matrix represents the probability that an asset in *ith* portfolio this month is allocated to *jth* portfolio next month if I sort assets by standardised value measure.

P	1	2	3	4	5	6	7	8	9	10	11	12	13	14	15
1	0.843	0.138	0.010	0.002	0.002	0.001	0.002	0.001	0.000	0.001	0.001	0.000	0.000	0.000	0.000
2	0.144	0.631	0.171	0.025	0.011	0.008	0.007	0.002	0.001	0.001	0.000	0.001	0.000	0.000	0.000
3	0.007	0.176	0.578	0.182	0.030	0.017	0.006	0.004	0.001	0.000	0.000	0.000	0.000	0.000	0.000
4	0.002	0.031	0.174	0.526	0.192	0.045	0.021	0.005	0.003	0.001	0.000	0.000	0.000	0.001	0.000
5	0.003	0.009	0.039	0.184	0.489	0.188	0.056	0.018	0.007	0.003	0.002	0.000	0.000	0.000	0.000
6	0.000	0.009	0.023	0.051	0.179	0.444	0.209	0.057	0.019	0.006	0.002	0.002	0.000	0.000	0.000
7	0.001	0.003	0.003	0.026	0.064	0.199	0.414	0.203	0.061	0.019	0.005	0.002	0.000	0.000	0.000
8	0.002	0.001	0.002	0.005	0.022	0.058	0.182	0.426	0.226	0.058	0.010	0.004	0.001	0.000	0.000
9	0.000	0.001	0.001	0.003	0.012	0.028	0.060	0.215	0.412	0.217	0.040	0.010	0.002	0.000	0.000
10	0.000	0.000	0.001	0.000	0.003	0.009	0.020	0.054	0.201	0.477	0.192	0.037	0.004	0.002	0.000
11	0.000	0.000	0.001	0.000	0.002	0.006	0.006	0.007	0.052	0.166	0.534	0.194	0.025	0.006	0.001
12	0.000	0.000	0.000	0.000	0.001	0.002	0.002	0.002	0.011	0.040	0.189	0.554	0.178	0.019	0.003
13	0.001	0.001	0.000	0.000	0.000	0.001	0.001	0.001	0.002	0.005	0.021	0.163	0.607	0.190	0.007
14	0.000	0.001	0.000	0.000	0.000	0.000	0.001	0.001	0.000	0.006	0.009	0.032	0.183	0.666	0.101
15	0.000	0.000	0.000	0.000	0.000	0.000	0.001	0.000	0.000	0.000	0.001	0.001	0.007	0.107	0.883

[2]For example, Menkhoff et al. (2014) report asset pricing test results for both returns before and after adjusted for transaction cost, returns and asset pricing test results are not much different after taking transaction cost into account. Asness et al. (2013) deliberately choose returns before transaction cost because they believe gross returns are most suitable to illuminate the relation between their returns and risks.

FIGURE 1.9: Transition Matrix of Non-segmented Carry Portfolio

The number in *ith* column and *jth* row of the transition matrix represents the probability that an asset in *ith* portfolio this month is allocated to *jth* portfolio next month if I sort assets by standardised carry measure.

P	1	2	3	4	5	6	7	8	9	10	11	12	13	14	15
1	0.825	0.134	0.018	0.008	0.001	0.002	0.000	0.002	0.003	0.002	0.001	0.001	0.000	0.000	0.003
2	0.138	0.627	0.166	0.030	0.012	0.008	0.004	0.006	0.004	0.001	0.002	0.000	0.002	0.000	0.000
3	0.016	0.168	0.532	0.190	0.037	0.017	0.016	0.010	0.004	0.003	0.001	0.003	0.001	0.000	0.000
4	0.010	0.030	0.180	0.476	0.199	0.052	0.022	0.010	0.008	0.007	0.003	0.002	0.000	0.001	0.001
5	0.002	0.012	0.046	0.197	0.472	0.190	0.046	0.016	0.006	0.003	0.004	0.001	0.002	0.002	0.000
6	0.001	0.006	0.023	0.044	0.200	0.451	0.192	0.053	0.010	0.006	0.006	0.004	0.001	0.002	0.000
7	0.002	0.007	0.013	0.025	0.045	0.197	0.442	0.194	0.047	0.016	0.006	0.003	0.003	0.001	0.000
8	0.003	0.006	0.011	0.013	0.015	0.050	0.207	0.432	0.185	0.051	0.013	0.005	0.003	0.004	0.001
9	0.001	0.004	0.006	0.004	0.010	0.015	0.047	0.209	0.461	0.191	0.038	0.008	0.004	0.003	0.001
10	0.001	0.003	0.005	0.004	0.006	0.010	0.014	0.049	0.208	0.462	0.177	0.037	0.016	0.005	0.003
11	0.001	0.002	0.002	0.004	0.003	0.005	0.007	0.013	0.040	0.203	0.479	0.188	0.038	0.008	0.008
12	0.001	0.001	0.002	0.001	0.002	0.002	0.005	0.006	0.009	0.034	0.204	0.540	0.165	0.024	0.004
13	0.000	0.000	0.001	0.002	0.001	0.002	0.001	0.002	0.006	0.020	0.038	0.175	0.577	0.162	0.015
14	0.000	0.001	0.000	0.001	0.002	0.001	0.002	0.002	0.003	0.004	0.009	0.024	0.167	0.664	0.120
15	0.003	0.000	0.001	0.001	0.000	0.002	0.000	0.001	0.001	0.002	0.006	0.007	0.015	0.119	0.843

FIGURE 1.10: Transition Matrix of Non-segmented Momentum Portfolio

The number in *ith* column and *jth* row of the transition matrix represents the probability that an asset in *ith* portfolio this month is allocated to *jth* portfolio next month if I sort assets by standardised momentum measure.

P	1	2	3	4	5	6	7	8	9	10	11	12	13	14	15
1	0.609	0.179	0.048	0.034	0.020	0.017	0.013	0.008	0.013	0.009	0.008	0.006	0.012	0.010	0.016
2	0.180	0.351	0.204	0.080	0.057	0.027	0.017	0.014	0.010	0.011	0.012	0.011	0.012	0.007	0.008
3	0.055	0.201	0.296	0.175	0.085	0.052	0.034	0.017	0.014	0.018	0.018	0.013	0.009	0.005	0.008
4	0.034	0.090	0.182	0.219	0.157	0.106	0.065	0.037	0.030	0.022	0.018	0.013	0.010	0.010	0.007
5	0.017	0.050	0.087	0.175	0.202	0.166	0.095	0.060	0.046	0.034	0.017	0.019	0.015	0.009	0.008
6	0.011	0.026	0.053	0.108	0.153	0.186	0.176	0.104	0.055	0.043	0.028	0.024	0.017	0.009	0.007
7	0.012	0.021	0.034	0.060	0.108	0.156	0.175	0.147	0.100	0.057	0.049	0.033	0.027	0.016	0.006
8	0.013	0.019	0.025	0.040	0.064	0.093	0.148	0.176	0.139	0.100	0.070	0.045	0.039	0.019	0.009
9	0.011	0.015	0.020	0.032	0.050	0.063	0.103	0.144	0.177	0.150	0.100	0.063	0.041	0.022	0.009
10	0.011	0.011	0.012	0.019	0.034	0.048	0.064	0.102	0.150	0.174	0.152	0.104	0.078	0.032	0.009
11	0.013	0.014	0.009	0.022	0.024	0.034	0.041	0.076	0.104	0.151	0.182	0.157	0.094	0.059	0.019
12	0.013	0.009	0.014	0.016	0.027	0.028	0.038	0.044	0.066	0.116	0.143	0.190	0.172	0.093	0.031
13	0.007	0.010	0.011	0.017	0.019	0.013	0.025	0.031	0.044	0.053	0.121	0.180	0.215	0.185	0.070
14	0.013	0.007	0.010	0.013	0.012	0.014	0.016	0.026	0.023	0.027	0.047	0.101	0.186	0.335	0.171
15	0.011	0.006	0.005	0.009	0.006	0.012	0.009	0.009	0.009	0.013	0.021	0.032	0.058	0.181	0.618

The HML returns of these standardised portfolios sorted by value, carry, and momentum are similar to those of the combined portfolios composed of one third of each asset class. Overall, these summarised statistics for the portfolios created from my aggregated cross-section – especially those of carry and momentum – indicate that an international investor can earn good rewards from investing across asset classes, regardless of whether they sort the assets into non-segmented portfolios by the signals from the beginning or diversify across asset classes after adopting the strategies within each asset class first. The results do not indicate that value, carry, and momentum returns in different asset classes are caused by the same factors. Therefore, I proceed to conduct asset pricing tests to identify the factors driving the variation in mean returns of my across-asset-class portfolios.

In the next stage, I focus on the three risk factors described in Section 1.4.3: a global 'market' factor equal to the equally weighted average of all asset returns in the aggregated cross section, a market volatility factor and a market liquidity factor.

Table 1.11 reports the two step OLS-FMB test results for the models containing global market risk and volatility risk factors. In the first-stage time series regressions, we see that all value portfolios load with roughly unit weight on the market, in line with the findings of Lustig et al. (2013). This confirms that the return of the equally-weighted market portfolio should always be included in the asset pricing test as a level factor. However, value and momentum returns do not significantly load on volatility risk, implying that the returns do not vary with the volatility factor over time. By contrast, most carry portfolios are exposed to the time variation of market volatility, as most carry returns load significantly on volatility in the first-step regression.

In the second-stage cross-sectional regressions, the risk premium of momentum portfolios on the volatility factor is negative and significant. Thus, portfolios with low exposure to volatility earn high mean returns. Ex ante, one might have expected the converse – in other words, that a portfolio with high volatility beta, which tends to pay off well when volatility is low, is not attractive to investors and thus has a high expected return. The p-value associated with J statistics is not 0, so we cannot reject the null hypothesis that the pricing error is 0. The adjusted R^2 is very small, suggesting that risk factors can only explain less than 20% of the cross-sectional difference in momentum returns. Meanwhile, most first-step loadings are not statistically significant, so the model with volatility risk cannot effectively rationalise my momentum returns. In addition, since returns of momentum portfolios can be partially explained by volatility risk, my sorting strategy purposely expose my portfolios more to this risk factor than those in Asness et al. (2013). Therefore, my strategy should generate a bigger return than the strategy in Asness et al. (2013) when market is less volatile and a smaller return when market is more volatile.

The second-stage results for value are much less impressive. The market factor appears to be significant and has the correct sign, but volatility plays a relatively insignificant role in explaining the cross section of mean returns. The volatility coefficient for value portfolios in the second-stage regression is slightly positive, indicating that high value portfolios – which pay well when volatility is high – should be more attractive to investors, but they have a higher expected return. This can be explained by the negative correlation between value and the more popular momentum trading strategy, as suggested by Asness et al. (2013).

Although most carry returns are exposed to volatility risks in the first-step regression, the exposure seems not to contribute to the cross-sectional difference in carry returns. Although volatility slightly explains the premium of non-segmented carry portfolio composed of currencies and bonds, it can not explain the carry premium when equities are added. The p-value associated with J statistics is 0, meaning that we can reject the null hypothesis that the pricing error is 0. We see from the table that assets with larger carry and larger expected returns are not significantly negatively correlated with the market volatility factor. These results confirm those of Cenedese et al. (2014), suggesting that only global equity factors can price international equity portfolios sorted by equity carry. Therefore, my return cross-section incorporating currencies, bonds, and equities cannot be justified by a common set of risk factors: thus, investors can take advantage of this by investing in carry portfolios across asset classes, without suffering a market-wide volatility risk.

I also attempt to explain the returns by the liquidity risk factor described by Pástor and Stambaugh (2003).[3] Table 1.12 indicates how exposure to market risk and liquidity risk influence mean returns on value and momentum portfolios. The results are very similar to those presented in Table 1.11. The first-stage results here are uniformly unimpressive for liquidity risk. The liquidity risk factor has little impact

[3]This factor has the drawback of relying on liquidity of individual US equities and thus we are relying on commonality in liquidity across asset classes and countries in its application here.

TABLE 1.11: Two Factor OLS-FMB of 15 Non-segmented Portfolios - Volatility Risk

Panel A reports OLS-FMB test results of non-segmented value/carry/momentum portfolios. 'Globe' is market mean return of all assets. 'Vol' is volatility factor constructed by daily data of currency and equity. Panel B reports estimated parameters in the 1st step regression model. * denotes a 10% significance and ** denotes a 5% significance.

Panel A: Test Results - Globe and Vol

	Value	Carry	MOM
Globe	0.0048	0.0063	0.0065
t-stats	9.0126	7.0625	10.6022
Vol	0.0494	-0.0287	-0.1033
t-stats	1.5838	-0.8599	-2.7777
r-squared	0.4278	0.0757	0.1761
adjr	0.3324	-0.0784	0.0387
J-stats	12.5468	46.8761	17.9598
p-value	0.4834	0	0.1591

Panel B: 1st step regression result

		Value		Carry		MOM
P	Globe	Vol	Globe	Vol	Globe	Vol
P1	0.9015**	0.0109	1.4143**	0.0294**	1.0138**	0.0089
P2	0.8709**	0.0043	1.0128**	0.0209**	1.1455**	0.0194
P3	0.9144**	-0.0068	0.7920**	0.0168**	1.0773**	0.0185*
P4	0.8323**	-0.0011	0.0773**	0.0138*	1.0901**	0.0158
P5	0.8450**	0.0149	0.8018**	0.0185**	1.1426**	0.0160
P6	0.8895**	0.0121	0.9209**	0.0331**	1.0589**	-0.0102
P7	0.8191**	-0.0148	0.9220**	-0.0273**	0.9826**	-0.0259**
P8	0.8624**	0.0116	0.9567**	0.0085	0.9970**	-0.0056
P9	0.9665**	0.0471**	0.9963**	-0.0280**	1.1070**	0.0285**
P10	0.8766**	- 0.0022	1.0615**	-0.0039	0.9100**	-0.0013
P11	0.8489**	-0.0059	1.1038**	-0.0301	0.9717**	-0.0195**
P12	0.9333**	0.0043	1.1189**	-0.0312**	0.9377**	0.0121
P13	1.0313**	0.0209**	1.1436**	-0.0626**	0.8595**	-0.0285**
P14	1.1671**	0.0245*	1.1320*	-0.0175	0.8252**	-0.0139
P15	1.1001**	-0.0082	0.9479	0.0100	0.7842**	-0.0147

on cross-sectional differences in the value or carry returns. In the second-stage regressions, liquidity risk plays a minor role: there is weak evidence that it helps to explain the cross-section of mean momentum portfolio returns. This result is similar to – albeit much weaker than – the asset pricing results for within-asset-class momentum reported by Asness et al. (2013), Pástor and Stambaugh (2003), and Sadka (2006).

Table 1.13 reports the results of the global asset pricing test, including market risk, volatility risk and liquidity risk factors. The results are broadly consistent with the two-factor asset pricing test results in Tables 1.11 and 1.12, and the first-step regression results demonstrate that no portfolios are exposed to time variations of market volatility or liquidity. The R^2 for each strategy remains very small. For value and momentum portfolios, we cannot reject the null hypothesis that the pricing error is 0, while we can reject the null hypothesis for carry portfolios. In summary, an asset pricing model with market-wide systematic risk factors across asset classes cannot rationalise my value, carry, or momentum returns.

Figures 1.11, 1.12, and 1.13 display the mean returns of the value, carry, and momentum portfolios alongside the pricing errors from the three-factor model. The portfolio returns clearly demonstrate a cross-sectional difference; however, even after accounting for the three risk factors, the pricing errors of value and momentum portfolios demonstrate an upward pattern while pricing errors of some carry portfolios are large. The results of the previous asset pricing tests, namely that the set of systematic risk factors cannot explain my return cross-section. However, my test results suggest that investors could take advantage of the diversification benefits across asset classes, as value, carry, and momentum portfolios in each asset class are only exposed to risk factors idiosyncratic to their own asset classes. This also explains why my returns are not better than an equally-weighted combined portfolio composed of value, carry, and momentum portfolios from each asset class, as both methods improve returns through diversification. Sorting assets by those signals, regardless of their asset classes, does not expose the portfolios to any across-asset-class

TABLE 1.12: Two Factor OLS-FMB of 15 Non-segmented Portfolios - Liquidity Risk

Panel A reports OLS-FMB test results non-segmented value/carry/momentum portfolios. 'Globe' is market mean return of all assets. 'Liquidity' factor is Pastor and Stambaugh's innovation in aggregate liquidity. Panel B reports estimated parameters in the 1st step regression model. * denotes a 10% significance and ** denotes a 5% significance.

Panel A: Test Results - Globe and Liquidity

	Value	Carry	MOM
Globe	0.0053	0.0063	0.0064
t-stats	10.0556	7.0619	10.1280
Liquidity	-0.0229	-0.0029	0.0336
t-stats	-1.1399	-0.1213	2.2438
r-squared	0.3180	0.0666	0.1125
adjr	0.2043	-0.0890	-0.0354
J-stats	15.3628	48.7032	18.4444
p-value	0.2853	0	0.1414

Panel B: 1st step regression result

		Value		Carry		MOM
P	Globe	Liquidity	Globe	Liquidity	Globe	Liquidity
P1	0.8789 **	-0.0160	1.0574 **	0.0534 **	1.0013 **	-0.0240
P2	0.8662 **	-0.0176	1.0838 **	-0.0172	1.1207 **	-0.0587 **
P3	0.9157 **	0.0444 **	1.0759 **	-0.0576 **	1.0483 **	-0.0421
P4	0.8323 **	0.0080	1.1104 **	0.0013	1.0539 **	-0.0064
P5	0.8091 **	-0.0087	0.9988 **	-0.0374 **	1.1047 **	-0.0036
P6	0.8718 **	-0.0375 *	1.0543 **	0.0101	1.0665 **	0.0450 *
P7	0.8596 **	-0.0039	0.9722 **	-0.0249	1.0496 **	-0.0091
P8	0.8308 **	0.0026	0.9520 **	-0.0459 **	1.0099 **	0.0021
P9	0.8747 **	-0.0484 **	1.0130 **	-0.0341 *	1.0469 **	-0.0248
P10	0.8766 **	0.0154	0.9540 **	-0.0350 *	0.9186 **	-0.0143
P11	0.8594 **	0.0133	0.9121 **	0.0183	1.0121 **	0.0193
P12	0.9328 **	-0.0288	0.8874 **	0.0295	0.9063 **	0.0045
P13	0.9737 **	0.0071	0.8265 **	-0.0136	0.9107 **	0.0480 **
P14	1.0950 **	0.0199	0.9499 **	0.0709 **	0.8451 **	0.0365
P15	1.1145 **	0.0191	1.0166 **	0.0838 **	0.7446 **	0.0089

TABLE 1.13: Three Factor OLS-FMB of 15 Non-segmented Standardised Portfolios

Panel A reports OLS-FMB test results. Vol is volatility factor constructed by daily data of currency and equity. Panel B reports estimated parameters in the 1st step regression model. * denotes a 10% significance and ** denotes a 5% significance.

Panel A: Test Result

	Value	Carry	MOM
Globe	0.0049	0.0063	0.0065
t-stats	8.5077	6.9620	10.2983
Vol	0.0473	0.0346	-0.0886
t-stats	1.4281	-0.9890	-1.9968
Liquidity	-0.0124	-0.0169	0.0262
t-stats	-0.6082	-0.5648	1.6238
r-squared	0.4326	0.1184	0.2061
adjr	0.2778	-0.1221	-0.0140
J-stats	11.5335	45.2779	17.6129
p-value	0.4838	0	0.1280

Panel B: 1st step regression result

		Value			Carry			MOM	
P	Globe	Vol	Liquidity	Globe	Vol	Liquidity	Globe	Vol	Liquidity
P1	0.9018**	0.0095	-0.0103	1.0288**	-0.0203*	0.0097	1.0135**	0.0057	-0.0196**
P2	0.8714**	0.0022	-0.0163	1.0858**	0.0031	-0.0063	1.1449**	0.0113	-0.0498
P3	0.9131**	-0.0011	0.0437**	0.9527**	-0.0142	0.0323	1.0770**	0.0134	-0.0317**
P4	0.8321**	-0.0001	0.0080	0.9457**	0.0002	-0.0085	1.0902**	0.0169	0.0068
P5	0.8450**	0.0149	0.0003	1.0438**	-0.0031	-0.0190	1.1427**	0.0177	0.0103
P6	0.8905**	0.0078	-0.0328	0.9384**	0.0135	0.0085	1.0594**	-0.0033	0.0425*
P7	0.8195**	-0.0166*	-0.0139	1.0001**	-0.0009	-0.0511**	0.9822**	-0.0314**	-0.0337
P8	0.8621**	0.0130	0.0105	0.9712**	-0.0081	0.0515**	0.9970**	-0.0060	-0.0026*
P9	0.9672**	0.0384**	-0.0252	1.0586**	0.0196*	0.0112	1.1070**	0.0280**	-0.0029**
P10	0.8762**	-0.0002	0.0152	1.0452**	-0.0139	-0.0056	0.9097**	-0.0041	-0.0176**
P11	0.8486**	-0.0045	0.0106	1.0165**	-0.0001	-0.0038	0.9718**	-0.0188*	0.0046
P12	0.9342**	0.0006	-0.0285	1.1315**	0.0141	0.0352	0.9379**	0.0147	0.0160**
P13	1.0306**	0.0237**	0.0214	0.9823**	0.0221*	-0.0059	0.8599**	-0.0237**	0.0295
P14	1.1659**	0.0295**	0.0377	1.0683**	0.0452**	-0.0022	0.8256 **	-0.0091	0.0294**
P15	1.0996**	-0.0062	0.0154	0.9141**	-0.0118	-0.0426	0.7844**	0.0185	0.0234

systematic risk factors and thus does not generate greater returns than combined portfolios after sorting within each asset class.

FIGURE 1.11: Value Pricing Errors

I plot mean returns of 15 non-segmented value portfolios and their pricing errors after conducting three-factor (market mean return, market volatility and liquidity risk) OLS-FMB asset pricing test.

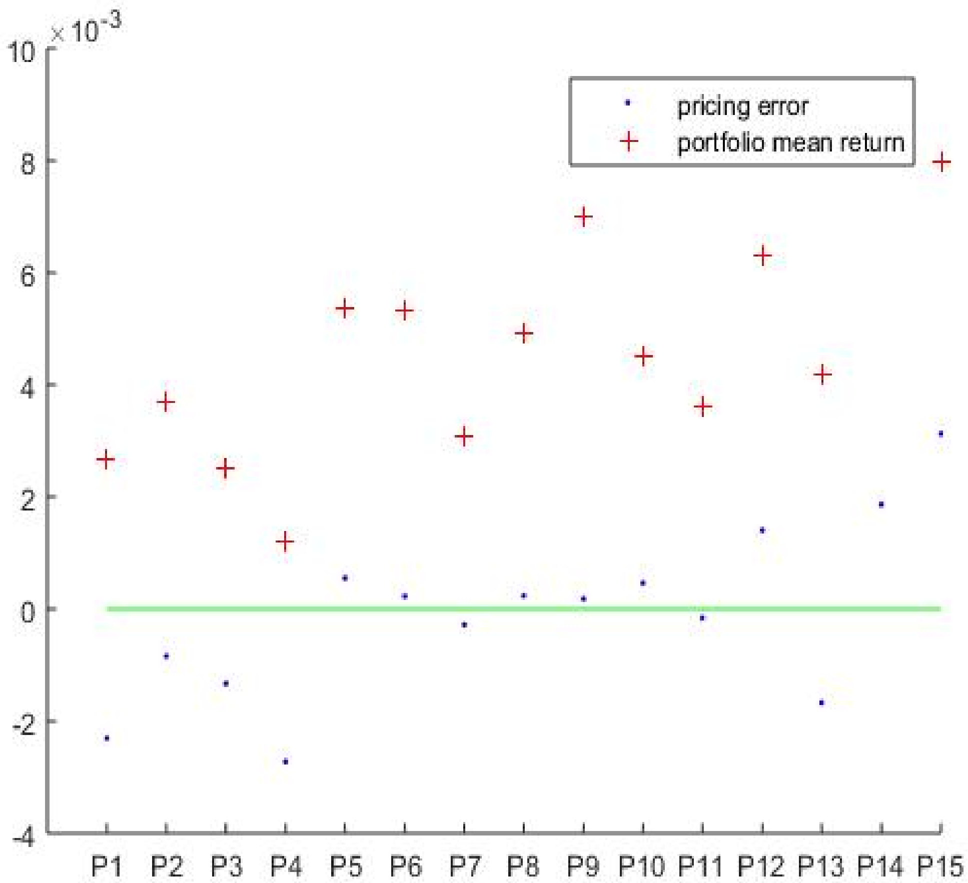

FIGURE 1.12: Carry Pricing Errors

I plot mean returns of 15 non-segmented carry portfolios and their pricing errors after conducting three-factor (market mean return, market volatility and liquidity risk) OLS-FMB asset pricing test.

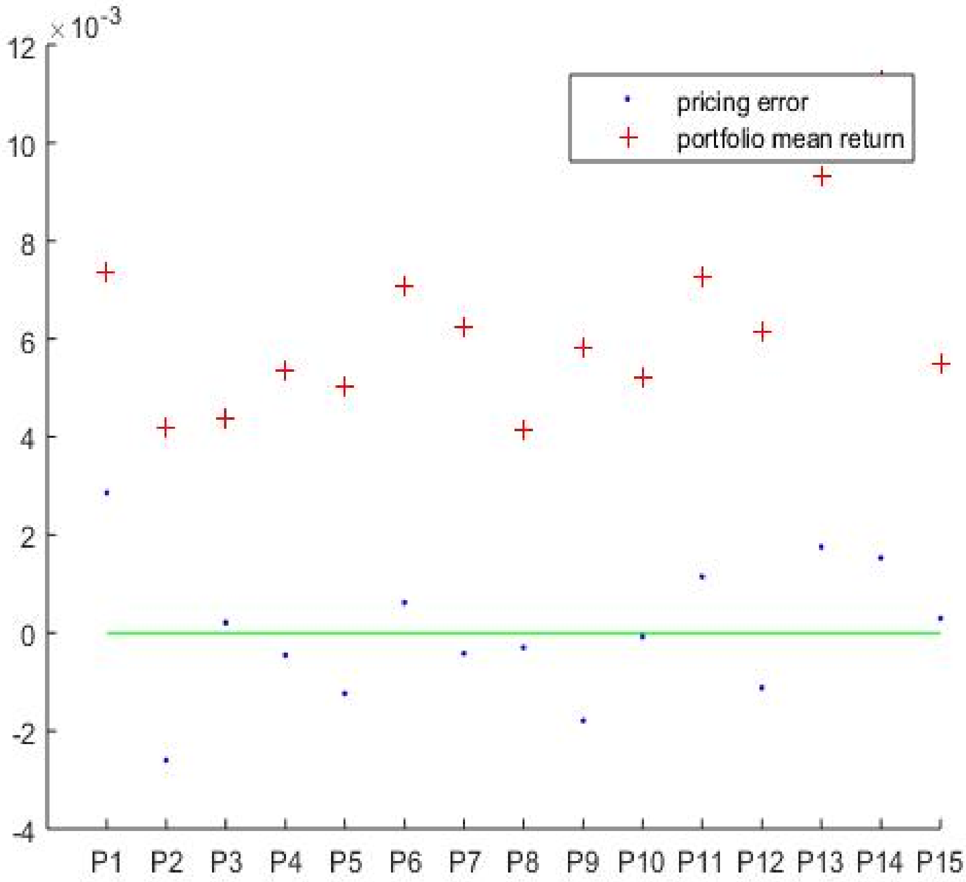

FIGURE 1.13: Momentum Pricing Error

I plot mean returns of 15 non-segmented momentum portfolios and their pricing errors after conducting three-factor (market mean return, market volatility and liquidity risks) OLS-FMB asset pricing test.

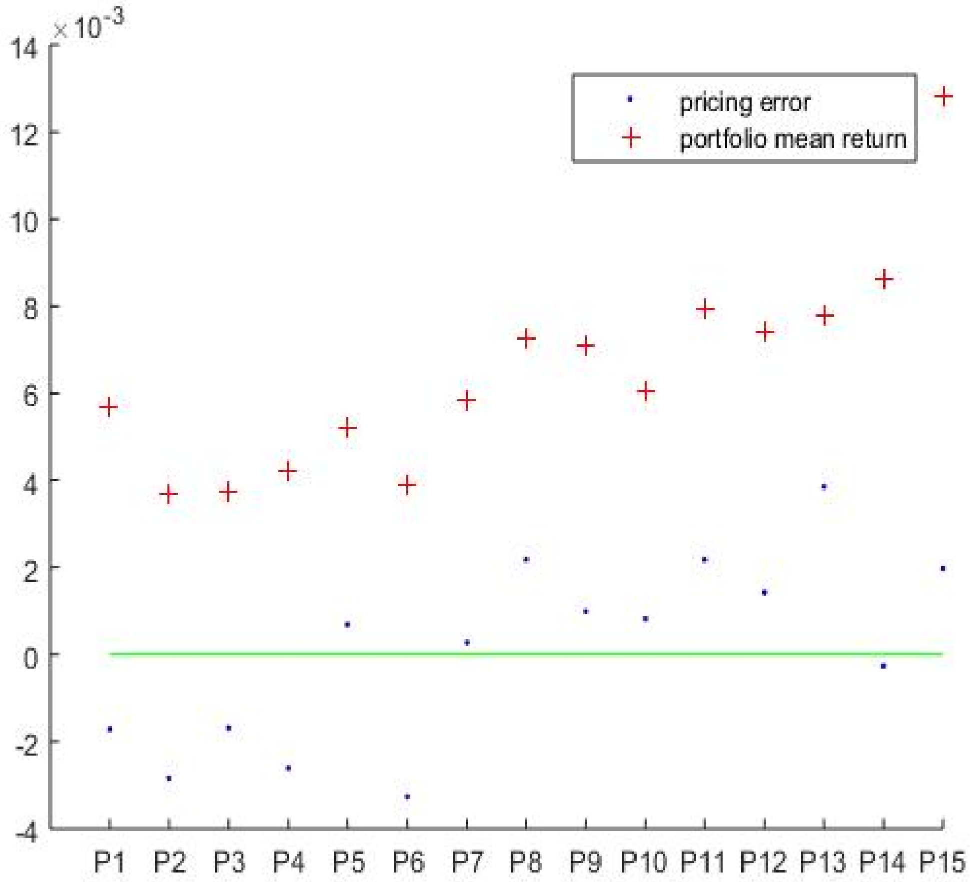

Above all, the volatility or liquidity factor effectively explains the returns within each asset class, but it fails across asset classes. The results imply that the currency, international bond, and equity markets are not fully integrated and thus reward the same risks with different prices. However, my test nevertheless suffers from the bad model problem, which is likely due to the fact that my risk factors cannot reflect the time variations of market-wide volatility or liquidity across asset classes. For example, the market portfolio I use is an equally-weighted portfolio, composed of all assets across asset classes. However, in reality, the trading volumes are quite different. In addition, my volatility factor is an equally-weighted realised volatility, constructed on the basis of currency and equity data. My liquidity factor is the Pastor-Stambaugh liquidity series, which covers only US data.

1.6 Conclusion

I apply value, carry, and momentum sorting rules to an aggregated cross-section containing global equity indices, bonds, and currencies. I treat assets from different classes as belonging to a unified cross-section, which differentiates my work from previous investigations into single asset classes, such as those of Asness et al. (2013), Lustig et al. (2013), Cenedese et al. (2014), Koijen et al. (2013), and Menkhoff et al. (2012).

I demonstrate that value/momentum strategies with standardised value/momentum predictors can generate significant mean returns for international investors who are willing to spread their wealth across asset classes. Carry is a particularly attractive strategy, generating HML returns of nearly 10% per annum, with a Sharpe ratio of more than 1. Momentum yields a mean HML return of around 7%, with a Sharpe ratio of roughly 0.6.

Asset pricing tests suggest that returns of cross-asset currency and bond portfolios sorted by carry signals can be partly explained by their exposure to a global volatility factor; however, when equity is added, the volatility risk factor does not work at all. In addition, market-wide volatility and liquidity risk factors across asset classes cannot explain the across-asset-class value, carry, or momentum returns. The results suggest that these returns in each asset class are exposed to risk factors idiosyncratic to their own asset classes; thus, investors can diversify across asset classes when adopting these strategies to improve their risk-adjusted returns. In addition, the three different asset classes are not fully integrated because within-asset-class asset pricing models do a better job than across-asset-class models of explaining value, carry, and momentum patterns in returns.

Chapter 2

Evaporating liquidity: information asymmetry or inventory control

2.1 Introduction

The liquidity of many asset classes declined drastically during the financial crisis between 2007 and 2009. Previous studies have provided two explanations for this. Nagel (2012) studies the US equity market and concludes that liquidity provision withdrawal due to liquidity providers' inventory control was the main driver of liquidity evaporation. The results confirm what Brunnermeier and Pedersen (2009) predict by their theory that contributes sudden liquidity dry-up to mutually reinforcing market liquidity and funding liquidity, and that speculators' capital is the driver of market liquidity and risk premium and volatility is a state variable affecting market liquidity. However, Gorton and Metrick (2012) argue that increased information asymmetry led to the liquidity evaporation in the securitised debt market because the external shock from subprime mortgages switched the information-insensitive assets to information-sensitive assets. The resulting adverse selection stopped people from trading and thus caused the market breakdown.

On one hand, information asymmetry may adversely affect liquidity providers' willingness to supply liquidity. The theoretical background is provided by Kyle (1985a) and Glosten and Milgrom (1985) whose models point out that market makers may suffer a loss providing liquidity to informed investors. Previous literature has proposed different models to explain how adverse selection triggers crisis. For example, Bolton et al. (2011) suggest that firms can choose either to sell early or late if adverse selection discount is too big, leaving only 'lemons' in the market. Morris and Shin (2012) propose that a small amount of adverse selection problem can lead to failure of 'market confidence' and thus market collapse. Similar to Gorton and Metrick (2012), Dang et al. (2009) believe that a shock that trigger private information production can be made worse due to adverse selection and may reduce trade to zero. Therefore, when the negative economic shock is large enough, investors are more worried that the assets in the market are 'lemons', and thus fear of adverse selection escalates. The liquidity providers who do not profit from producing private information are worried about being taken advantage of, and the fear of adverse selection will reduce their liquidity provision. On the other hand, liquidity providers' constrained inventory-absorption capacity due to tighter funding, elevated risk or less competition can also lead to liquidity dry-up. According to Nagel (2012), the expected return of liquidity provision will increase during the crisis, different from liquidity dry-up due to adverse selection problem. This paper examines whether the evaporating liquidity in the UK equity market during the global financial crisis was caused by an amplified adverse selection problem or by liquidity providers' constrained inventory absorption capacity and the increased inventory control cost. As claimed in O'Hara (2003), price discovery and liquidity are two functions of market for asset pricing. Separating the two processes help to identify which function of financial market went wrong during the crisis. Many debates arose regarding how to regulate the financial institutions and at the same time, maintain their functions such as liquidity provision after the crisis. Identifying whether information asymmetry or inventory control cause liquidity dry-up provides insights to regulators and policymakers how to maintain liquidity during market downturn.

Nagel (2012) has used the returns from reversal strategies as a proxy for the returns of liquidity provision, as liquidity providers buy when the public sells, which coincides with falling prices, and then sell when the public buys, which coincides with rising prices. However, there are many different versions of reversal strategies, and it is extremely difficult to determine which version is the best proxy. Previous research has considered how inventory control influences liquidity through market makers' inventory data. However, as described by Grossman and Miller (1988) and Campbell et al. (1993), liquidity providers are not just specialists or dealers but anyone who accommodates liquidity needs in exchange for higher expected returns. Hendershott et al. (2011) claim that algorithmic traders and quantitative investors perform the role of providing liquidity without being officially designated as market makers. Due to the difficulty accessing the inventory data of all liquidity providers and determining the specification of reversal strategies, I take a different approach.

Inspired by Hendershott and Menkveld (2014), I decompose stock prices into unobserved fundamental values and pricing errors. Theoretically, on the one hand, prices move towards assets' fundamental values in response to information contained in customers' order flows; and these changes due to private information are permanent, which makes the fundamental value process a random walk. On the other hand, the pricing error, the deviation of price from fundamental value, is transitory, so the pricing error is a stationary process. Therefore, I use state space form (SSF) approach to isolate the two unobserved time series and obtain estimates of unknown parameters in the model through Kalman Filter. In addition, the reaction of fundamental values and pricing errors to customers' order flows could reflect how information asymmetry and inventory control varied during the crisis. Information asymmetry influences liquidity because investors who require immediate liquidity may have better access to information concerning a particular security than liquidity suppliers. Therefore, liquidity providers ask for a higher (lower) price when they sell (buy) an asset to compensate for the adverse selection problem arising from a bad market shock, leading fundamental value changes to be more sensitive to customers' orders in the crisis. Meanwhile, the pricing error emerges as liquidity providers increase (decrease) their price quotes after net buy (sell) flow to induce customers' sell (buy) orders so that liquidity providers could move inventory back to their desired level. If liquidity providers tighten liquidity provision, pricing errors induced by each customers' order increase.

I find that pricing errors became more sensitive to customers' order flows from

June to December 2008, indicating that liquidity providers charged a larger premium for providing liquidity as the financial crisis developed. Meanwhile, the fundamental values of most stocks, especially big-cap stocks, did not become more sensitive to customers' order flows during the crisis, meaning that adverse selection problem was not severely amplified for most stocks in the UK market. The Brunnermeier and Pedersen (2009) model suggests that an exogenous negative shock might trigger the market to a low-liquidity/ high margin status in which constraint funding, market illiquidity, and increasing volatility reinforce one another. Thus, the model implies that liquidity can dry up suddenly, and this sudden dry-up is related to volatility. My results suggest that pricing errors' sensitivity to customers' order flows increases together with the VIX, supplying evidence that liquidity providers' tighter inventory control in a much more volatile market led to the liquidity dry-up during the crisis. It might be good news to regulators and policymakers that the liquidity dry-up is caused by inventory control rather than adverse selection. Therefore, as long as the liquidity provision sector has enough funding and more risk bearing capacity, liquidity will not evaporate. To liquidity providers, my results can assure them that they would not suffer a bigger loss due to adverse selection. In contrast, consistent with the results in Nagel (2012), liquidity providers should make a bigger return during market downturn when liquidity becomes a scare resource.

The remainder of this chapter is organised as follows. Section 2.2 presents a review of previous literature that proposes theories and provides evidence for both information asymmetry and inventory control channels. Sections 2.3 and 2.4 describe the data and methodology used in this paper. Section 2.5 presents empirical results, and Section 2.6 concludes.

2.2 Literature review

Recent financial crises have shown that, at times, liquidity can decline or even disappear. Levine and Zervos (1998) emphasise the importance of liquidity and contend that more liquid financial markets can promote investment, productivity, and economic growth. Therefore, many microstructure researchers have studied the reasons for liquidity crises, presenting theoretical models and empirical evidence to explain liquidity fluctuations. These models typically involve two sources of market friction: information asymmetry and inventory control.

Liquidity is broadly defined as the ability to quickly trade large quantities of risky assets, at low costs, and without moving the price. However, the question of how liquidity should be measured remains. Bid-ask spread is usually employed, as market makers provide immediate liquidity to those asynchronously and stochastically arriving investors who are unwilling to bear the costs associated with constantly monitoring the market (Townsend (1978)). However, Grossman and Miller (1988) believe that the bid-ask spread cannot fully capture market liquidity because it only measures market makers' return when they 'cross' both sides of the trade simultaneously; therefore, they propose autocorrelation in rates of return as a liquidity measure. Campbell et al. (1993), in line with previous studies, state that price changes accompanied by large trading volumes tend to be reversed because risk-averse market makers have higher expected returns after accommodating non-informational traders' exogenous liquidity demand, which has inspired a set of papers that estimate liquidity through temporary price changes induced by volume (or order flow). For example, Pastor and Stambaugh (2001) estimate liquidity using the effect of a given volume on returns, finding liquidity to be a priced factor. In addition, to measure the time variation of liquidity provision, Nagel (2012) use returns from a reversal strategy to measure liquidity after proving that reversal strategy returns closely track the returns earned by liquidity providers.

On the one hand, a group of researchers have studied liquidity through information asymmetry. Information leads to permanent changes in price. Kyle (1985a) and Glosten and Milgrom (1985) have developed models suggesting that, since liquidity providers react to order flows due to information asymmetry, price fluctuates in response to order flow innovations, and the impact from information asymmetry is permanent. Evans and Lyons (2002a) also find that investors' order flow may contain private information and make permanent price changes using foreign exchange trading data. In addition, they show that uninformed liquidity providers are informationally disadvantaged when trading with informed agents; thus, liquidity providers should be compensated based on the probability that a coming order contains private information. Similarly, as mentioned by Weill (2007), market makers should be compensated for the adverse selection problem because they temporarily lean against the market to match the asynchronous stochastic arrivals of impatient buyers and sellers across time. Together, these studies argue that the reaction of liquidity providers to customers' orders is determined by the extent of information asymmetry in the market. In addition, some studies have confirmed that uninformed liquidity providers are compensated for adverse selection by bid-ask spreads. Hasbrouck (1991a) and Hasbrouck (1991b) define information impact as the persistent impact of trade innovations, concluding that large trades are associated with widening bid-ask spreads because a large trade is more likely to contain private information and, as a result, has a larger price impact. He also finds that trades are more informative for firms with small market capitalisation. Barclay and Hendershott (2004) observe that trading costs are much larger after trading hours than during the trading day, but dealers do not achieve greater profits, as the larger spread compensates for greater adverse selection problems after the normal trading hours.

On the other hand, previous studies have provided abundant evidence that temporary price changes are caused by liquidity providers' inventory management. Hendershott and Seasholes (2007) and Comerton-Forde et al. (2010) use specialists' inventory data from the New York Stock Exchange (NYSE) to show that specialists' inventory position can explain time variation in liquidity. Hansch et al. (1998) find evidence that inventory has a substantial impact on price formation and liquidity in dealership markets. Reiss and Werner (1998) also find that inventory positions determine dealers' trading behaviour, while Naik and Yadav (2003) conclude that individual dealers focus on the position risk of stocks held by themselves, rather than the position risk of the entire portfolio managed by the firm. These studies all present evidence that liquidity providers manage risk by keeping their inventories at a target level.

To separate information asymmetry and inventory control I use the SSF inspired by Hendershott and Menkveld (2014) and Brogaard et al. (2014) that adopt the SSF to separate the permanent price changes and transitory price changes. Hendershott and Menkveld (2014) first apply the model to daily US equity price and liquidity providers' inventory to study the price pressure that liquidity providers' inventory control exerts on price. The model is further developed in Brogaard et al. (2014) to divide the order flows into orders of HFTs and non-HFTs in SSF to study how orders of different types of investors influence fundamental value and pricing error. But in nature, the model is still based on the different ways that orders drive price due to information or inventory control.

Many researcher further studied the relationships between market declines, volatility, and liquidity as a result of liquidity providers' inventory control after liquidity dry-ups that occurred during the 1998 LTCM crisis and the 2008 global financial crisis. Some theoretical papers propose models to explain why liquidity decreases after market declines and becomes more volatile. Brunnermeier and Pedersen (2009) develop a theoretical model in which intermediary capital positions influence liquidity provision, and they suggest that volatility and liquidity simultaneously influence one another at the same time during crises, leading to liquidity dry-up. Anshuman and Viswanathan (2005) focus on the relationship between liquidity and market returns, and present a slightly different model, in which market makers are less able to finance in the repo market when leveraged investors' defaults lead to asset liquidation. Garleanu and Pedersen (2007b) show that tighter risk management by institutions in volatile markets reduces their risk bearing capacity and thus lowers market liquidity, suggesting that volatility is the underlying state variable that drives liquidity reductions. Kyle and Xiong (2001) and Xiong (2001) propose limit-to-arbitrage models, indicating that, in normal times, when shocks to noise trades move prices away from fundamental values, arbitrageurs provide liquidity and take advantage of the opportunities; however, in market downturns, when those liquidity providers have increased risk aversion or tighter capital constraints, they are less willing to hold risky assets. Chordia et al. (2005) find that innovations to liquidity and volatility in stock and bond markets are significantly correlated, indicating that common factors drive liquidity and volatility in these markets. Deuskar (2006) provides some initial support for a link between volatility misperception and liquidity, consistent with the theory that liquidity providers are less willing to hold risky assets when volatility is perceived to be high. However, the liquidity measure used in these papers captures both the persistent and temporary price impacts of trades; thus, it cannot distinguish between adverse selection and inventory control. In addition, Chung and Chuwonganant (2014) further demonstrate that how liquidity reacts to volatility change depends on market structure.

After the global financial crisis, liquidity evaporation has attracted more attention from researchers, investors and regulators than ever before because no one wants to see that a local financial toxicity drags the whole system into a mess due to liquidity dry-up again. Empirical studies have presented mixed evidence regarding how liquidity providers' unwillingness to provide liquidity lead to liquidity evaporation during financial crisis. On the one hand, Gorton and Metrick (2012) show that in securitised debt markets, information asymmetry was amplified during the financial crisis, increasing the information sensitivity of asset prices. On the other hand, Nagel (2012) finds that the time variation in liquidity provision can be predicted by the VIX index. This demonstrates that the evaporating liquidity in 2008 can be partly explained by liquidity providers' inventory control, but it is still unclear whether the VIX itself is the state variable that drives the time variation in liquidity or other state variables correlated with the VIX influence liquidity. Mitchell et al. (2007) note that convertible arbitrage hedge funds, which provide liquidity in normal times, were forced to liquidate their convertible bond positions due to binding capital constraints following large capital redemptions from investors in 2005 and the significant decline in security values during the LTCM crisis. Many regulatory changes followed to make the system more resistant to negative shocks. However, more debates arose regarding whether these regulations make the financial system more resistant or more fragile. Musto et al. (2018) suggest that policies to offset the liquidity feedback in less liquid securities could help mitigate a potential illiquidity spiral during a crisis. Regarding the Volcker Rule that limits liquidity provision of banks in the US bond market, Trebbi and Xiao (2019) believe that liquidity did not deteriorate after negative shocks because non-banker liquidity providers could fill the gap while Bao et al. (2018) holds a different opinion.

My research makes the contribution that I separate the effects of customers' order flows on pricing error and on fundamental value, enabling me to study separately how information asymmetry and inventory control lead to liquidity decline. In addition, my research does not rely on market makers' inventory data or returns of reversal strategies. Such convenience is given by the minute data of prices and order flows, which are more informative than the daily public stock prices mostly used in previous papers. As I have a straightforward measure of market liquidity, I can further study how market liquidity varies with underlying state variables such as volatility and funding. As not many studies have discussed the liquidity evaporation in the UK equity market, my research tries to test liquidity evaporation theories by UK equity data.

2.3 Data and summary statistics

2.3.1 Data

I use trading data for 100 common stocks[1] , FTSE100 constituents, from the London Stock Exchange (LSE) to construct mid-quotes (average of bid and ask prices) and market order flows every minute for all trading hours from June to December 2008.[2] Order flow data is from the electronic platform of LSE. Majority of trading activities of FTSE100 stocks are included in my dataset. Other trading platforms such as Chi-X, BATS, and Turquoise only account for less than 20% of all transactions of most FTSE100 constituents till 2008. Therefore, my dataset includes almost all orders that determine the prices of these equities in my research.

The daily closing price of FTSE100 during the global financial crisis is shown in Figure 2.1. The financial crisis of 2007-2008 started from plummet of mortgage related secrurities, and then gradually developed into an international banking crisis. It culminated with the bankruptcy of Leman Brothers In Sep 2008. Global equity markets all crashed during the crisis. Both the TED spread and LIBOR spiked to historical record highs in September 2008. Additionally, after Leman Brothers went to bankruptcy in mid September, all big banks were perceived to be risky and western governments started to inject capital to prevent them from collapsing. These six months' data provide a good window for us to look at how liquidity disappeared. To facilitate comparison across stocks, stocks are sorted into five quantiles based on market capitalisation. Quantile 1 refers to small market-cap companies and Quantile 5 corresponds to big market-cap companies. Although I call them small cap equities in this chapter, their market capitalisations are bigger than many equities in the UK market, but relatively small compared with the other constituents of FTSE100. I only apply the SSF to FTSE 100 constituents because those equities are traded frequently enough for me to estimate the parameters of my SSF.

[1]One stock is removed due to infrequent trading.

[2]Minutely prices and order flows are removed if returns (in b.p.) with absolute values are bigger than 500, or bid-ask spreads (in b.p.) are smaller than 0 or bigger than 500 within this minute.

FIGURE 2.1: Price Change of FTSE100 from 2007 to 2008

The chart shows price change of FTSE100 during the financial crisis.

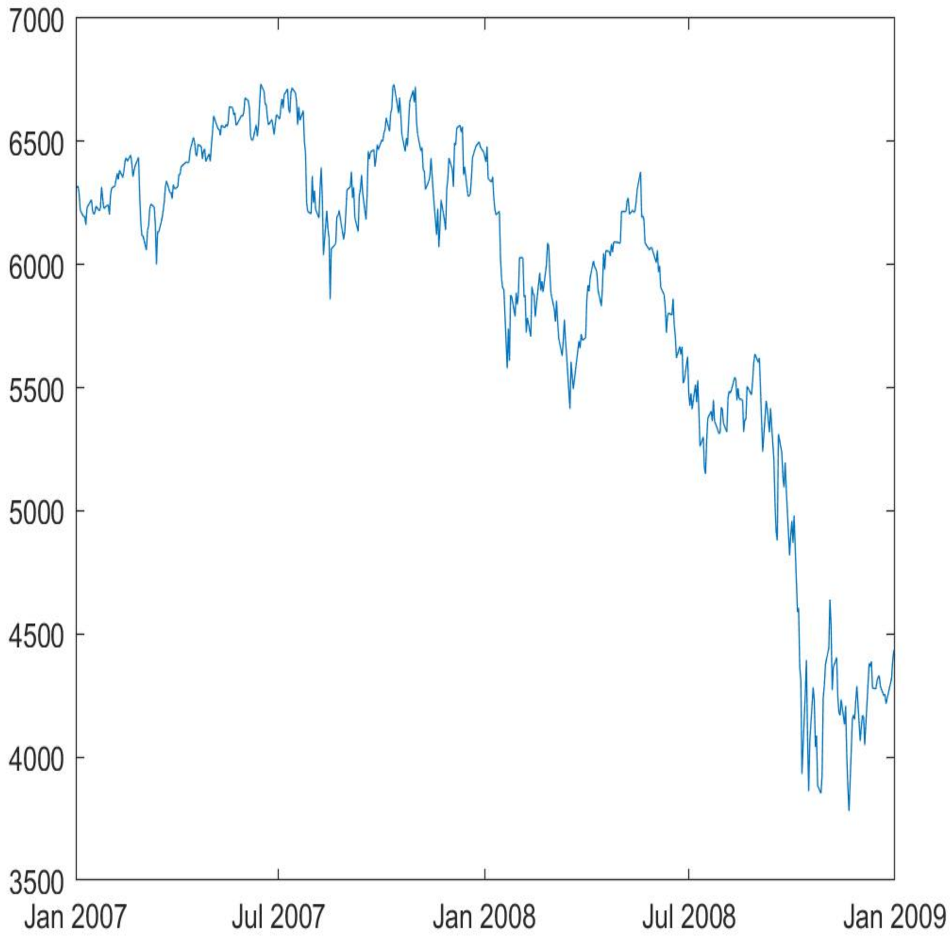

2.3.2 Summary statistics

Table 2.1 reports mean, standard deviation and first autocorrelation of both returns and order flows for all five quantiles. Mean returns are all negative, indicating a declining market. The first autocorrelation of return is negative, which confirms return reversal within an extremely short period. The first autocorrelation of order flow is positive because traders are working to minimize price impact by converting big trades to continuous small trades.

Figure 2.2 and Figure 2.3 display distribution of minute order flows and trading

TABLE 2.1: Summary Statistics

This table presents summary statistics of returns and order flows every minute from June to December 2008 of 99 stocks traded on LSE. Stocks are sorted into five quantiles based on market capitalisation where Q1 includes companies with the smallest market-caps. All six statistics reported in this table are calculated by minute return, order flow or volume of each stock first, and then averaged within each quantile. Returns are in b.p. while order flows are in 10,000 shares.

	return			order flow		
	mean	st. dev.	1st autoco.	mean	st.dev.	1st autoco.
All	-0.0434	22.9081	-0.0293	-0.0141	1.8217	0.0922
Q1	-0.0847	28.3903	-0.0158	-0.0127	1.7304	0.0885
Q2	-0.0784	28.1486	-0.0173	-0.0113	1.6403	0.0891
Q3	-0.0169	20.7071	-0.0273	-0.0152	1.5888	0.0947
Q4	-0.0319	19.6624	-0.0415	-0.0068	1.0304	0.0966
Q5	-0.0073	17.9065	-0.0440	-0.0246	3.1142	0.0916

volumes (in number of shares) for all companies and companies in each quantile. Distribution of order flows is nearly bell-shaped with most companies' order flows around zero. Even during the crisis, order flows of FTSE100 stocks seemed not very left skewed. Order flow and volume are much bigger for big-cap equities, suggesting that although all these FTSE100 constituents are frequently traded, Q5 equities are much more frequently traded with bigger volumes.

FIGURE 2.2: Distribution of Order Flow

The histograms in this figure show distribution of order flows for all companies and companies in each quantile. Stocks are sorted into five quantiles based on market capitalisation where Q1 includes companies with the smallest market-caps.

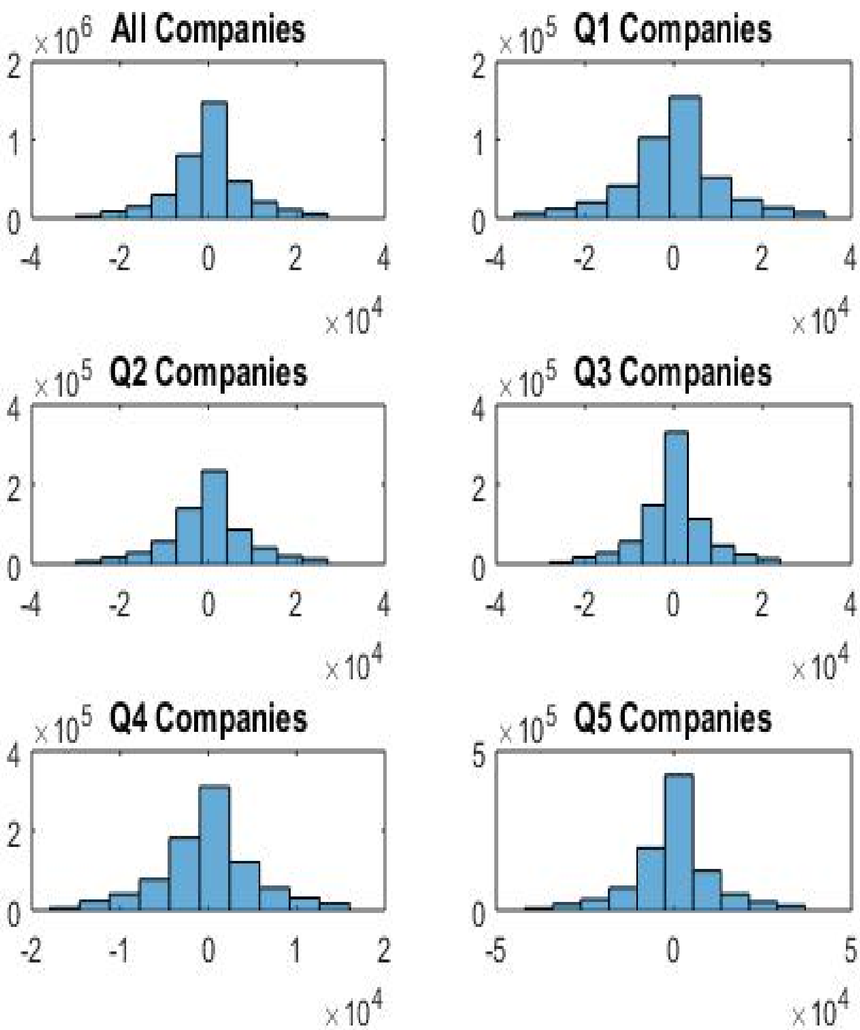

FIGURE 2.3: Distribution of Volume

The histograms in this figure show distribution of trading volume for all companies and companies in each quantile. Stocks are sorted into five quantiles based on market capitalisation where Q1 includes companies with the smallest market-caps.

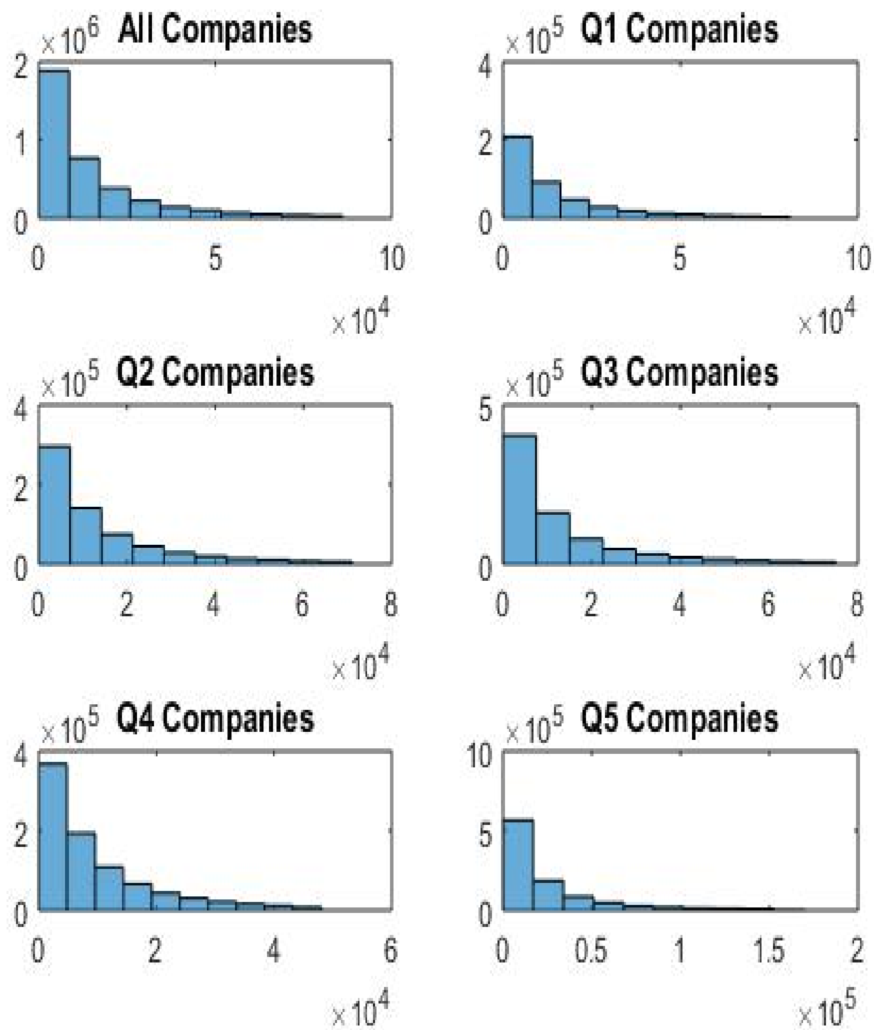

Figure 2.4 presents how bid-ask spreads change over time during the crisis. The average spreads for all stocks increased sharply in September 2008. The increase was significant for companies with small market caps and the spreads did not go back to their original level. Spreads for companies with big market caps reverted gradually to their original level after the spike in September, indicating that the financial crisis

had a much bigger and prolonged impact on liquidity of small market caps.

FIGURE 2.4: Bid-ask Spread

This figure presents bid-ask spreads (in b.p.) of 99 stocks traded on London Stock Exchange from June to December 2008. The bid-ask spread is averaged each day with minute data for each stock first. Then the spreads are averaged cross-sectionally for all stocks and stocks in five quantiles. Companies are sorted into five quantiles based on market capitalisation where Q1 refers to companies with the smallest market caps. The bid-ask spread is the bid-ask difference as percentage of mid-quotes.

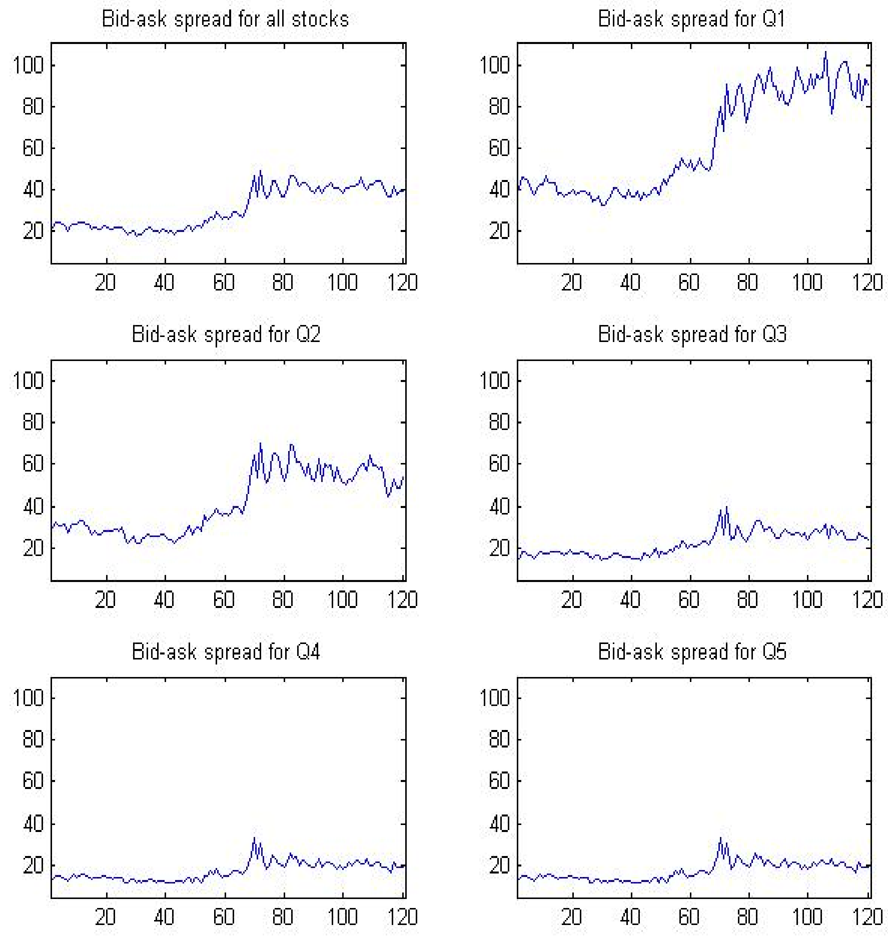

2.4 Methodology

Since price change is caused by both private information and liquidity providers' inventory control, my challenge is to isolate the two unobserved parts from the observed price. I use a state space form (SSF) approach, similar to that used by Hendershott and Menkveld (2014) which models the observed price as the sum of two unobserved time series: one random walk process that represents fundamental value and one stationary process that captures the pricing error. The SSF is shown below:

$$p_t = m_t + s_t \tag{2.1}$$

$$m_t = m_{t-1} + \beta \hat{X}_t + e_t \tag{2.2}$$

$$s_t = \alpha X_t + u_t \tag{2.3}$$

where p_t is the observed log price of stock; m_t is fundamental value and s_t is pricing error; e_t and u_t are uncorrelated i.i.d. process. X_t is investors' order flow. $\hat{X}_t$ is investors' order flow 'surprise'. $\hat{X}_t$ is estimated by the residual term of the equation below:

$$X_t = \gamma_1 X_{t-1} + \gamma_2 X_{t-2} + \gamma_3 X_{t-3} + ... + v_t \tag{2.4}$$

The number of lagged order flows in equation (2.4) is determined by the Schwarz information criterion.

I add up all previous minute log returns as minute log price p_t and all order flows of all trades within a minute as minute order flow X_t for each stock every minute. At the end of each day, a set of parameters in the SSF are estimated by Kalman Filter with minute data for each stock separately. Then parameters for each stock every day are averaged cross-sectionally, and standard errors are calculated with the cross-section. The daily parameters thus show the time variation of the impact of order flows on fundamental value and pricing error. The details of Kalman Filter and simulation results given by the method are shown in Appendix I.

Unobserved efficient price process. Fundamental value m_t in equation (2.2) is a random walk process. Fundamental value change is determined by contemporaneous private information. Since informed traders tend to split big trades into continuous small trades to decrease price impact, order flow is usually positively autocorrelated. Additionally, informed traders want immediate liquidity to take advantage of their private information. Only unexpected trading activity of informed traders should represent private information that has an impact on fundamental value of a security and the impact is permanent. Based on this assumption, order flow innovation $\hat{X}_t$ is the independent variable in equation (2.2). Liquidity providers are disadvantaged regarding information compared with investors who require immediate liquidity. Therefore, they adjust the fundamental value when new information arrives, and then quote a price based on the probability that the order is driven by private information. The parameter β thus reflects how fundamental value responds to private information. During the global financial crisis, β may increase due to market panic regarding the intrinsic value of risky assets, and thus the amplified adverse selection problem may cause the liquidity dry-up.

Unobserved pricing error process. Pricing error s_t, is primarily caused by liquidity providers' inventory control. Liquidity providers' inventory is determined by investors' order flows. When liquidity providers provide immediate liquidity to investors, they have to bear the risk associated with their inventory change. When liquidity providers have more (less) inventory of a security than their target level, they will decrease (increase) price to induce more buy (sell) orders to bring their inventory back to their original level. Therefore, we should expect that price deviates from fundamental value when liquidity providers' inventory deviates from their target level. Therefore, α measures how pricing error responds to liquidity providers' inventory change (as well as other microstructure frictions). If liquidity providers become more risk averse or have less risk-bearing capacity, we should expect that α increases. But once inventory goes back to the original level, the pricing error should disappear. Therefore, s_t is a stationary process.

The above SSF is similar to what is adopted in Hendershott and Menkveld (2014).

The difference is that their research is based on daily data and they use specialists' inventory as independent variable while I use minute order flows as independent variable. However, since they use daily data, the pricing error may disappear in one day. therefore, there is no autocorrelation term in equation (2.3) in their model. The pricing error on day t is only determined by how specialists' inventory deviates from their original level on that day. While my model is applied to minute data, the pricing error from the previous minute may not disappear immediately. As a result, I add an AR(1) term and adopt the following pricing error process to capture the dynamics of my minute data.

$$s_t = \phi s_{t-1} + \alpha X_t + u_t \tag{2.5}$$

The disadvantage of this specification is the greater difficulty in obtaining accurate estimates due to the extra parameter added. I report estimates of SSF given by equations (2.1), (2.2) and (2.5) in the following section and estimates of SSF given by equations (2.1), (2.2) and (2.3) in Appendix II as the latter is a less reasonable model.

2.5 Empirical results

Tables 2.2 and 2.4 report the means and standard errors of SSF estimates, as defined by equations (2.1), (2.2), and (2.5) for all companies and those companies from Q1 to Q5, each month. Daily parameters for each stock are first estimated from minute data, then averaged cross-sectionally. Monthly mean and standard errors (in brackets) are then calculated based on the daily parameters. Both parameters α and β have conjectured positive signs. α is positive and statistically significant, indicating that customers' buy (sell) orders cause a temporary positive (negative) pricing error. The temporary positive (negative) pricing error occurs as customers' buy (sell) orders decrease (increase) liquidity providers' inventory, and to bring the inventory back to the original level, liquidity providers must offer a higher (lower) price to induce more sell (buy) orders. According to Table 2.2, α rises from 5.40 in July to its apex of 10.47 in November; thus, in July, every 10,000 shares of net order inflow increased the pricing error by 0.054%, while, in November, every customer buy order increased the pricing error by 0.1047%. Hendershott and Menkveld (2014) find that a US$100,000 inventory shock causes price pressure of 0.02% for the large-cap stocks traded on the NYSE. My estimates suggest that from July to December, customer orders of US$100,000 caused an average price pressure of 0.0013%.[3] This result is smaller than that identified by Hendershott and Menkveld (2014), as the NYSE is a specialist market and adopts specialists' inventory data in their SSF, while I use customers' order flows as proxy for liquidity providers' inventory change. The time variation of α in the table also suggests that the pricing error was more sensitive to customers' order flows in November than in July. This shows that liquidity providers controlled their inventories more cautiously and were less willing to provide liquidity, leading to larger pricing errors for every subsequent order. It can also be interpreted as liquidity providers requiring larger expected returns from pricing

[3] Average α during the six months is 7.87, meaning that 10,000 shares of buy (sell) order cause the pricing error to increase (decrease) by 0.0787%. Average stock price of FTSE100 is GBP455 from July to December and average exchange rate of GBP/USD is 0.78. Therefore, the pricing error caused by USD100,000 is

$$0.0787\% * 100,000 * 0.78/455/10,000 = 0.0013\%$$

.

errors to compensate for their liquidity provision during the financial crisis. In addition, α is cross-sectionally different among the five quantiles. For companies with the largest market caps, α is small and increases from 4.29 in July to 7.05 in December, while α of Q2 and Q3 companies exhibit the most significant increase between July and December. This confirms that liquidity providers' inventory control had less impact on companies with larger market caps. This cross-sectional difference is similar to that of bid-ask spreads, implying that both liquidity measures (bid-ask spreads and temporary price changes) for companies with big market capitalisation, did not increase substantially during the crisis. Hendershott and Menkveld (2014) use money amounts rather than number of shares in the SSF. Money amounts and number of shares might generate different estimates of parameters in the SSF. However, my results suggest that α increased during the six months when most equity prices fell. If I replace number of shares with money amounts, α should increase more. The results are shown in Table 2.3. α increases over the six months for all stocks.

The estimates for β in Table 2.4 are positive and statistically significant for all five quantiles. This is consistent with my hypothesis that order flow innovations contain private information that is impounded into stock prices, permanently changing them. The table also shows that just β of Q1 companies increases significantly from 1.41 in July to 4.84 in December, and β of Q2 companies increases slightly from 1.14 in July to 2.24 in December, while β of the other companies remains at the same level throughout the crisis. The results indicate that, as the crisis deepened, for small-cap companies, fundamental values increased (decreased) more significantly when customers' buy (sell) orders were accommodated, due to a greater probability that customers' orders of these stocks contained private information. As a result, liquidity providers with no private information were more worried about their information disadvantage and thus unwilling to provide liquidity, leading to decreasing liquidity for these companies. However, the adverse selection problem was not amplified for most stocks, especially big-cap stocks in the UK market, as fundamental values retained the same sensitivity to customers' order flow innovations. For example, β of

Q5 companies in July is 0.42; thus, 10,000 more customer buy order surprise would increase the fundamental value by 0.0042%, and β does not change substantially in the following five months, indicating that the effect of one more customer buy (sell) order on fundamental value did not change during the crisis. Therefore, for most companies, the evaporation of liquidity was due to liquidity providers' inventory control, while, for the companies with the smallest market capitalisation, liquidity dried up due to both information asymmetry and inventory control.

TABLE 2.2: Monthly α

This table presents mean and standard error (in bracket) of parameter α in the following state space model:

$$\begin{aligned} p_t &= m_t + s_t \\ m_t &= m_{t-1} + \beta \hat{X}_t + e_t \\ s_t &= \phi s_{t-1} + \alpha X_t + u_t \end{aligned}$$

where p_t is the observed log price of stock; m_t is fundamental value; s_t is pricing error; e_t and u_t are uncorrelated i.i.d. processes. $\hat{X}_t$ is investors' order flow innovation. X_t is investors' order flow.

Companies are sorted into five quantiles based on their market capitalisation. Q1 refers to companies with smallest market caps. α is reported for each month from June to December 2008. Daily parameters for each stock are estimated from minute data first and averaged cross-sectionally. Monthly mean and standard errors are then calculated by the daily parameters.

		JUL	AUG	SEP	OCT	NOV	DEC
All	mean	5.4044	6.1140	6.2155	9.5329	10.4705	9.5022
		(0.1516)	(0.1751)	(0.2017)	(0.2858)	(0.3266)	(0.3192)
Q1	mean	4.2119	4.9151	4.9576	7.1750	7.2880	5.1561
		(0.3406)	(0.3843)	(0.4381)	(0.5796)	(0.7775)	(0.5867)
Q2	mean	5.3666	6.9379	6.8385	10.4859	12.0096	10.0439
		(0.3484)	(0.3859)	(0.4999)	(0.6702)	(0.8378)	(0.7244)
Q3	mean	6.0835	6.5487	7.3996	11.2150	12.0738	13.3162
		(0.3523)	(0.3814)	(0.5142)	(0.6935)	(0.7401)	(0.9728)
Q4	mean	7.1605	8.1680	7.4404	11.8421	13.8196	12.0453
		(0.4144)	(0.5680)	(0.4873)	(0.7093)	(0.7861)	(0.7792)
Q5	mean	4.2916	4.2396	4.3402	6.9804	7.0205	7.0491
		(0.2383)	(0.2515)	(0.2707)	(0.5345)	(0.4421)	(0.4664)

Figure 2.5 illustrates how α varies over time. I find that α increases with the development of the crisis, with a trend similar to that of the VIX. Figure 2.6 plots α

TABLE 2.3: Monthly α – Order Flow in Money Amount

This table presents mean and standard error (in bracket) of parameter α in the following state space model:

$$p_t = m_t + s_t$$
$$m_t = m_{t-1} + \beta \hat{X}_t + e_t$$
$$s_t = \phi s_{t-1} + \alpha X_t + u_t$$

where p_t is the observed log price of stock; m_t is fundamental value; s_t is pricing error; e_t and u_t are uncorrelated i.i.d. processes. $\hat{X}_t$ is investors' order flow innovation (in money amount). X_t is investors' order flow (in money amount).
Companies are sorted into five quantiles based on their market capitalisation. Q1 refers to companies with smallest market caps. α is reported for each month from June to December 2008. Daily parameters for each stock are estimated from minute data first and averaged cross-sectionally. Monthly mean and standard errors are then calculated by the daily parameters.

		JUL	AUG	SEP	OCT	NOV	DEC
All	mean	0.0196	0.0206	0.0203	0.0444	0.0605	0.0553
		(0.0007)	(0.0007)	(0.0009)	(0.0018)	(0.0018)	(0.0030)
Q1	mean	0.0326	0.0350	0.0380	0.0926	0.1179	0.0862
		(0.0044)	(0.0038)	(0.0052)	(0.0100)	(0.0204)	(0.0209)
Q2	mean	0.0212	0.0234	0.0220	0.0467	0.0628	0.0679
		(0.0013)	(0.0014)	(0.0015)	(0.0030)	(0.0046)	(0.0048)
Q3	mean	0.0272	0.0276	0.0247	0.0564	0.0773	0.0718
		(0.0017)	(0.0018)	(0.0019)	(0.0036)	(0.0057)	(0.0061)
Q4	mean	0.0160	0.0152	0.0146	0.0275	0.0423	0.0384
		(0.0011)	(0.0011)	(0.0009)	(0.0020)	(0.0038)	(0.0029)
Q5	mean	0.0064	0.0058	0.0062	0.0102	0.0147	0.0156
		(0.0003)	(0.0004)	(0.0004)	(0.0006)	(0.0009)	(0.0010)

TABLE 2.4: Monthly β

This table presents mean and standard error (in bracket) of parameter β in the following state space model:

$$p_t = m_t + s_t$$
$$m_t = m_{t-1} + \beta \hat{X}_t + e_t$$
$$s_t = \phi s_{t-1} + \alpha X_t + u_t$$

where p_t is the observed log price of stock; m_t is fundamental value; s_t is pricing error; e_t and u_t are uncorrelated i.i.d. processes. $\hat{X}_t$ is investors' order flow innovation. X_t is investors' order flow.
Companies are sorted into five quantiles based on their market capitalisation. Q1 refers to companies with smallest market caps. β is reported for each month from June to December 2008 . Daily parameters for each stock are estimated from minute data first and averaged cross-sectionally. Monthly mean and standard errors are then calculated by the daily parameters.

		JUL	AUG	SEP	OCT	NOV	DEC
All	mean	0.9732	0.7905	1.2421	1.7154	1.3328	1.6960
		(0.1395)	(0.1544)	(0.1825)	(0.2454)	(0.2928)	(0.2757)
Q1	mean	1.4085	1.4535	2.2411	3.4166	4.4487	4.8365
		(0.3392)	(0.3670)	(0.4403)	(0.5494)	(0.7871)	(0.6452)
Q2	mean	1.1403	0.7520	1.8468	3.1866	1.9081	2.2381
		(0.3298)	(0.3412)	(0.4689)	(0.5863)	(0.7683)	(0.6405)
Q3	mean	0.2637	0.3189	0.2343	0.2872	0.4373	0.0755
		(0.3196)	(0.3196)	(0.4334)	(0.5448)	(0.6143)	(0.7833)
Q4	mean	1.6375	0.8115	1.2894	1.4158	-0.0741	0.9069
		(0.3947)	(0.5086)	(0.4544)	(0.6399)	(0.6867)	(0.6705)
Q5	mean	0.4163	0.4881	0.6746	0.3729	0.2098	0.4618
		(0.1819)	(0.2071)	(0.2276)	(0.4276)	(0.3603)	(0.3638)

against the VIX, and indicates a positive correlation between the two. The correlation coefficient is 0.7976, suggesting that the impact of order flows on pricing errors is highly correlated with market volatility. Thus, liquidity providers control their inventory more cautiously and are less willing or less capable to provide liquidity when the market becomes more volatile. This result is consistent with the findings of Nagel (2012) and Hameed et al. (2010), suggesting that the VIX can predict the profit of a reversal strategy. However, a larger pricing error can, at the same time, make the stock market more volatile, leading to a strong correlation between volatility and market liquidity. For companies with the biggest market caps, the correlation coefficient (0.5685) is the smallest among all five quantiles, indicating that big-cap stock prices deviate less from fundamental value after a substantial negative market shock and liquidity dry-up. These results also provide evidence that liquidity providers can make larger profits when the market is volatile and in decline, perhaps due to elevated risk, reduced competition, or tighter funding constraints.

FIGURE 2.5: Time Variation of α

This figure depicts how α changes over time. The estimate is obtained from the following state space model

$$p_t = m_t + s_t$$
$$m_t = m_{t-1} + \beta \hat{X}_t + e_t$$
$$s_t = \phi s_{t-1} + \alpha X_t + u_t$$

Companies are sorted into five quantiles based on market caps where Q1 refers to companies with the smallest market caps. The VIX is also plotted to show the trend.

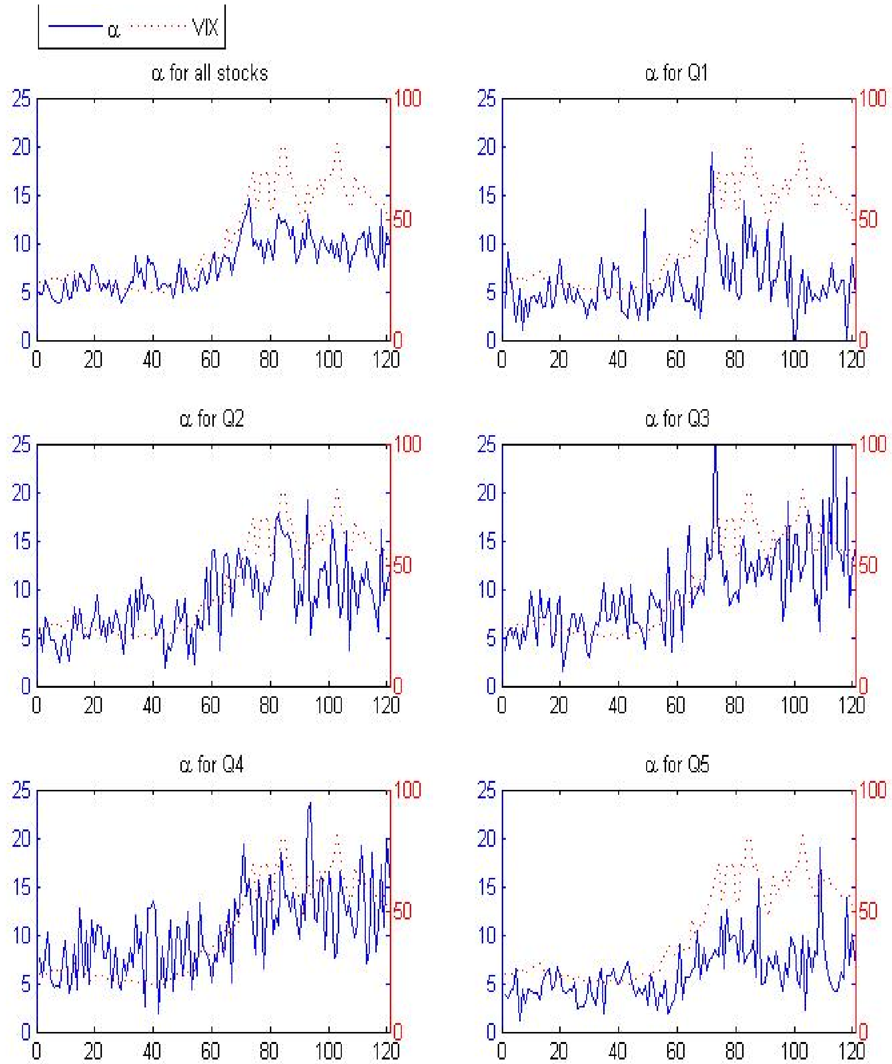

FIGURE 2.6: α against VIX

This figure shows how α (in the following state space model) is correlated with the VIX from June to December 2008.

$$p_t = m_t + s_t$$
$$m_t = m_{t-1} + \beta \hat{X}_t + e_t$$
$$s_t = \phi s_{t-1} + \alpha X_t + u_t$$

Companies are sorted into five quantiles based on market caps where Q1 refers to companies with the smallest market caps.

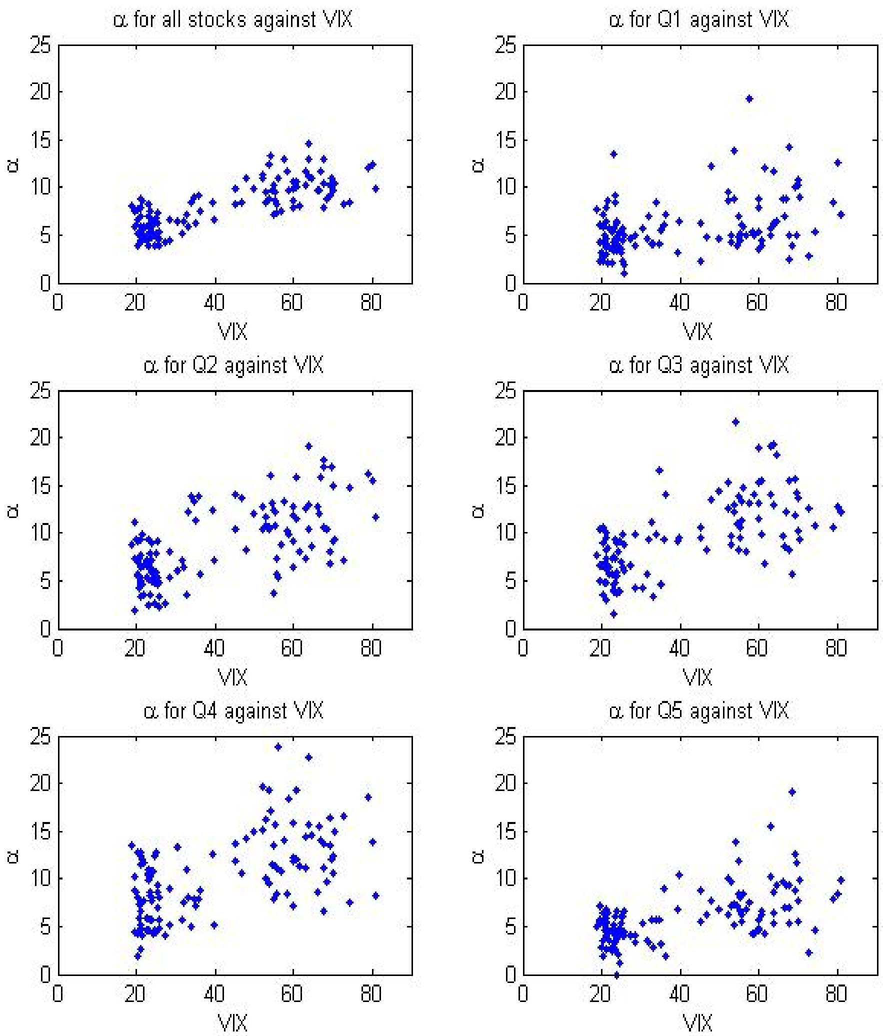

Figure 2.7 shows how β varies; we see that for Q1 companies, β increases over time. For the other quantiles, β maintains the same level over the six-month period. Figure 2.8 demonstrates the correlation between β and the VIX. β for Q1 has a positive correlation with the VIX. The correlation coefficient for this is 0.4118, while those of the other quantiles are all around zero. These two figures indicate that β, unlike α, does not change over time; therefore, information asymmetry was not a significant problem in the UK equity market during the crisis and, thus, not the cause of the liquidity dry-up. In addition, there is no obvious relationship between the VIX and the adverse selection problem. The VIX, either as a state variable itself or through its correlation with other state variables, cannot predict when traders will have more private information or when insiders will trade more aggressively in the equity market. In addition, since it appears that only companies with small market caps have a positive correlation with the VIX, we infer that only 'low-quality' securities had greater adverse selection problems during the crisis. I further sort companies based on trading volume and plot their β against the VIX, as shown in Figure 2.9. This reveals that β was not influenced by the crisis or the increasing volatility of most stocks during the crisis. However, for companies with small trading volumes, β increases with the VIX, indicating a larger probability that these stocks were traded by insiders during the market turmoil. Both Figures 2.8 and 2.9 present evidence that only small companies with illiquid stocks suffered greater adverse selection problems during the crisis, while most other stocks were not influenced.

FIGURE 2.7: Time Variation of β

This figure depicts how β changes over time. The estimate is obtained from the following state space model

$$p_t = m_t + s_t$$
$$m_t = m_{t-1} + \beta\hat{X}_t + e_t$$
$$s_t = \phi s_{t-1} + \alpha X_t + u_t$$

Companies are sorted into five quantiles based on market caps where Q1 refers to companies with the smallest market caps. The VIX is also plotted to show the trend.

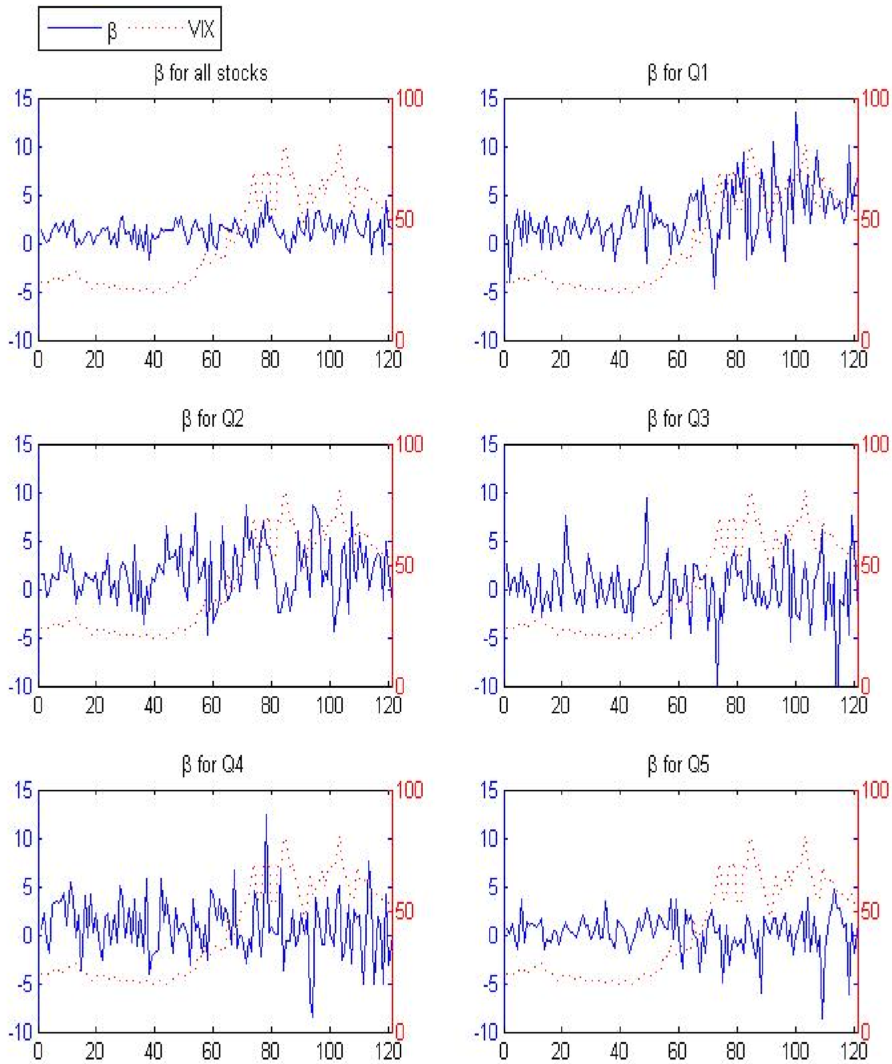

FIGURE 2.8: β against VIX - market capitalisation

This figure shows how β (in the following state space model) is correlated with the VIX from June to December 2008.

$$p_t = m_t + s_t$$
$$m_t = m_{t-1} + \beta \hat{X}_t + e_t$$
$$s_t = \phi s_{t-1} + \alpha X_t + u_t$$

Companies are sorted into five quantiles based on market caps where Q1 refers to companies with the smallest market caps.

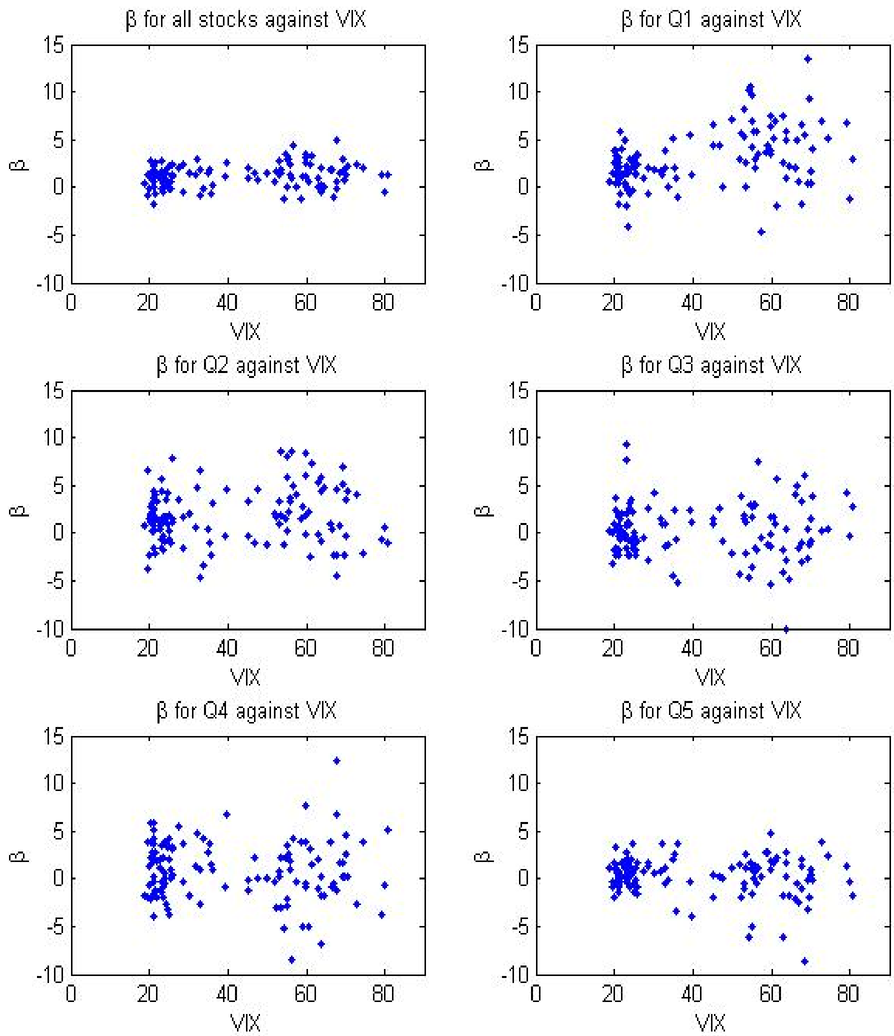

FIGURE 2.9: β against VIX - trading volume

This figure shows how β (in the following state space model) is correlated with the VIX from June to December 2008.

$$p_t = m_t + s_t$$
$$m_t = m_{t-1} + \beta \hat{X}_t + e_t$$
$$s_t = \phi s_{t-1} + \alpha X_t + u_t$$

Companies are sorted into five quantiles based on trading volume where Q1 refers to companies with the smallest trading volume.

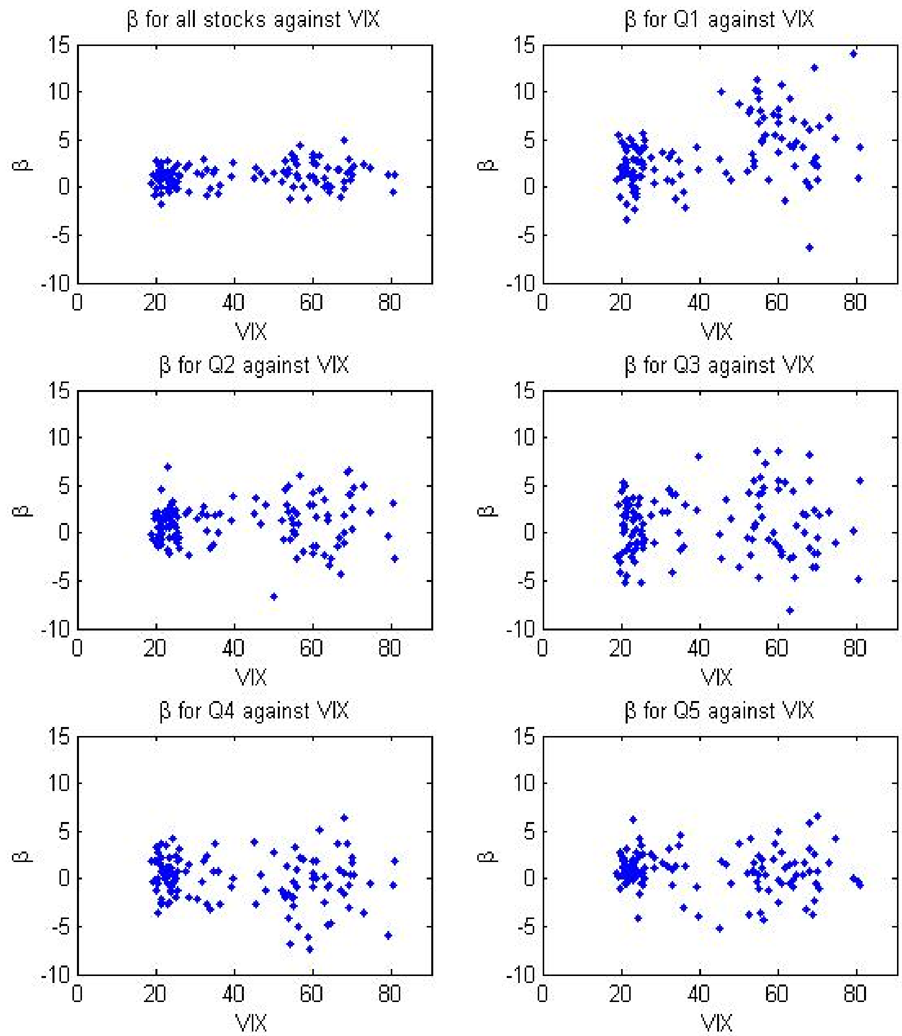

When the model defined by equations (2.1), (2.2), and (2.5) are applied to the data, Table 2.5 reveals that the coefficient for the AR(1) term in the pricing error equation is significantly positive. This demonstrates that the pricing error in the previous minute does not immediately disappear. The parameter ϕ is around 0.7 for the entire six-month period, indicating that 70% of the pricing error at time t can be explained by the pricing error at time $t-1$. Therefore, this specification should better capture the dynamics of the two unobserved processes than SSF without AR(1) in the pricing error. The above results prove that liquidity provision generates larger

TABLE 2.5: Monthly ϕ

This table presents mean and standard error (in bracket) of parameter ϕ in the following state space model:

$$p_t = m_t + s_t$$
$$m_t = m_{t-1} + \beta \hat{X}_t + e_t$$
$$s_t = \phi s_{t-1} + \alpha X_t + u_t$$

where p_t is the observed log price of stock; m_t is fundamental value; s_t is pricing error; e_t and u_t are uncorrelated i.i.d. processes. $\hat{X}_t$ is investors' order flow innovation. X_t is investors' order flow.
Companies are sorted into five quantiles based on their market capitalisation. Q1 refers to companies with smallest market caps. ϕ is reported for each month from June to December 2008 . Daily parameters for each stock are estimated from minute date first and averaged cross-sectionally. Monthly mean and standard errors are then calculated by the daily parameters.

		JUL	AUG	SEP	OCT	NOV	DEC
All	mean	0.7595	0.7367	0.7184	0.7325	0.7038	0.6664
		(0.0111)	(0.0119)	(0.0124)	(0.0116)	(0.1128)	(0.0134)
Q1	mean	0.7515	0.6675	0.6931	0.7226	0.6498	0.6411
		(0.0238)	(0.0293)	(0.0285)	(0.0256)	(0.0290)	(0.0296)
Q2	mean	0.7325	0.7681	0.6760	0.7808	0.7396	0.6991
		(0.0264)	(0.0253)	(0.0293)	(0.0216)	(0.0261)	(0.0275)
Q3	mean	0.7830	0.7268	0.7467	0.7566	0.7052	0.6497
		(0.0240)	(0.0274)	(0.0264)	(0.0255)	(0.0291)	(0.0304)
Q4	mean	0.7102	0.6955	0.6928	0.6768	0.6862	0.6376
		(0.0280)	(0.0289)	(0.0297)	(0.0295)	(0.0304)	(0.0321)
Q5	mean	0.8158	0.8216	0.7820	0.7252	0.7356	0.7031
		(0.0214)	(0.0208)	(0.0240)	(0.0271)	(0.0279)	(0.0301)

profits in a falling and volatile market, since liquidity providers can seize a larger return from the pricing error without incurring more substantial losses from the information asymmetry. However, the higher return may simply be the result of the larger risk borne by the liquidity providers. Another possible reason is that most financial intermediaries are financially constrained, so there is less competition in liquidity provision. Liquidity providers can therefore earn a larger risk-adjusted return. For example, quantitative hedge funds may stop providing liquidity due to insufficient capital, as documented by Ben-David et al. (2012).

2.6 Conclusion

I use SSF to decompose observed stock prices into unobserved fundamental value (a random walk process determined by information contained in orders), and pricing error (a mean-reversal process influenced by liquidity providers' inventory control). My results are similar to those reported by Hendershott and Menkveld (2014), but the pricing error caused by order flow on the LSE (0.0013% by orders of USD100,000) is smaller than the pricing error caused by specialists' inventory change on the NYSE (0.02% by inventory change of USD100,000). The time variation of my estimation during the financial crisis indicates that liquidity providers' inventory control was the main cause of the liquidity dry-up in the UK equity market in 2008. Increases in asymmetric information played a much smaller role. When the market became more volatile with the development of the crisis, liquidity providers became less willing to absorb the extra risky assets, not because there was a greater probability of adverse selection but because the liquidity providers were less willing to devote capital to maintaining risky market-making positions. However, for small market capitalisation companies with illiquid stock issues, liquidity seems to have declined due to asymmetric information concerns.

My results in the UK equity market are consistent with those in Nagel (2012). Although the sample of Nagel (2012) covers US equity market including NYSE, AMEX and Nasdaq stocks while my sample covers FTSE100 stocks traded on LSE, we both find that inventory control is the primary cause of liquidity evaporation for big stocks with big market capitalisation. Our results also confirms the connection between volatility and market liquidity, as suggested by the model in Brunnermeier and Pedersen (2009). My results in the UK equity market do not support the adverse selection theory prosed by Gorton and Metrick (2012) probably because the assets in their study were information insensitive before the crisis and became information sensitive after the external shock. As suggested by Pagano and Volpin (2012), issuers of asset-backed securities choose to release coarse information to enhance liquidity. Dang et al. (2009) suggest that the debt market is more liquid without private information generation. However, equity market heavily relies on private information generation and adverse selection always exists. Therefore, liquidity providers do not lose 'market confidence' due to the external shock. My results can be generalised to other markets where assets are information sensitive. In addition, policy makers do not need to rebuild 'market confidence' but inject capital to restore liquidity provision instead. Liquidity providers of big market cap stocks do not need to worry about adverse selection problem during a crisis, and the survivors can make even bigger profits. It is a relief for all liquidity demanders that market liquidity can be restored quickly after crisis as long as liquidity provision sector has sufficient capital and risk-bearing capacity.

Although I conclude that liquidity providers could make larger profits due to pricing errors during the financial crisis, which is consistent with what Nagel (2012) has found via a reversal strategy, it is unclear whether the profit is generated by greater risks borne by liquidity providers or by scarcity of capital in the market. As predicted by the model of Brunnermeier and Pedersen (2009), funding triggers a switch from a high-liquidity/low-volatility equilibrium to a low-liquidity/high-volatility equilibrium, leading to liquidity dry-up. Therefore, we can further add state variables such as VIX and LIBOR-OIS to SSF to test whether scarcity of capital leads to liquidity providers' inventory control.

2.7 Appendix I: Kalman Filter and simulation results

Kalman Filter is used to estimate the parameters in the SSF. The method first takes all observations into account to decompose the observed price time series into two unobserved processes which represent the underlying states, and then generates the estimates through maximum likelihood. Therefore, the estimates should be unbiased and efficient.

As this paper aims to find out how α and β in SSF vary during the financial crisis, I need relatively accurate estimates of parameters obtained through Kalman Filter for each trading day. Therefore, before applying the method to real data, I test its accuracy through simulation.

I put actual order flow data of a certain stock into SSF with pre-specified parameters to simulate a time-series stock price. I then estimate the parameters in SSF with stock price and customers' order flow using the same methodology as described in Section 2.4. I replicate the simulation for 100 times, and report the mean and variance of the 100 replications for each parameter.

The true parameters and corresponding simulated results are reported in Table 2.6 for equations (2.2) and (2.3) and in Table 2.7 for equations (2.2) and (2.5) .

The simulation results show that if there is no AR(1) term as in equation (2.3), Kalman Filter generates very accurate estimates for α and β. However, as I add the AR(1) term in the unobserved pricing error process, the estimates are less accurate and variances become larger. However, as equation (2.5) should be more appropriate to represent the dynamics of the pricing error process theoretically, I still use this specification to decompose the stock price.

TABLE 2.6: Simulation Results (1)

This table presents simulation results for parameters in the following state space model:

$$p_t = m_t + s_t$$
$$m_t = m_{t-1} + \beta \hat{X}_t + e_t$$
$$s_t = \alpha X_t + u_t$$

where p_t is the observed log price of stock; m_t is fundamental value; s_t is pricing error; e_t and u_t are uncorrelated i.i.d. process. $\hat{X}_t$ is investors' order flow innovation. X_t is investors' order flow.
Order flows of three stocks are picked as independent variables for simulation. Stock 1 is Home Retail Group (GB00B19NKB76); Stock 2 is Vodaphone Group (GB00B16GWD56); Stock 3 is BT Group (GB0030913577).

	True	Stock 1		Stock 2		Stock 3	
		mean	variance	mean	variance	mean	variance
Panel A: Simulation 1							
β	16	16.0833	0.3776	15.9621	0.5721	16.0008	5.7084
α	0.2	0.2060	0.2648	0.2085	0.2898	0.2661	3.0979
$var(e)$	100	97.3417	67.1841	97.8731	74.4382	96.5315	69.7272
$var(u)$	1	2.7294	10.6975	2.2380	8.4848	2.5239	8.8021
Panel B: Simulation 2							
β	10	10.0303	0.0409	9.9920	0.0573	9.9817	0.6233
α	0.5	0.5028	0.0280	0.5065	0.0320	0.5395	0.3544
$var(e)$	10	10.0267	1.3110	10.0597	1.2710	9.8484	1.1979
$var(u)$	1	1.0152	0.3466	0.9463	0.2714	1.0501	0.2690
Panel C: Simulation 3							
β	3	3.0088	0.0041	2.9974	0.0057	.9942	0.0630
α	0.8	0.8009	0.0028	0.8021	0.0032	0.8125	0.0355
$var(e)$	1	0.9978	0.0127	1.0024	0.0126	0.9817	0.0119
$var(u)$	0.1	0.1032	0.0033	0.0956	0.0027	0.1059	0.0027

TABLE 2.7: Simulation Results (2)

This table presents simulation results for parameters in the following state space model:

$$p_t = m_t + s_t$$
$$m_t = m_{t-1} + \beta \hat{X}_t + e_t$$
$$s_t = \phi s_{t-1} + \alpha X_t + u_t$$

where p_t is the observed log price of stock; m_t is fundamental value; s_t is pricing error; e_t and u_t are uncorrelated i.i.d. process. $\hat{X}_t$ is investors' order flow innovation. X_t is investors' order flow.
Order flows of three stocks are picked as independent variables for simulation. Stock 1 is Home Retail Group (GB00B19NKB76); Stock 2 is Vodaphone Group (GB00B16GWD56); Stock 3 is BT Group (GB0030913577).

	True	Stock 1		Stock 2		Stock 3	
		mean	variance	mean	variance	mean	variance
Panel A: Simulation 1							
β	16	16.3225	6.8684	16.6296	35.3779	15.7020	100.7817
α	0.2	-0.1807	6.5013	-0.3692	35.1359	0.5608	102.5754
ϕ	0.8	0.5748	0.4341	0.5931	0.4439	0.9385	0.0099
$var(e)$	100	70.2227	1200	67.9790	1653	53.2882	1563
$var(u)$	1	29.1293	1208	31.6668	1647	46.7702	1555
Panel B: Simulation 2							
β	10	10.5319	1.2589	9.8592	2.0768	9.9721	7.7493
α	0.5	-0.0471	1.2404	0.6596	2.0541	0.5692	7.9637
ϕ	0.5	0.7683	0.0912	0.6476	0.1154	0.6544	0.3262
$var(e)$	10	7.1178	10.6338	8.0088	10.9792	6.6941	17.3782
$var(u)$	1	3.9017	11.6083	2.9453	11.5354	4.3764	17.1434
Panel C: Simulation 3							
β	3	5.1760	1.6049	3.0171	0.0457	3.2157	0.8363
α	0.8	-1.3895	1.5908	0.7886	0.0376	0.5936	0.8069
ϕ	0.2	0.7917	0.1143	0.2161	0.0180	0.5588	0.1692
$var(e)$	1	1.2942	0.0546	0.9701	0.0324	0.7387	0.1358
$var(u)$	0.1	0.0392	0.0037	0.1278	0.0359	0.3715	0.1541

2.8 Appendix II: Estimates of SSF without AR(1)

Table 2.8 and 2.9 report estimates of SSF defined by equations (2.1), (2.2) and (2.3) each month. βs are positive for all stocks, consistent with our hypothesis that order flow innovations contain private information which will be impounded into stock prices. α has constantly negative sign which is statistically significant. The result can be interpreted as saying that order flows reduce pricing error, which is inconsistent with theories of liquidity providers' inventory control. Theoretically, if liquidity demanders' buy (sell) order decreases (increases) liquidity providers' inventory, liquidity providers should purposely increase (decrease) the price they offer to induce more sell (buy) orders which bring their inventory to original level. Therefore, net positive (negative) order flows should increase (decrease) pricing error. Figure 2.10 and 2.11 show how α varies over time and how it changes with VIX. The result indicates that α was constant during the financial crisis, meaning that liquidity providers did not change their liquidity provision in the declining and volatile market. This result is very different from the ones reported by Nagel (2012) and Hameed et al. (2010), which find that market volatility and market return can predict liquidity provision. Figure 2.12 and 2.13 demonstrate that β increased all the time during the six months and was positively correlated to the VIX, suggesting that information asymmetry in the UK equity market was more significant and there was a bigger probability that private information drove investors' order flows at that time. Therefore, adverse selection problem was the main cause of liquidity dry-up. However, the results for α is very unreasonable, which might be caused by the mis-specified equation (2.3). The equation does not allow autocorrelation in pricing errors, and thus cannot capture the dynamics of the unobserved pricing error process. Therefore, all the variations go to the fundamental value process, leading to the increase of β. As a result, we should not rely on the results of model specified by equations (2.1), (2.2) and (2.3).

TABLE 2.8: Monthly α

This table presents mean and standard error (in bracket) of parameter α in the following state space model:

$$p_t = m_t + s_t$$
$$m_t = m_{t-1} + \beta\hat{X}_t + e_t$$
$$s_t = \alpha X_t + u_t$$

where p_t is the observed log price of stock; m_t is fundamental value; s_t is pricing error; e_t and u_t are uncorrelated i.i.d. processes. $\hat{X}_t$ is investors' order flow innovation. X_t is investors' order flow.
Companies are sorted into five quantiles based on their market capitalisation. Q1 refers to companies with smallest market caps. α is reported for each month from June to December 2008. Daily parameters for each stock are estimated from minute date first and averaged cross-sectionally. Monthly mean and standard errors are then calculated by the daily parameters.

		JUL	AUG	SEP	OCT	NOV	DEC
All	mean	-0.6059	-0.6600	-0.6211	-0.7841	-1.4233	-0.9201
		(0.0243)	(0.0279)	(0.0373)	(0.0518)	(0.0578)	(0.0510)
Q1	mean	-0.9830	-0.9877	-1.1436	-2.2473	-2.3935	-1.8214
		(0.0543)	(0.0683)	(0.0880)	(0.1327)	(0.1549)	(0.1292)
Q2	mean	-0.6809	-0.9636	-0.8518	-1.4115	-2.6191	-1.5425
		(0.0507)	(0.0633)	(0.0876)	(0.1260)	(0.1482)	(0.1164)
Q3	mean	-0.5789	-0.5893	-0.3972	-0.2945	-1.0661	-0.6971
		(0.0531)	(0.0610)	(0.0903)	(0.0935)	(0.1095)	(0.1245)
Q4	mean	-0.6429	-0.7416	-0.6435	-0.0369	-0.9785	-0.5797
		(0.0717)	(0.0715)	(0.0895)	(0.1078)	(0.1175)	(0.1156)
Q5	mean	-0.1704	-0.0449	-0.0959	-0.0091	-0.1525	-0.0169
		(0.0342)	(0.0360)	(0.0491)	(0.0828)	(0.0714)	(0.0646)

TABLE 2.9: Monthly β

This table presents mean and standard error (in bracket) of parameter β in the following state space model:

$$p_t = m_t + s_t$$
$$m_t = m_{t-1} + \beta \hat{X}_t + e_t$$
$$s_t = \alpha X_t + u_t$$

where p_t is the observed log price of stock; m_t is fundamental value; s_t is pricing error; e_t and u_t are uncorrelated i.i.d. processes. $\hat{X}_t$ is investors' order flow innovation. X_t is investors' order flow.
Companies are sorted into five quantiles based on their market capitalisation. Q1 refers to companies with smallest market caps. β is reported for each month from June to December 2008. Daily parameters for each stock are estimated from minute date first and averaged cross-sectionally. Monthly mean and standard errors are then calculated by the daily parameters.

		JUL	AUG	SEP	OCT	NOV	DEC
All	mean	6.9653	7.5219	8.0520	12.0465	13.2608	12.1460
		(0.1010)	(0.1154)	(0.1338)	(0.2016)	(0.2183)	(0.1943)
Q1	mean	6.6069	7.2506	8.2395	12.9076	14.0539	11.8085
		(0.1748)	(0.1914)	(0.2238)	(0.4093)	(0.4175)	(0.3791)
Q2	mean	7.1562	8.6723	9.5085	15.1837	16.6022	13.7788
		(0.1828)	(0.2408)	(0.3195)	(0.4952)	(0.5586)	(0.4148)
Q3	mean	6.8764	7.4021	8.0531	11.7005	13.5883	14.0994
		(0.2254)	(0.2689)	(0.3263)	(0.4311)	(0.4815)	(0.5010)
Q4	mean	9.4699	9.6567	9.3845	13.2028	14.7742	13.5971
		(0.3207)	(0.3256)	(0.3402)	(0.4902)	(0.5174)	(0.4803)
Q5	mean	4.9349	4.7456	5.1506	7.3480	7.4095	7.5149
		(0.1795)	(0.1952)	(0.2169)	(0.3185)	(0.3128)	(0.2860)

FIGURE 2.10: Time Variation of α

This figure depicts how α changes over time. The estimate is obtained from the following state space model

$$p_t = m_t + s_t$$
$$m_t = m_{t-1} + \beta \hat{X}_t + e_t$$
$$s_t = \alpha X_t + u_t$$

Companies are sorted into five quantiles based on market caps where Q1 refers to companies with the smallest market caps. The VIX is also plotted to show the trend.

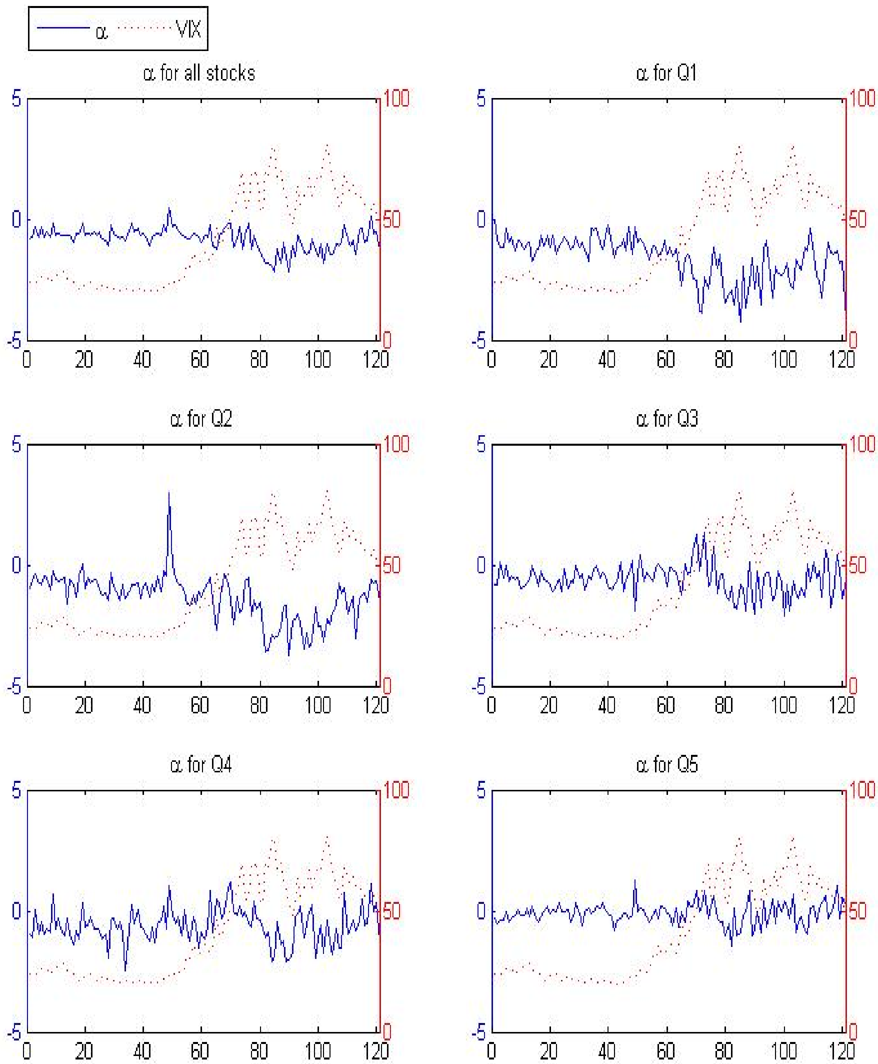

FIGURE 2.11: α against VIX

This figure shows how α (in the following state space model) is correlated with the VIX from June to December 2008.

$$p_t = m_t + s_t$$
$$m_t = m_{t-1} + \beta \hat{X}_t + e_t$$
$$s_t = \alpha X_t + u_t$$

Companies are sorted into five quantiles based on market caps where Q1 refers to companies with the smallest market caps.

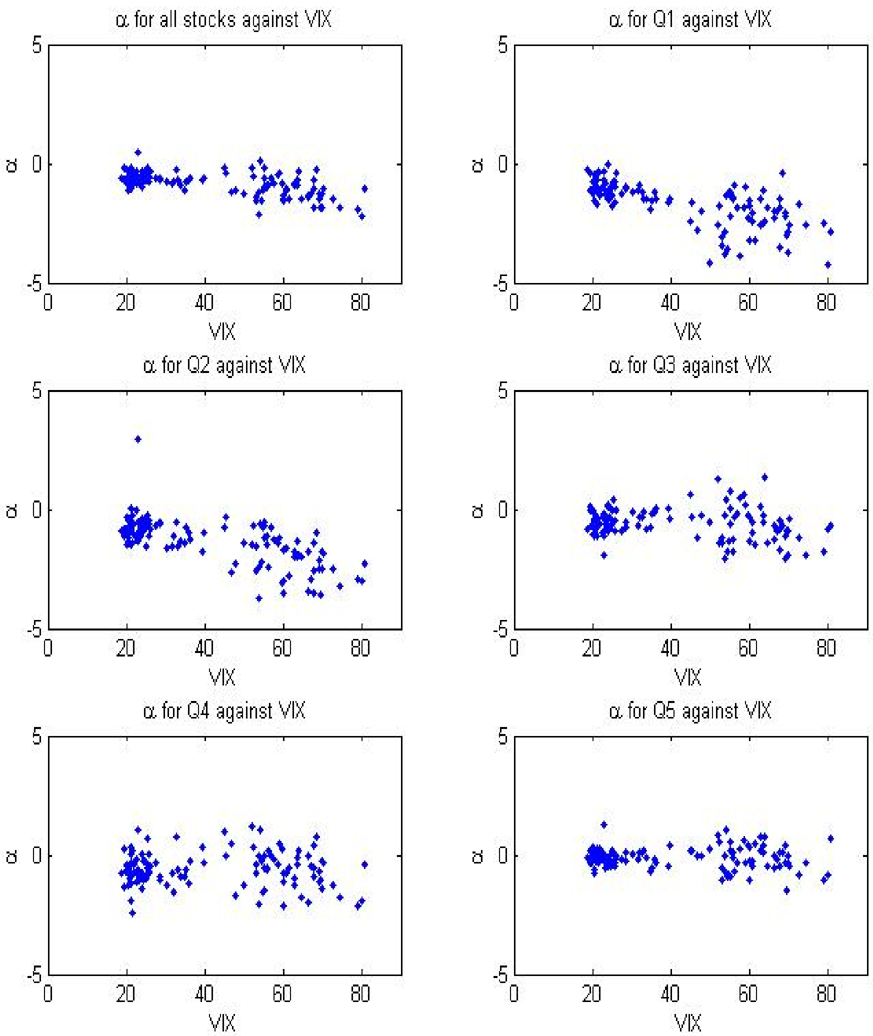

FIGURE 2.12: Time Variation of β

This figure depicts how β changes over time. The estimate is obtained from the following state space model

$$p_t = m_t + s_t$$
$$m_t = m_{t-1} + \beta\hat{X}_t + e_t$$
$$s_t = \alpha X_t + u_t$$

Companies are sorted into five quantiles based on market caps where Q1 refers to companies with the smallest market caps.VIX is also plotted to show the trend.

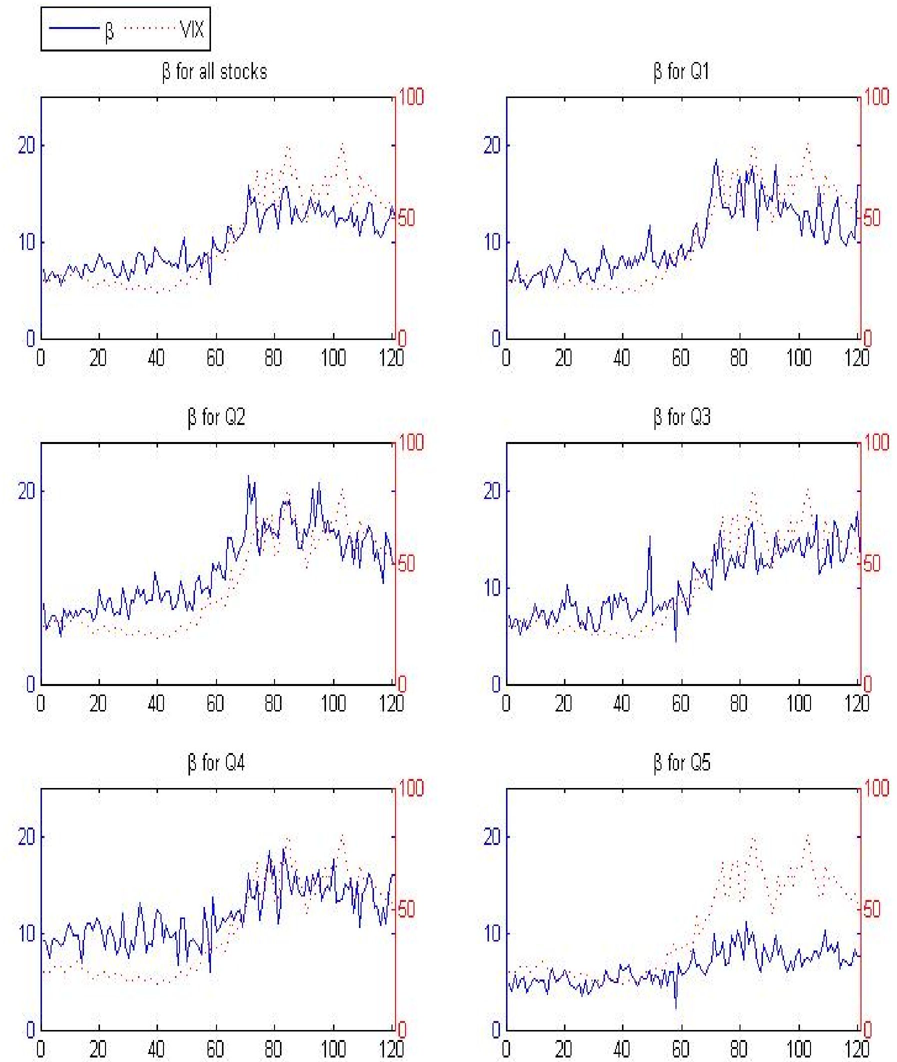

FIGURE 2.13: β against VIX

This figure shows how β (in the following state space model) is correlated with the VIX from June to December 2008.

$$p_t = m_t + s_t$$
$$m_t = m_{t-1} + \beta \hat{X}_t + e_t$$
$$s_t = \alpha X_t + u_t$$

Companies are sorted into five quantiles based on market caps where Q1 refers to companies with the smallest market caps.

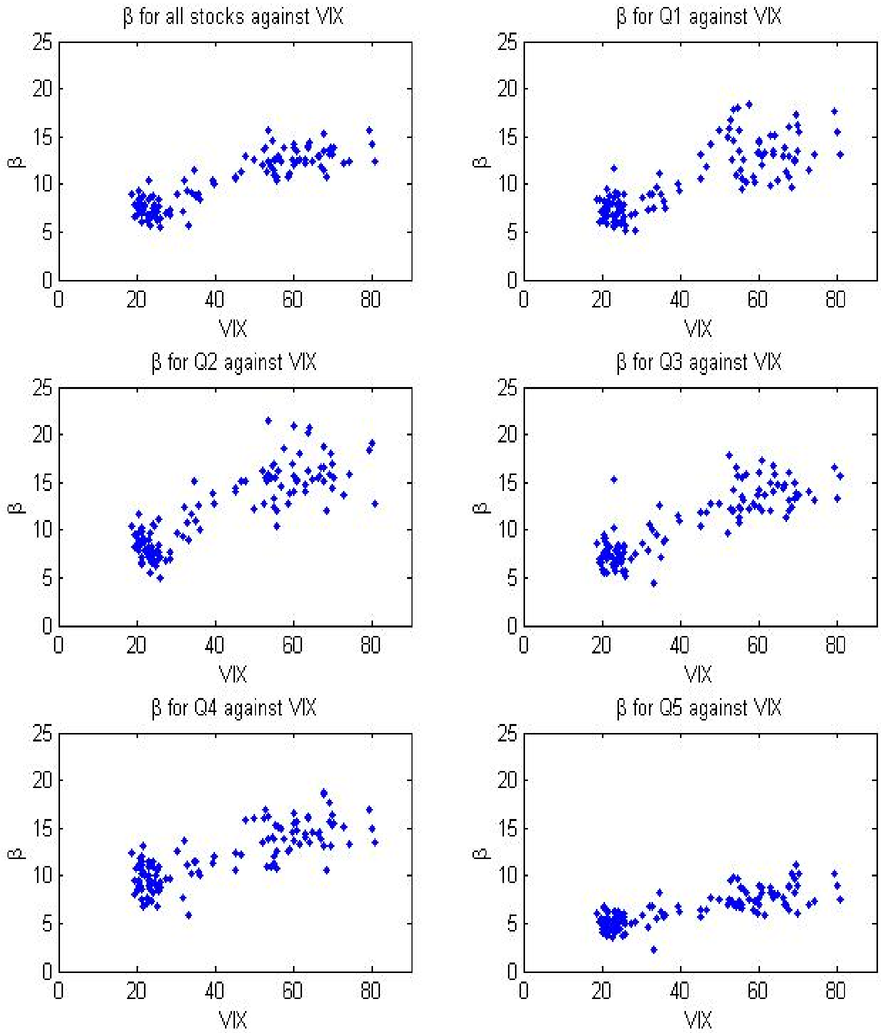

Chapter 3

What drives price changes in cryptocurrency market

3.1 Introduction

The total market capitalisation of cryptocurrency had risen to more than US$800 billion by January 2018, becoming an emerging asset class that investors cannot overlook. Bitcoin is the most popular of thousands of different cryptocurrencies. The price shot up to US$20,000 per Bitcoin in December 2017 and fell back to US$4,000 in November 2018. Although the huge returns and volatility of cryptocurrency have attracted the attention of many investors, little is known about how prices are determined. Previous literature has tried to study the statistical characteristics of cryptocurrency returns and risk factors associated with returns (e.g. Liu et al. (2019), Shen et al. (2020), Urquhart (2017), Bouoiyour et al. (2016) etc.), fair value of some cryptocurrencies (e.g. Biais et al. (2020), Dimpfl and Peter (2020), Sockin and Xiong (2020), Ciaian et al. (2016) etc.), and correlations between cryptocurrencies and other asset classes (e.g. Baur et al. (2018), Dyhrberg (2016) Pal and Mitra (2019), Klein et al. (2018) etc.). However, as no strong evidence that cryptocurrency can bring future cash flow is presented, it is difficult to determine its price from a traditional asset price perspective. Interestingly, cryptocurrencies, for the first time, show the world that some assets that have not generated any cash flows in the past and no sign of generating certain cash flows in the future are traded with a big volume at a high price. Therefore, the cryptocurrency market provides us with a good place to study how trading activity drives price, and thus I take a microstructure perspective to find out how cryptocurrency price is determined through trading. In this chapter, I attempt to answer the question 'how cryptocurrency price is determined' from the microstructure finance perspective, identifying how order flow – the most important variable in the field of microstructure finance, according to Evans and Lyons (2002b) – affects cryptocurrency prices. This will help us to understand what caused the bubble in December 2017, as well as its bursting in January 2018. Previous studies have found that order flows play an important role in determining asset prices, either through price discovery or price pressure. Evans and Lyons (2002b) suggest that private information from informed investors is impounded into price by order flows. Love and Payne (2008) argue that public announcements are impounded into price largely by order flows. This strand of the literature suggests that order flows influence price through price discovery because order flows contain information that reflects investors' views of the asset's fundamental value, thus permanently changing the fundamental value. Additionally, Campbell et al. (1993) and Pastor and Stambaugh (2001) consider temporary pricing errors induced by order flows, concluding that order flows influence price due to liquidity providers' inventory control through price pressure. Thus, in this chapter, I ask whether cryptocurrency price changes are driven by information contained in order flows and whether liquidity providers' willingness to hold risky inventory on the cryptocurrency exchanges affects price changes. Second, since information asymmetry and liquidity providers' inventory control vary when market conditions change, I wish to determine how the impact of orders on cryptocurrency price through these two channels changes over time, as well as how this change contributed to the bubble and its bursting. Finally, it is worth considering whether the order flows of one cryptocurrency on one exchange affect the price of another cryptocurrency or another exchange and whether these effects are through price discovery or price pressure, as the previous literature does provide evidence of liquidity and volatility spill-over effects across countries and assets due to constrained funding and increased risk aversion (Chordia et al. (2005); Kyle and Xiong (2001); Brunnermeier and Pedersen (2009); Comerton-Forde et al. (2010); etc.). In the cryptocurrency market, Makarov and Schoar (2019a) document a heterogeneity where price discovery happens across exchanges and time, and they indicate that the most important market for price discovery of Bitcoin is Bitfinex. Therefore, I also test the existence of spill-over effects across exchanges and cryptocurrencies.

Hendershott and Menkveld (2014) have applied State Space Form (SSF) to decompose stock prices into fundamental value and pricing error, both as functions of order flows, to reflect processes of price discovery and price pressure. I use the method to analyse the price determination of Bitcoin and Ethereum. Bitcoin and Ethereum represent more than 70% of the total cryptocurrency market capitalisation, and they are the primary funding cryptocurrencies for Initial Coin Offerings (ICOs). Bitcoin is the first and largest cryptocurrency, and it attracts investors by providing a safe means of wealth storage. The technical revolution of Ethereum Smart Contracts in 2017 brought block-chain technology and cryptocurrencies to a new generation, allowing developers to build and deploy decentralised applications. I choose SSF to analyse cryptocurrency price because it is difficult to tell what is 'fundamental value' of cryptocurrencies, and thus I regard the price as a long-term information aggregation plus a temporary pricing error.

Many exchanges exist in the cryptocurrency market in the first place because no licenses are needed to open new exchanges (especially if no fiat currency is involved in trading). Different exchanges target different types of investors. For example, Kraken mainly targets European investors. The extreme situation is that in China where fiat trading is controlled by the government, some exchanges provide Chinese investors with a platform to buy/sell cryptocurrencies with CNY. In addition, every year new cryptocurrencies are listed on different exchanges, and new derivatives are constantly introduced into the market by new exchanges. Therefore, many exchanges still have their own customer base as they provide unique products and services, similar to brokers in the decentralized foreign exchange market. However, as the market is still evolving, people are still discussing the most efficient structure of the cryptocurrency market. Jeon et al. (2021) holds the view that fragmented bitcoin orders increase transaction cost and thus decrease market efficiency. As the market is still new and evolving, more research needs to be done and more regulations need to be introduced to make the market more fair and efficient. My research is also initiated for this purpose.

As the structure of the cryptocurrency market is similar to the decentralized currency market, it is worth asking whether there is information transmission between exchanges and between cryptocurrencies. Makarov and Schoar (2018) documents large deviations in bitcoin prices across exchanges in different countries. No previous literature has discussed how different cryptocurrencies influence each other. Therefore, I want to use the SSF to explore information transmission and price discovery between exchanges and between cryptocurrencies through trading. I gather data from Bitfinex and Kraken, which are among the largest cryptocurrency exchanges in the world today. Although they are leading exchanges in the cryptocurrency market, their market share combined are less than 50%. Like other exchanges, cryptocurrency exchanges have liquidity demanders and providers, and both Bitfinex and Kraken encourage liquidity provision by charging lower fees to 'maker orders' (who have no private information) than to 'taker orders' (who have private information and try to profit from the information immediately through orders). In addition, although order flows should reflect heterogeneous expectations on asset fundamentals, those who provide liquidity have no idea of their counterparties who consume liquidity and thus cannot know whether the orders contain private information. Therefore, it is worth studying the responsiveness of fundamental value to order flows and how 'informativeness' in orders changes in the cryptocurrency market. By comparison, price pressure – primarily caused by liquidity providers' inventory control, as demonstrated in the literature[1] – is also affected by orders and varies over time, which could have played an important role in the bubble.

[1] Grossman and Miller (1988) proposed the market marking inventory model, which suggests that liquidity providers' inventory could predict return reversal. Hendershott and Seasholes (2007) and Comerton-Forde et al. (2010) confirmed the predictions of the model with the New York Stock Exchange specialists' inventory data. Naik and Yadav (2003) and Reiss and Werner (1998) confirmed the predictions with the London Stock Exchange market maker data.

My results suggest that for both Bitcoin and Ethereum on both Bitfinex and Kraken, information is impounded into price through order flows, and unexpected buy (sell) orders thus cause fundamental value to increase (decrease). At the same time, order flows generate temporary pricing errors, which diminish in minutes. Therefore, order flows influence prices through both price discovery and price pressure processes in the cryptocurrency market, similar to other asset classes. Although cryptocurrency market is an emerging asset class, the process how price is determined from the microstructure perspective has no difference from other asset classes. Therefore, investors can regulators can borrow experience from the development of other asset classes to better invest in or regulate this emerging market. In addition, both the fundamental value and pricing error were more sensitive to orders at the beginning of the boom and of the crash. Therefore, both increased information asymmetry and tighter inventory control by liquidity providers contributed to the growth and bursting of the bubble. In contrast, Nagel (2012) argues that liquidity dry-up in the US equity market during the financial crisis was primarily caused by the inventory channel. In addition, my results in the previous chapter demonstrate that liquidity evaporation of FTSE 100 stocks during the crisis was also caused by liquidity providers' tighter inventory control. My results for the cryptocurrency market suggest that the Bitcoin bubble on Bitfinex could have been caused by liquidity providers' different responses to informed investors' buy and sell orders, although this hypothesis could be tested directly in future research. The result is consistent with Griffin and Shams (2018) that accused the sister company of Bitfinex of manipulating Bitcoin price with Tether in 2017, and thus confirms that regulation is urgently needed in the market as the market capitalisation keeps growing, especially when more leveraged products are introduced. My results confirm that cryptocurrency market is still a very immature market where information asymmetry is rampant, leading to the bubble. Therefore, although it is difficult to decide the fair value of cryptocurrencies, regulators still need to regulate trading activities and platforms to make the market more fair and efficient. Finally, I find out that Bitcoin order flows contain relevant information that changes Ethereum prices and vice versa, suggesting an information spill-over between cryptocurrencies. Although both cryptocurrencies are more influenced by the information contained in orders of their own, some of the information simultaneously influences the cryptocurrencies. Information also spreads between exchanges through order flows, so different exchanges could keep the same prices for certain cryptocurrencies. This confirms the important role of order flows in price discovery. This result is consistent with that of Makarov and Schoar (2018), who suggests that Bitcoin prices differ across countries but to a much less extent between the US and Europe. Information asymmetry is more pronounced on Kraken than on Bitfinex, as information contained in orders on Kraken has a more substantial impact on both Bitcoin and Ethereum fundamental values. This study helps investors develop trading strategies across exchanges and cryptocurrencies, and helps regulators understand the landscape of the fragmented market and thus how different exchanges and different cryptocurrencies are connected.

This paper is structured as follows. Section 3.2 presents a review of previous literature on cryptocurrency as an asset, highlighting the theories of how order flows influence asset prices in traditional asset classes and the empirical evidence. Sections 3.3 and 3.4 describe the data and methodology used in this paper, respectively. Section 3.5 provides the empirical results. A final section concludes.

3.2 Literature review

When it was created, cryptocurrency was seen only as a kind of currency (similar to US dollars and British pounds, for example) because of its function as a medium of exchange. However, it is now generally believed to be an emerging asset class of its own due to its price characteristics. Gronwald (2014) argues that the return on Bitcoin price is characterised by extreme movements and conditional heteroscedasticity; thus, it can be categorised as an immature asset class. Yermack (2015) notes that cryptocurrency appears to behave more as a speculative investment than a currency. Some researchers have applied regression or portfolio models to study cryptocurrency returns, highlighting the similarities with other asset classes. Makarov and Schoar (2018) find substantial arbitrage opportunities across exchanges in cryptocurrency markets. Borri and Shakhnov (2018) probe the risks associated with the across-exchange arbitrage activities, as well as the limits to arbitrage, and find that the largest price deviations occur in exchanges with greater probability of shut down, smaller Bitcoin supply, and larger volume and return volatility. Balcilar et al. (2017) study time-series Bitcoin data and find that volume contains information with which to predict Bitcoin return but fails in bear and bull market regimes. Hubrich (2017) uses carry, value, and momentum factors to construct cryptocurrency portfolios and concludes that these factors are effective for forecasting cryptocurrency returns. The above literature inspires us to consider the price formation of cryptocurrency as similar to other asset classes, such as foreign exchanges, stocks and bonds.

The literature on how asset price is determined, from the perspective of microstructure finance, has achieved some impressive results in the traditional asset classes. According to the theoretical model proposed by Hendershott and Menkveld (2014), price can be decomposed into two parts – fundamental value and pricing error, which are driven by order flows through 'price discovery' and 'price pressure', respectively. The findings of Hasbrouck (1991a) and Hasbrouck (1991b) suggest that private information contained in order flows can permanently affect stock price. Albuquerque et al. (2009) further argue that equity order flows driven by market-wide private information predict both equity and currency returns because order flows represent investors' heterogeneous expectations regarding firm values. Brandt and Kavajecz (2004) find that the yield curve in the US treasury market is permanently influenced by order flow imbalances, which they describe as the aggregation of heterogeneous private information. Regarding currencies, Evans and Lyons (2002b) suggest a similar framework in the FX market, where price can be largely explained by contemporaneous order flows and order flows do a better job than macro factors of explaining currency returns, especially at the high-frequency level. Even macroeconomic news and public information are impounded into FX price changes through order flows, as shown by Love and Payne (2008). Menkhoff et al. (2016) report substantial heterogeneity across different end-user segments in their trading style and risk exposure, such that order flows influence price in different ways.

In my research, I use SSF to decompose the observed price into fundamental value and pricing error, as done by, Hendershott and Menkveld (2014) because my purpose is to explore how order flows directly and simultaneously affect prices through both 'price discovery' and 'price pressure'. Evans and Lyons (2002b) adopt a regression method to explain currency returns by order flows, but they focus on how the fundamental values of currencies are determined by information. Hasbrouck (1991a), Hasbrouck (1991b), and Love and Payne (2008) study the informativeness of orders with a VAR model by decomposing return variance into trade-related and untrade-related components. Nagel (2012) uses a return reversal strategy to measure pricing errors, and Menkhoff et al. (2016) sort portfolios based on order flows to track informativeness. These methods all work well for tracking informativeness or pricing errors over time, capturing the time variation and relating this variation to other factors, but these methods can not simultaneously measure the direct effects of order flows on both parts of the prices. Therefore, although the purpose of this research is similar to those of these previous studies, I take a different approach.

Little research has studied the cryptocurrency market or its bubble in 2017 to 2018. It is typically believed that the value of cryptocurrency depends on two factors. First, characterised as a decentralised currency because no central bank could control the number of Bitcoin in the market, it can be seen as a libertarian response to central bank's failure to manage the financial crisis. Bitcoin can bypass national restrictions on international transfers, probably at a lower cost, according to Bariviera et al. (2017). Second, Bitcoin is a reward in the block-chain system; thus, as explained by Hileman and Rauchs (2017), its value depends on the development of block-chain technology. However, there are different views on the value of cryptocurrency, and various researchers attribute the bubble to different causes. Cheah and Fry (2015) argue that the fundamental value of Bitcoin is zero and that its price is a speculative bubble. Fry and Cheah (2016) find that certain events do have a detectable impact on the market previous bubble before it is brought to an end by an exogenous shock — a picture that seems qualitatively similar to the bursting of the internet stocks bubble in 2000. This comparison of the Bitcoin and dot com bubbles is made in purely qualitative terms by Yermack (2015). Li et al. (2018) and Xu and Livshits (2018) conclude that pump-and-dump schemes are pervasive in cryptocurrency, while the latter authors argue that these schemes drive the substantial Bitcoin price change between July and November 2017. In addition, Baur and Dimpfl (2018) find that positive shocks increase volatility by more than negative shocks, reflecting uninformed investors' fear-of-missing-out (FOMO) and the existence of pump-and-dump schemes. Most studies explain the bubble through the price discovery channel since they all contribute the bubbles to investors' misperception about fundamental values of cryptocurrencies.

The key contribution of this work is that it separates the fundamental value and the pricing error of a specific cryptocurrency, showing directly how order flows influence price through the processes of 'price discovery' and 'price pressure'. Although it is questionable whether the fundamental value reflects the real value, information permanently changes prices and makes the value part a random walk process. Using SSF, I can further study how order flows influence price across cryptocurrencies and across exchanges. The results may help cryptocurrency investors and regulators to better understand how the bubble formed and burst.

3.3 Data and summary statistics

3.3.1 Data

I obtain tick by tick trading data (including price, order flow and volume) of BTCUSD and ETHUSD for all trading hours between January 2017 and January 2018 on Bitfinex and Kraken from Kaiko, a data provider in cryptocurrency market that collects data directly from exchanges. Both cryptocurrencies are traded 24 hours per day and seven days per week, but sometimes there is no data available from the exchanges. For example, the longest closed period for BTCUSD trading on Bitfinex is about three days from 4th August to 6th August, because the exchange was hacked according to the company's announcement. Although Kraken was never hacked, no BTCUSD trading data on 6th August was available from the provider. I also exclude those days with less than 1,000 transactions per day and those minutes when returns (in b.p.) are larger than 500 .

3.3.2 Summary statistics

Figure 3.1 shows how Bitcoin and Ethereum prices vary over time on Bitfinex and Kraken, respectively. Both Bitfinex and Kraken are leading exchanges in cryptocurrency market. Bitfinex is based in Hong Kong (owned by a US parent company) with world wide clients. Kraken is based in San Francisco but it is the largest Bitcoin exchange in Euro volume. The figures demonstrate that prices on two exchanges are nearly the same, consistent with Makarov and Schoar (2018) who have found that price deviations between the most liquid exchanges in the US and Europe are small.

Figure 3.1a demonstrates that Bitcoin price becomes volatile in May, and then increases significantly from May to December 2017. After mid-December, the price becomes even more volatile and declines rapidly. Before May, the price is volatile in January and March, due to two exogenous impacts. In January 2017, the People's bank of China, China's central bank, tightened its oversight of the country's Bitcoin exchanges. Some biggest Bitcoin exchanges then halted withdrawals followed by shut-downs later that year. The regulations led to a big fall in Bitcoin trading volume but its price was not much influenced in the end. In March 2017, a Bitcoin ETF was rejected by the US Securities and Exchange Commission (SEC). But the SEC left the door open for future Bitcoin exchange products. Therefore, although Bitcoin price fell immediately after the rejection, it recovered to its previous level after a few days. From May to December, Bitcoin price climbed all the way till a history record of US$20,000 accompanied by a big number of initial coin offerings (ICOs).

Figure 3.1b shows that Ethereum price increases rapidly from May to June 2018 to US$400, then lingers for four months, and shoots up to US$1,600 from mid-November 2017 to mid-January 2018. Ethereum became an important cryptocurrency after May 2017 because with the idea of smart contracts, Ethereum could provide some technology companies with a good platform for ICOs.

Figure 3.2 shows daily returns of Bitcoin and Ethereum traded on both exchanges. Returns are volatile during the whole period, but we can still find volatility clusters, common in other asset classes, on both exchanges.

FIGURE 3.1: Bitcoin & Ethereum Prices

This figure depicts how Bitcoin and Ethereum prices change over time from January 2017 to January 2018.

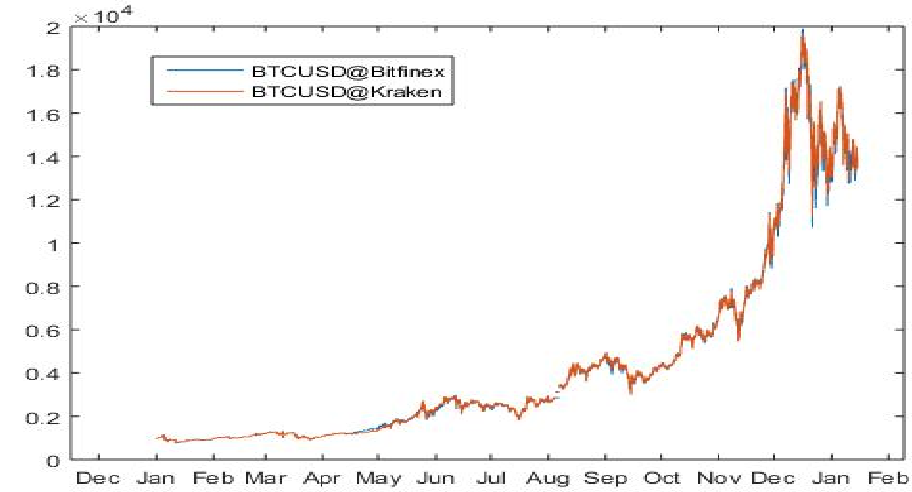

(A) BTCUSD

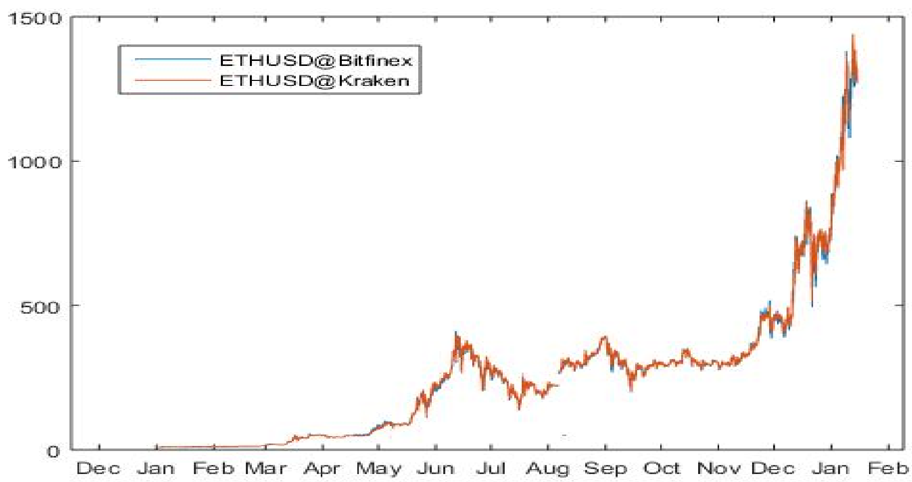

(B) ETHUSD

FIGURE 3.2: Bitcoin & Ethereum Returns

This figure depicts how Bitcoin and Ethereum returns change over time from January 2017 to January 2018.

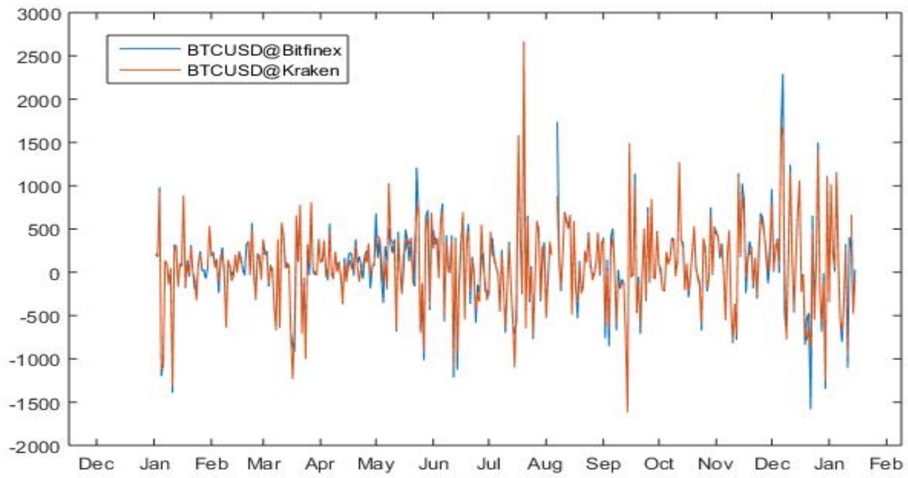

(A) BTCUSD

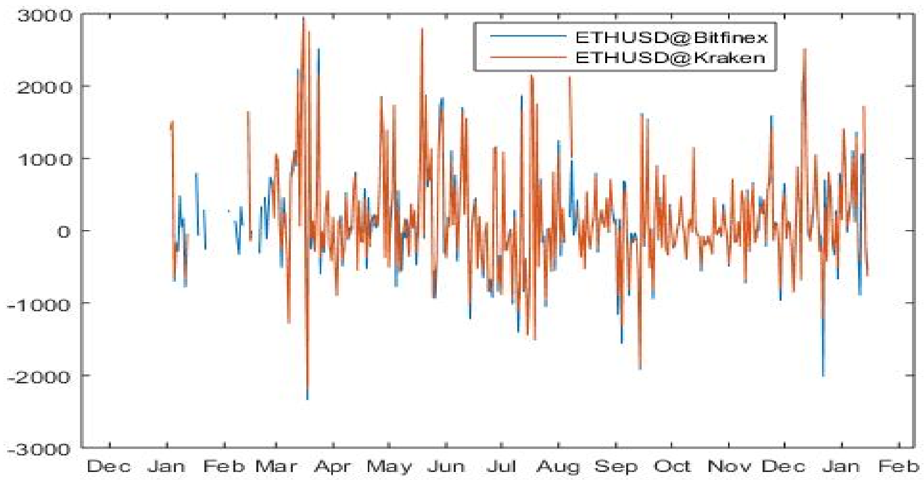

(B) ETHUSD

Table 3.1 reports mean, standard deviation, first autocorrelation, skewness and kurtosis of returns (in b.p.), order flows and trading volumes (in number of cryptocurrency and in USD) of both cryptocurrencies on Bitfinex and Kraken, aggregated every 10 minutes. Both cryptocurrencies have positive returns during the period with big standard deviations, slightly negative 1st autocorrelation, negative skewness, and huge kurtosis (due to some outliers). Mean returns, return standard deviations, and mean order flows are all similar between the two exchanges, but order flow standard deviations on Kraken are much smaller than those on Bitfinex. Volumes of both cryptocurrencies on Bitfinex are five times more than on Kraken. During my sample period, mean return of Bitcoin is positive while mean order flow on both exchanges are negative.

Figure 3.3 demonstrates trading volumes of BTCUSD and ETHUSD for each day within a week. As shown in the figure, unlike most assets, Bitcoin is most actively traded during weekends in 2017. It seems that most participators in the market are non-institutional investors. Ethereum has the largest trading volumes on Wednesdays and Thursdays. Figure 3.4 shows trading volumes every two hours in one day from mid-night (12:00 UTC). The figures indicate that on both exchanges, Bitcoin and Ethereum are actively traded throughout a day, with 14:00-16:00 slightly more actively traded than other time. Table 3.2 summarises trading information of BTCUSD and ETHUSD on Bitfinex and Kraken. The average trade size during my sample period is very small, with a big number of daily transactions. It confirms that most participants in the market are non-institutional investors.

TABLE 3.1: Summary Statistics

This table presents summary statistics of return, order flow and trading volume of Bitcoin and Ethereum, aggregated every 10 minutes from January 2017 to January 2018, traded on Bitfinex and Kraken. Returns (in b.p.) are calculated by the price of the last trade within the 10 minutes, while order flows and volumes are combined every 10 minutes.

Panel A: BTCUSD on Bitfinex

	mean	st. dev.	1st autoco.	skew	kurtosis
Return	0.7232	48.0123	-0.0574	-0.2481	15.6890
Order Flow	-2.0210	167.1504	0.1793	-1.5468	78.7349
Volume (in no. of cryptocurrency)	212.6146	325.7770	0.6438	6.0280	91.4554
Volume (in USD)	1298100	2614100	0.8118	4.5111	35.9912

Panel B: ETHUSD on Bitfinex

	mean	st. dev.	1st autoco.	skew	kurtosis
Return	1.1587	65.9245	-0.0580	-0.0125	10.9796
Order Flow	12.7988	1218.2	0.2267	-1.1010	69.0527
Volume (in no. of cryptocurrency)	1364.1	2017.8	0.5938	4.7295	42.6998
Volume (in USD)	427710	765690	0.7971	4.3693	42.6998

Panel C: BTCUSD on Kraken

	mean	st. dev.	1st autoco.	skew	kurtosis
Return	0.5752	47.2959	-0.0505	-0.3605	14.6890
Order Flow	-1.7517	29.0941	0.1974	-0.5367	51.4132
Volume (in no. of cryptocurrency)	33.0141	40.4923	0.5342	3.8729	34.0581
Volume (in USD)	140490	216190	0.6480	4.2766	33.5024

Panel D: ETHUSD on Kraken

	mean	st. dev.	1st autoco.	skew	kurtosis
Return	1.1135	68.8310	-0.1071	-0.0378	10.6146
Order Flow	25.6904	561.3235	0.2340	1.7841	74.5016
Volume (in no. of cryptocurrency)	459.5386	767.8794	0.5380	5.3164	56.4448
Volume (in USD)	104890	169890	0.6186	4.4294	56.4448

FIGURE 3.3: Trading Volume by Weekday

This figure depicts trading volume (in no. of cryptocurrency) of Bitcoin and Ethereum on Bitfinex and Kraken each day within a week from Sunday to Saturday.

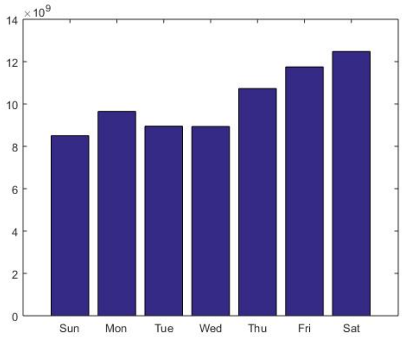

(A) BTCUSD on Bitfinex

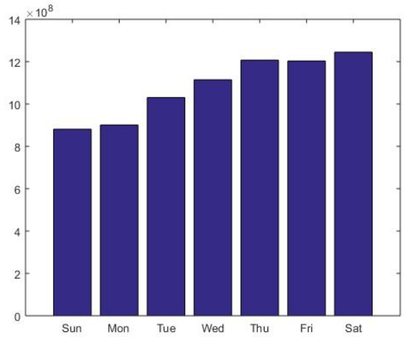

(B) BTCUSD on Kraken

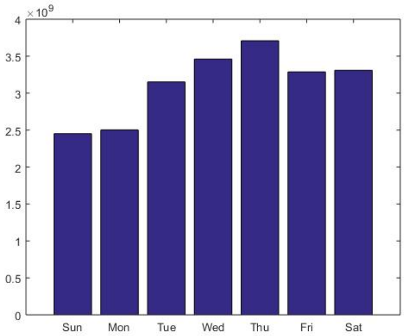

(C) ETHUSD on Bitfinex

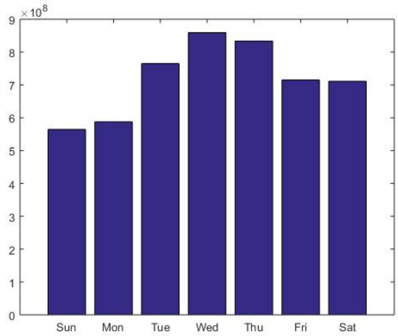

(D) ETHUSD on Kraken

FIGURE 3.4: Trading Volume by Hour

This figure depicts trading volume (in no. of cryptocurrency) of Bitcoin and Ethereum on Bitfinex and Kraken every two hours from 12:00 (in UST).

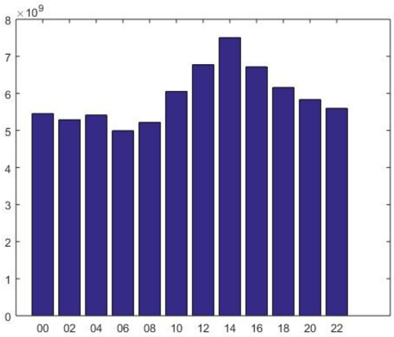

(A) BTCUSD on Bitfinex

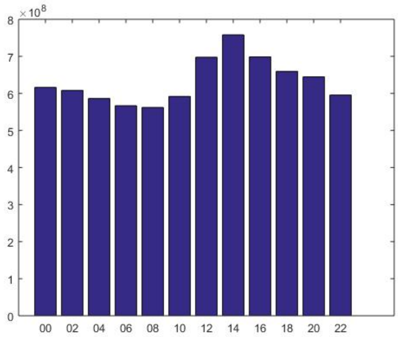

(B) BTCUSD on Kraken

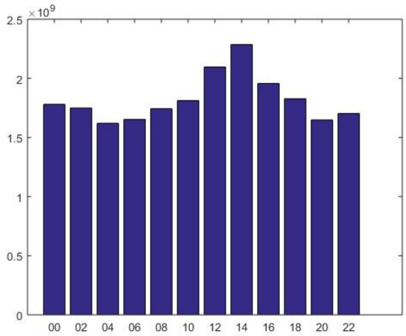

(C) ETHUSD on Bitfinex

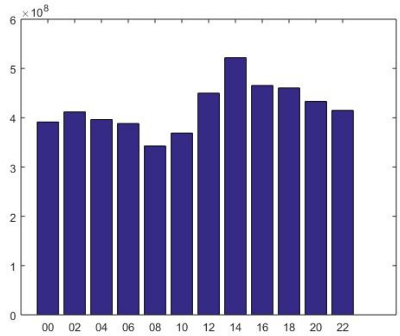

(D) ETHUSD on Kraken

TABLE 3.2: Trading Frequency

This table presents average trade size (in number of shares) and number of trades every day for BTCUSD and ETHUSD traded on Bitfinex and Kraken from 01/01/2017 to 15/01/2018.

	BTC/Bitfinex	BTC/Kraken	ETH/Bitfinex	ETH/Kraken
Trade Size	0.5500	0.3434	5.8590	5.4777
No. of Trades	55720	13689	31850	11097

3.4 Methodology

I use a state space form (SSF) approach, the same as the one used in the previous chapter. The SSF is shown below:

$$p_t = m_t + s_t \tag{3.1}$$

$$m_t = m_{t-1} + \beta \hat{X}_t + e_t \tag{3.2}$$

$$s_t = \phi s_{t-1} + \alpha X_t + u_t \tag{3.3}$$

where p_t is the observed log price of cryptocurrency; m_t is unobserved efficient price process and s_t is unobserved pricing error process; e_t and u_t are uncorrelated i.i.d. process. X_t is investors' order flow. $\hat{X}_t$ is investors' order flow 'surprise'. $\hat{X}_t$ is estimated by the residual term of the equation below:

$$X_t = \gamma_1 X_{t-1} + \gamma_2 X_{t-2} + \gamma_3 X_{t-3} + ... + v_t \tag{3.4}$$

The number of lagged order flows in equation (3.4) is determined by the Schwarz information criterion.

I add up order flows every 10 minutes as X_t, and obtain the price of the last trade within the 10 minutes as the corresponding price p_t.[2]At the end of each day, I obtain the SSF estimates and a Hessian matrix associated with the estimates with those 10-minute prices and order flows within the most recent week by Kalman Filter. Standard errors are then calculated by the Hessian matrix. Therefore, the daily parameter β in equation 3.2 indicates the impact of private information contained in orders on the fundamental value and α in equation 3.3 demonstrates the impact of liquidity providers' inventory control on the pricing error.

Although the unobserved efficient price process m_t is referred to as 'fundamental value' in my research, in the same way as the model of Hendershott and Menkveld (2014), it does not necessarily mean that m_t reflects the 'true' intrinsic value of the

[2]In application, p_t is cumulative log returns from the beginning of the week.

security determined by its future cash flows, especially in our case – an irrational exuberance in cryptocurrency market. The 'fundamental value' in my research refers to an unobserved random walk process determined by information contained in informed investors' orders and how uninformed investors react to those orders. While the remaining part of price is a mean-reversal process mainly caused by liquidity providers' inventory control. In 2017, the total market value of cryptocurrencies increased by more than 30 times and then in 2018 decreased by nearly 80%. Therefore, over a long time span, much of Bitcoin or Ethereum price during the bubble is transitory. However, in my setting, only the immediate mean-reversal part of price is deemed as 'pricing error' because liquidity providers would not hold extra inventory for long, while the random walk part is deemed as 'fundamental value', because all the historical information is impounded into this part.

To study how order flows of one cryptocurrency on one exchange influence the price of another cryptocurrency on the same exchange or the price of the same cryptocurrency on another exchange, I add one more order flow factor to the SSF as follows:

$$m_t = m_{t-1} + \beta_1 \hat{X}_{t1} + \beta_2 \hat{X}_{t2} + e_t \quad (3.5)$$

$$s_t = \phi s_{t-1} + \alpha_1 X_{t1} + \alpha_2 X_{t2} + u_t \quad (3.6)$$

where p_t is the observed log price of a certain cryptocurrency; e_t and u_t are uncorrelated i.i.d. process. X_{t1} is investors' order flow of the same cryptocurrency on the same exchange. X_{t2} is investors' order flow of another cryptocurrency or on another exchange. $\hat{X}_{t1}$ is investors' order flow 'surprise'. $\hat{X}_{t2}$ is investors' order flow 'surprise' of another cryptocurrency or on another exchange.

3.5 Empirical results

Table 3.3 presents the estimates of SSF, defined by equations (3.1), (3.2), and (3.3), for BTCUSD traded on Bitfinex each month. Parameters are estimated based on price and order flow data, aggregated every 10 minutes for a one-week rolling window, at the end of each day. The monthly mean is then calculated using the parameters estimated every day. The estimates for β in Table 3.3 are all significantly positive and thus consistent with our hypothesis that order flow innovations contain information impounded into Bitcoin prices. In addition, this suggests either that some people in the market have private information about Bitcoin (according to Evans and Lyons (2002a)) or that some people make 'smarter' decisions than others when public information is released (according to Love and Payne (2008)). Similar to other asset classes, buy (sell) orders increase (decrease) the fundamental value of Bitcoin; thus, on Bitfinex, order flows of Bitcoin influence price through price discovery. For example, in June 2017, β is 0.2544, suggesting that, on average, one more buy (sell) order (in number of Bitcoin) initiated by investors increased (decreased) its fundamental value by 0.2544 (in b.p.) in that month. Therefore, buy order 'surprise' contains 'good news', and reflects informed investors' optimistic views of the fundamental value of Bitcoin, leading to an increase in its fundamental value, while sell order 'surprise' leads to a decrease in its fundamental value.

The relationship between fundamental value and order flow surprise is shown in Figure 3.5a. However, the figure indicates that, from January 2017 to January 2018, monthly average order surprises of Bitcoin are negative in most months, suggesting that, on average, 'bad news' led informed investors to 'unexpectedly' sell Bitcoin on Bitfinex, while monthly fundamental value changes are positive in most months before 2018. For example, in May, β is significantly positive and larger than in previous months, and monthly mean of order flow surprises is negative; however, fundamental value change is positive on average. A possible explanation for these seemingly contradictory results is that fundamental value is more sensitive to unexpected buy orders of informed investors than to unexpected sell orders. Therefore, we can infer two possible causes of the bubble: liquidity providers significantly increasing their

TABLE 3.3: Monthly SSF parameters - Bitcoin on Bitfinex

This table presents estimated parameters in the following state space model:

$$p_t = m_t + s_t$$
$$m_t = m_{t-1} + \beta \hat{X}_t + e_t$$
$$s_t = \phi s_{t-1} + \alpha X_t + u_t$$

where p_t is the observed log price (cumulative log return from the beginning of the week); m_t is the fundamental value; s_t is pricing error; e_t and u_t are uncorrelated i.i.d. processes. $\hat{X}_t$ is investors' order flow innovation. X_t is investors' order flow. Daily parameters are estimated by 10-minute price and order flow of BTCUSD from January 2017 to January 2018 on Bitfinex, and then averaged every month.

	β	t-stats	α	t-stats	ϕ	σ_e	σ_u
17-Jan	0.1291	23.2197	0.0406	8.5781	0.5692	642.2040	250.3840
17-Feb	0.1070	31.6820	0.0135	5.5648	0.2883	161.6082	72.7879
17-Mar	0.0978	24.1884	0.0278	8.3805	0.1846	581.6286	166.8791
17-Apr	0.0919	18.3876	0.0381	6.9139	0.5847	163.9524	106.1653
17-May	0.1948	16.9662	0.0718	6.9775	0.4506	1255.6012	199.8808
17-Jun	0.2592	19.9043	0.1164	8.7528	0.4839	1338.5778	657.0468
17-Jul	0.1884	18.8293	0.0605	9.5242	0.3817	1375.4687	345.5362
17-Aug	0.1336	14.3883	0.0559	7.7015	0.5475	504.4355	389.1771
17-Sep	0.1304	22.2606	0.0167	4.1490	0.2503	849.7834	425.7388
17-Oct	0.0882	28.3848	0.0194	8.1781	0.5157	282.3755	257.0814
17-Nov	0.1235	31.8711	0.0252	5.7069	0.2597	731.3254	300.2367
17-Dec	0.2251	23.2744	0.1474	11.7585	0.6461	2471.5626	1491.8629
18-Jan	0.2669	26.2210	0.1391	14.2113	0.4893	1964.9388	561.0867

quotes when buy orders arrived, and not adjusting their quotes accordingly when sell orders arrived.

FIGURE 3.5: Bitcoin Monthly Order Flows and Returns

The figures display average order flow innovations and fundamental value changes of Bitcoin every month from January 2017 to January 2018 on Bitfinex and Kraken. Fundamental value is obtained from the following state space form:

$$p_t = m_t + s_t$$
$$m_t = m_{t-1} + \beta\hat{X}_t + e_t$$
$$s_t = \phi s_{t-1} + \alpha X_t + u_t$$

where p_t is the observed log price (cumulative log return from the beginning of the week) of the currency; m_t is the information part (and $\delta m_t = m_t - m_{t-1}$); s_t is pricing error; e_t and u_t are uncorrelated i.i.d. processes. $\hat{X}_t$ is investors' order flow innovation. X_t is investors' order flow.

Investors' order flow$\hat{X}_t$ is the residual term of the following equation:

$$X_t = \gamma_1 X_{t-1} + \gamma_2 X_{t-2} + \gamma_3 X_{t-3} + ... + v_t$$

Fundamental value change is thus δm_t and order flow innovation is $\hat{X}_t$.

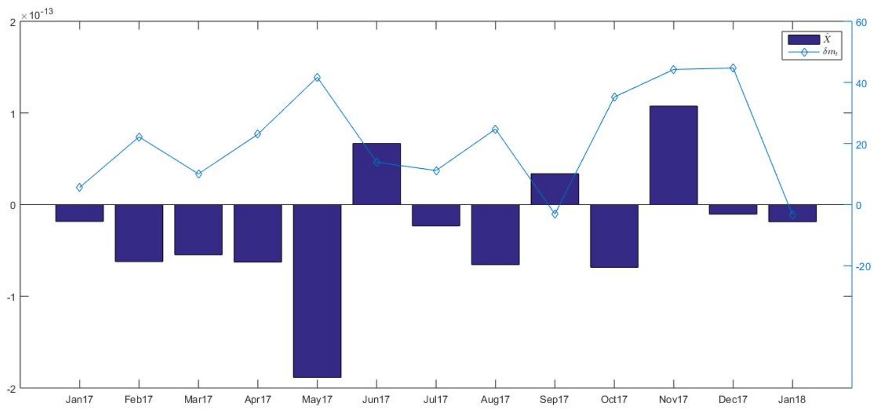

(A) BTCUSD on Bitfinex

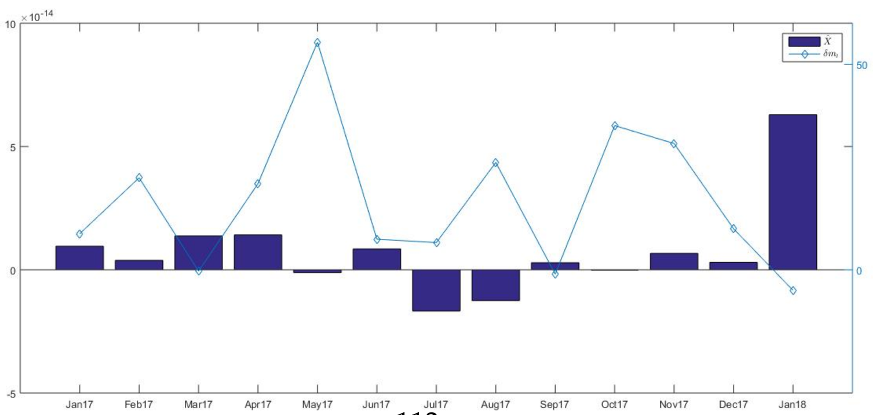

(B) BTCUSD on Kraken

First, liquidity providers may significantly increase their quotes in response to buy orders due to FOMO. From May 2017, many ICOs were launched, which confirmed investors' expectations that the cryptocurrency market would prosper and become an important payment and clearing method. Figure 3.6 shows the total funds raised for ICOs every month after January 2017, with most funded through Bitcoin or Ethereum. Some cryptocurrency prices increased sharply and immediately after their ICOs. For example, the price of Nexus increased by more than 50% immediately after the Project Research and Development scheme began. As more investors sought to invest in those ICOs and trade the newly issued cryptocurrencies, the convenience yield of Bitcoin (and Ethereum) increased significantly, corresponding to the theory proposed by Cochrane (2002) to explain the tech-stock bubble. The Cochrane (2002) theory of convenience yield associates high prices with high volume, high volatility, low supply of shares, wide dispersion of opinion, and restrictions on long-term short selling. The cryptocurrency market shared these characteristics during the bubble in 2017. In addition, Li et al. (2018) review the existence of a 'pump-and-dump' scheme during the bubble. They argue that the fake ICOs, due to lack of regulation in the market, led to a surging demand for Bitcoin (and Ethereum) and 'pumped' the prices of some newly issued cryptocurrencies to attract more people to join the exuberance. As noted by Kyle (1985b) and Hasbrouck (1991b), the influence of order flows on fundamental value reflects the extent of information asymmetry, and the impact reflects the probability that such an order is informed. Therefore, the information about ICOs and technology revolutions misled the uninformed liquidity providers to believe that an unexpected buy order always contained much information and that an unexpected sell order was probably from noise traders. Second, the fundamental value of Bitcoin being less responsive to sell orders may be due to manipulated support from Tether. As mentioned by Griffin and Shams (2018), Bitfinex's sister company, Tether Ltd., backed the Bitcoin price by falsely issuing Tether whenever the price dropped. My results are consistent with this theory as, despite many sell orders, Tether Ltd. could always quote a price to prevent a Bitcoin price drop. It is emphasised that, although I call the random walk process decided by order innovation 'fundamental value', it does not reflect the real 'value', especially during a bubble. In my case, the fundamental value part of the asset price cannot guarantee a rational expectation of future cash flows, but it does reflect investors' irrational responses to both private and public information.

FIGURE 3.6: ICO Fund Raised in USD

This figure depicts the total fund (in USD) raised during ICOs each month from January 2017 to April 2018. The data is obtained from www.icodata.io. In this database, the total fund raised each month is calculated as the sum of the funds raised for all ICOs that ends within that month. For example, the ICO of Dragon coin (DRG) began in December 2017, and finished in March 2018. Therefore, the total USD$320, 000, 000 is said to have been raised in March 2018.

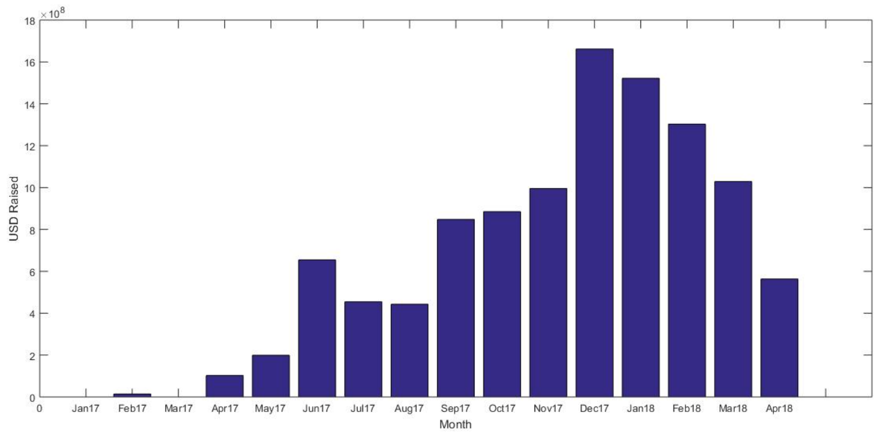

Table 3.3 also indicates that β in each month changes over time. During May to July 2017 and mid-December 2017 to January 2018, β is much larger than in other months, demonstrating that information asymmetry exacerbated during these periods. For example, β in October is 0.0882; thus, one more customer buy order surprise would increase the fundamental value by 8.82% (in b.p.), while, in January 2018, β rises to 0.2469. This suggests that the fundamental value part is more sensitive to orders in May, June, July, and December 2017 and January 2018. Figure 3.7a illustrates how the β of Bitcoin on Bitfinex and its 95% confidence interval change over the period. In addition, in May to July and late December 2017 to January 2018, β is larger

than in other months, confirming that the fundamental value of Bitcoin is more sensitive to order flows in those months on Bitfinex. According to Gorton and Metrick (2009), one theory that may explain the sudden increase in information asymmetry is that a large adverse shock increases information sensitivity and thus aggravates the adverse selection problem. For example, the previous chapter concludes that the average β of small-cap FTSE100 stocks increased from 6.61 to 14.05 during the 2008 global financial crisis, likely due to the aggravated adverse selection problem. However, this theory only explains increased information asymmetry after a negative shock, and it cannot explain the situation in May, June, and July, when the bubble began in the cryptocurrency market. The results indicate that uninformed investors in the cryptocurrency market believed orders (especially buy orders) contained more private information regarding the cryptocurrency's value from May to July, leading to the bubble. However, this paper does not test how impacts of buy orders and sell orders on price change, respectively. By discriminating between buy orders and sell orders in SSF, future research could directly test the hypothesis that the fundamental value of Bitcoin price was more sensitive to buy orders than sell orders when the bubble began.

FIGURE 3.7: Time Variation of β

This figure depicts how β changes over time from January 2017 to January 2018 with its 95% confidence interval. The estimate is obtained from the following state space model

$$p_t = m_t + s_t$$
$$m_t = m_{t-1} + \beta \hat{X}_t + e_t$$
$$s_t = \phi s_{t-1} + \alpha X_t + u_t$$

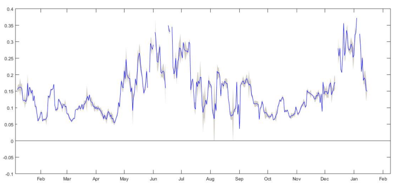

(A) BTCUSD on Bitfinex

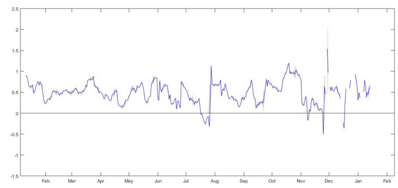

(B) BTCUSD on Kraken

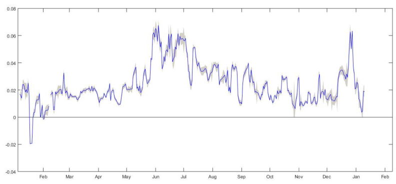

(C) ETHUSD on Bitfinex

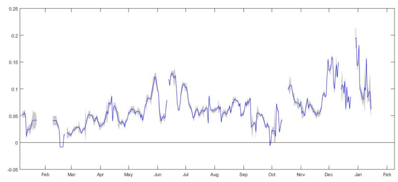

(D) ETHUSD on Kraken

As demonstrated in Table 3.3, α is significantly positive in every month, indicating that customers' buy (sell) orders caused temporary positive (negative) pricing errors in intra-day trading. The results are consistent with the inventory-control theory. The temporary positive (negative) pricing error occur because customers' buy (sell) orders decrease (increase) liquidity providers' inventory, and, to bring their inventory back to the original level, liquidity providers are obliged to offer a higher (lower) price to induce more sell (buy) orders. Additionally, α is much larger in June, December, and January. For example, if investors bough one more Bitcoin in November, this increased the pricing error by 2.5% (in b.p.), while, in December, every Bitcoin that investors bought increased it by 14% (in b.p.). The results suggest that liquidity providers were less willing to provide liquidity and tended to control their inventory more cautiously, which led to larger pricing errors for every order in June, December, and January. This could also be interpreted as liquidity providers requiring a higher expected return through pricing errors to compensate for increased liquidity provision costs in those months. The variation of α in Figure 3.8a confirms that α increases from May to June 2017 and from December 2017 to January 2018. The increased α after December followed a negative shock, while the increased α from May to June did not. Therefore, the literature proposing models to explain tighter inventory control after a large negative shock (such as Brunnermeier and Pedersen (2009) and Chordia et al. (2002)) cannot explain the increased α from May to June.

FIGURE 3.8: Time Variation of α

This figure depicts how α changes over time from January 2017 to January 2018 with its 95% confidence interval. The estimate is obtained from the following state space model

$$p_t = m_t + s_t$$
$$m_t = m_{t-1} + \beta \hat{X}_t + e_t$$
$$s_t = \phi s_{t-1} + \alpha X_t + u_t$$

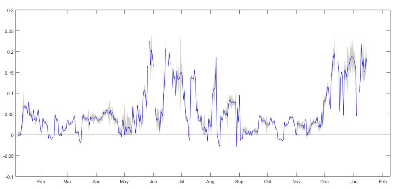

(A) BTCUSD on Bitfinex

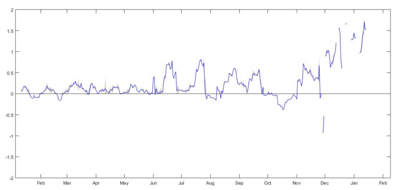

(B) BTCUSD on Kraken

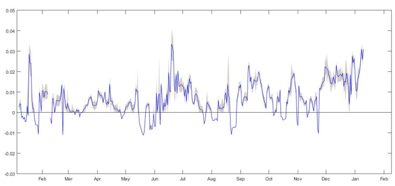

(C) ETHUSD on Bitfinex

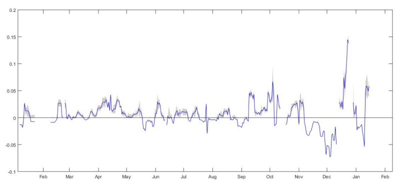

(D) ETHUSD on Kraken

Table 3.4 presents the β and α of Bitcoin traded on Kraken from January 2017 to January 2018. β is positive and significant in each month throughout the whole period. This confirms that, on Kraken, private information is also impounded into price through order flows. Compared to the results estimated by Bitfinex data, β is much larger, suggesting that information contained in order flows on Kraken has a greater impact on the fundamental value. Therefore, information asymmetry is more pronounced on Kraken. As suggested by Table 3.1 and Figure 3.5b, the trading volume and absolute values of both order flow and order flow surprise on Kraken are much smaller than those on Bitfinex, but Bitcoin prices are very similar between two exchanges. Thus, it is reasonable that orders on Kraken are more informative. Figure 3.7b shows that β on Kraken does not vary as extensively as β on Bitfinex. The results suggest that, on Kraken, information asymmetry was not aggravated when the boom started. Therefore, the variations in information asymmetry over time differ slightly between the two exchanges, probably because most investors on Bitfinex are from the US and Asia Pacific, while most of Kraken's customers are in Europe. The results also provide evidence for the argument that Tether, related only to Bitfinex, played an important role in 'supporting' Bitcoin price. Makarov and Schoar (2019a) also conclude that Bitfinex (Tether) is the most important market for price discovery. α is also positive and significant most of the time, larger than α on Bitfinex, meaning that one unit of order flow had a more significant impact on pricing error on Kraken. In late December 2017 and January 2018, when the market declined, α increased (as shown in the table and in Figure 3.8b), suggesting that liquidity providers were less willing to provide liquidity during that period, as in other asset classes after a negative market shock.

Figure 3.9 displays the fundamental value and pricing error obtained from observed price (weekly cumulative log returns in my research) separately. Figures 3.9a and 3.9b demonstrate that the fundamental value is the dominant component of Bitcoin price, and the pricing error diminishes very quickly and does not accumulate over time. Thus, Bitcoin price is primarily determined by information.

TABLE 3.4: Monthly parameters - Bitcoin on Kraken

This table presents estimated parameters in the following state space model:

$$p_t = m_t + s_t$$
$$m_t = m_{t-1} + \beta\hat{X}_t + e_t$$
$$s_t = \phi s_{t-1} + \alpha X_t + u_t$$

where p_t is the observed log price (cumulative log return from the beginning of the week); m_t is the fundamental value; s_t is pricing error; e_t and u_t are uncorrelated i.i.d. processes. $\hat{X}_t$ is investors' order flow innovation. X_t is investors' order flow. Daily parameters are estimated by 10-minute price and order flow of BTCUSD from January 2017 to January 2018 on Kraken, and then averaged every month.

	β	t-stats	α	t-stats	ϕ	σ_e	σ_u
17-Jan	0.7354	22.7436	0.0064	0.2481	0.2006	9642.1093	9182.9866
17-Feb	0.4548	29.0582	0.0253	1.4811	0.1191	359.1098	198.1281
17-Mar	0.6127	33.6936	0.1478	7.5574	0.0539	1106.4072	741.8906
17-Apr	0.3463	24.8722	0.0758	3.7341	0.2099	198.5200	282.1554
17-May	0.5694	33.4660	0.0757	5.4600	-0.0037	1592.3095	452.2081
17-Jun	0.4530	27.8300	0.3029	14.1216	0.4750	1529.5792	293.4830
17-Jul	0.2328	6.1445	0.2602	10.2742	0.4462	5542.7547	4687.7926
17-Aug	0.4552	35.8495	0.1987	19.2096	0.6555	465.3547	516.9785
17-Sep	0.4706	21.2305	0.2487	14.1716	0.8102	603.5621	805.3443
17-Oct	0.8189	52.3842	-0.1281	-12.4450	0.0072	547.7920	66.0117
17-Nov	0.3139	5.1486	0.2585	5.6668	0.6268	20876.3207	3215.0226
17-Dec	0.6050	16.4278	1.0615	30.3378	0.9045	14140.1583	6783.4480
18-Jan	0.5903	23.7461	1.2275	51.3894	0.9278	1277.6579	1114.1873

FIGURE 3.9: Fundamental Value and Pricing Error

The figures display fundamental values and pricing errors obtained from the state space form below:

$$p_t = m_t + s_t$$
$$m_t = m_{t-1} + \beta \hat{X}_t + e_t$$
$$s_t = \phi s_{t-1} + \alpha X_t + u_t$$

where p_t is the observed log price (cumulative log return from the beginning of the week) of the cryptocurrency; m_t is the fundamental value part; s_t is the pricing error part; e_t and u_t are uncorrelated i.i.d. processes. $\hat{X}_t$ is investors' order flow innovation. X_t is investors' order flow.

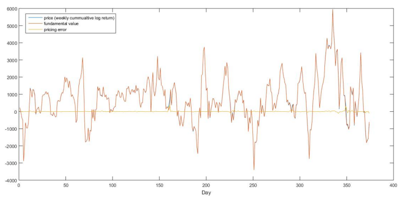

(A) BTCUSD on Bitfinex

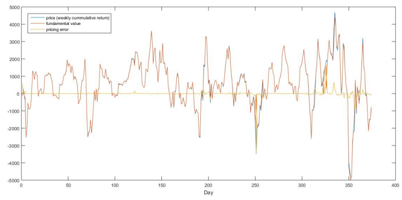

(B) BTCUSD on Kraken

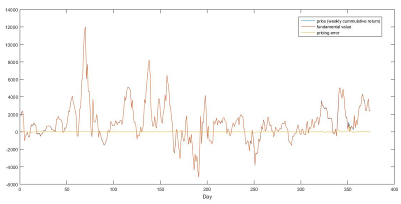

(C) ETHUSD on Bitfinex

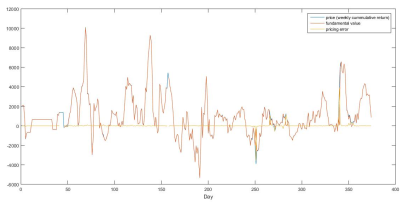

(D) ETHUSD on Kraken

Tables 3.5 and 3.6 indicate that βs of Ethereum traded on Bitfinex and Kraken from January 2017 to January 2018 are also positive and significant, demonstrating that information is impounded into the Ethereum price through order flows. Figure 3.7c shows that the β of Ethereum on Bitfinex is much larger in June and July 2017, and January 2018, immediately following the increase of β for Bitcoin on Bitfinex. Table 3.5 also shows that α is significantly positive on Bitfinex most of the time, consistent with Bitcoin results. However, estimates for α of Ethereum on Kraken are not statistically significant. Figure 3.8c suggests that α varies over time and increases in June 2017, December 2017, and January 2018. Figures 3.7d and 3.8d illustrate the variation in β and α of Ethereum traded on Kraken between June 2017 and January 2018. The results are similar to those for Bitcoin traded on Kraken, which proves that information was the key to the bubble and its bursting.

TABLE 3.5: Monthly SSF parameters - Ethereum on Bitfinex

This table presents estimated parameter in the following state space model:

$$p_t = m_t + s_t$$
$$m_t = m_{t-1} + \beta \hat{X}_t + e_t$$
$$s_t = \phi s_{t-1} + \alpha X_t + u_t$$

where p_t is the observed price (cumulative log return from the beginning of the week); m_t is the fundamental value; s_t is pricing error; e_t and u_t are uncorrelated i.i.d. processes. $\hat{X}_t$ is investors' order flow innovation. X_t is investors' order flow. Daily parameters are estimated by 10-minute price and order flow of ETHUSD from January 2017 to January 2018 on Bitfinex, and then averaged every month.

	β	t-stats	α	t-stats	ϕ	σ_e	σ_u
17-Jan	0.0096	4.9010	0.0026	1.1562	0.4896	1219.1967	909.3222
17-Feb	0.0165	10.6048	0.0029	1.6740	0.3048	417.7813	404.6383
17-Mar	0.0178	22.6461	0.0021	2.8561	-0.0891	3215.2168	877.5785
17-Apr	0.0160	17.5382	0.0042	3.9174	0.2772	797.1743	665.6256
17-May	0.0297	19.6685	-0.0001	-0.1041	0.1340	3060.9228	1076.5851
17-Jun	0.0528	19.9906	0.0104	3.7632	0.4078	2960.2500	1283.6409
17-Jul	0.0382	20.3581	0.0059	3.9119	-0.0553	3548.2909	373.6030
17-Aug	0.0293	20.3061	0.0010	0.5987	0.2910	890.1353	389.1772
17-Sep	0.0237	15.8610	0.0118	10.5951	0.6100	1536.6385	597.9873
17-Oct	0.0179	12.5917	0.0060	5.5064	0.4856	523.3284	211.2586
17-Nov	0.0148	11.3539	0.0060	6.1226	0.7138	675.4424	350.3982
17-Dec	0.0281	11.8684	0.0174	7.8979	0.8651	1796.1728	2933.6846
18-Jan	0.0196	7.6064	0.0266	13.3388	0.8592	2952.6091	694.4994

As shown in Figures 3.1a and 3.1b, the cryptocurrency market was volatile between May and June 2017, which was the start of the cryptocurrency boom, following the Ethereum revolution. Due to active ICOs, the cryptocurrency market as a whole increased from June to December 2017, with less volatility. After mid-December, the bubble burst. Bitcoin price fell and became volatile first, followed by Ethereum price. The previous tables and figures show that β and α are also larger in May, June, December, and January than in other months. Figures 3.10 and 3.11 demonstrate how β and α of Bitcoin and Ethereum correlate with daily realised

TABLE 3.6: Monthly parameters – Ethereum on Kraken

This table presents estimated parameters in the following state space model:

$$p_t = m_t + s_t$$
$$m_t = m_{t-1} + \beta \hat{X}_t + e_t$$
$$s_t = \phi s_{t-1} + \alpha X_t + u_t$$

where p_t is the observed price (cumulative log return from the beginning of the week); m_t is the fundamental value; s_t is pricing error; e_t and u_t are uncorrelated i.i.d. processes. $\hat{X}_t$ is investors' order flow innovation. X_t is investors' order flow. Daily parameters are estimated by 10-minute price and order flow of ETHUSD from June 2017 to January 2018 on Kraken, and then averaged every month.

	β	t-stats	α	t-stats	ϕ	σ_e	σ_u
17-Jan	0.0382	7.9307	-0.0007	-0.1642	0.5038	1451.8213	2149.8679
17-Feb	0.0268	7.3619	0.0001	0.0327	0.4140	571.0846	1120.6063
17-Mar	0.0341	14.8920	0.0032	1.3590	0.1261	4141.2617	2579.8925
17-Apr	0.0485	13.7706	0.0208	4.9539	0.3096	800.5308	1346.3850
17-May	0.0716	21.7103	-0.0017	-0.4461	0.1687	2886.3923	1458.9455
17-Jun	0.0871	2.3157	0.0061	0.1656	0.0807	3223.5338	878.4638
17-Jul	0.0645	23.4090	0.0005	0.2093	0.1417	4229.6961	1415.3066
17-Aug	0.0630	18.5133	-0.0001	-0.0247	0.3201	647.6130	666.9573
17-Sep	0.0453	12.3887	0.0150	4.7846	0.5988	1363.4341	2750.9476
17-Oct	0.0762	5.6710	0.0102	0.7205	0.2272	145358.7071	72141.4262
17-Nov	0.0713	21.3767	-0.0149	-4.5365	0.1878	665.9035	316.3801
17-Dec	0.1005	14.5109	0.0425	5.4762	0.6001	1670.2785	7969.7828
18-Jan	0.1289	22.6361	-0.0221	-5.0187	-0.2377	2983.9332	245.8693

volatility over time, from January 2017 to January 2018, on Bitfinex and Kraken. The figures suggest that both β and α are positively correlated with the realised volatility. The results indicate that, when the market is more volatile, information asymmetry is more pronounced and liquidity provision becomes tighter. Notably, in the cryptocurrency market, according to Makarov and Schoar (2019b), volatility is increased more by positive shocks than by negative shocks. Therefore, fundamental values and pricing errors may have been more sensitive to orders after positive shocks from May to July due to greater volatility. In addition, if volatility in order flows (or, say, uncertainty in information) remains unchanged, larger β and α will make the market more volatile. Therefore, if β and α increase, market volatility also increases. My results provide evidence for the model proposed by Deuskar (2006), who argues that clusters of volatility and liquidity arise endogenously even through fundamentals are homoskedastic, as well as the feedback theory proposed by Garleanu and Pedersen (2007a).

FIGURE 3.10: β against Volatility

This figure depicts how β changes over time against daily realized volatility of the cryptocurrency during the same period. The estimate is obtained from the following state space model

$$p_t = m_t + s_t$$
$$m_t = m_{t-1} + \beta \hat{X}_t + e_t$$
$$s_t = \phi s_{t-1} + \alpha X_t + u_t$$

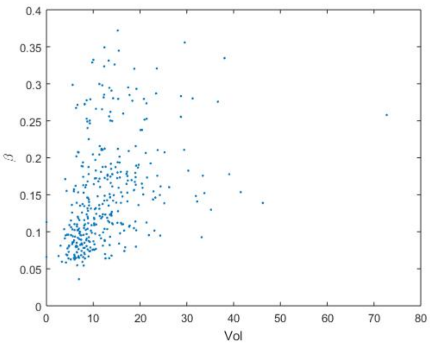

(A) BTCUSD on Bitfinex

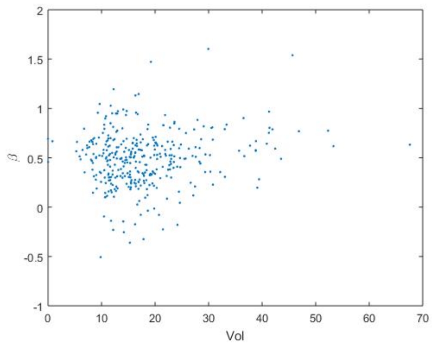

(B) BTCUSD on Kraken

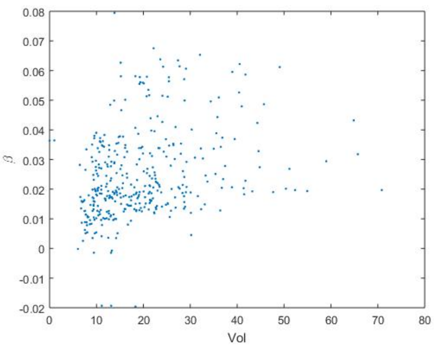

(C) ETHUSD on Bitfinex

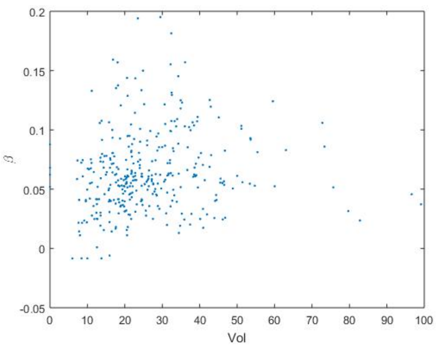

(D) ETHUSD on Kraken

FIGURE 3.11: α against Volatility

This figure depicts how α changes over time against daily realized volatility of the cryptocurrency during the same period. The estimate is obtained from the following state space model

$$p_t = m_t + s_t$$
$$m_t = m_{t-1} + \beta \hat{X}_t + e_t$$
$$s_t = \phi s_{t-1} + \alpha X_t + u_t$$

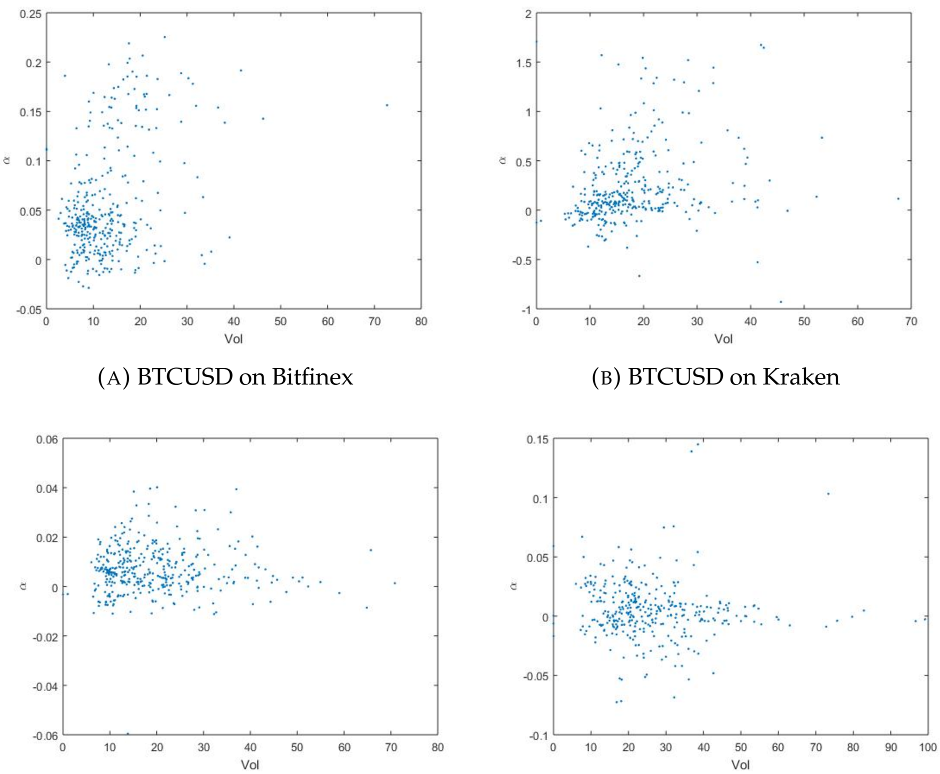

(A) BTCUSD on Bitfinex

(B) BTCUSD on Kraken

(C) ETHUSD on Bitfinex

(D) ETHUSD on Kraken

Tables 3.7 and 3.8 present estimates of SSF, defined by equations (3.1), (3.5), and (3.6), and thus indicate how Bitcoin and Ethereum orders affect Bitcoin price on Bitfinex and Kraken, respectively. Both β_1 and α_1 in the tables demonstrate that, when I add Ethereum orders to the model, Bitcoin orders retain a significantly positive impact on both the fundamental value and the pricing error of the Bitcoin price, consistent with our previous results. Meanwhile, Ethereum orders have only a significantly positive impact on the fundamental value of the Bitcoin price, as β_2 is significantly positive most of the time, while α_2 is not. The Bitfinex and Kraken results are very similar, suggesting that, on both exchanges, Ethereum orders contain private information that influences Bitcoin price, as well as proving the existence of information spill-over between these two cryptocurrencies. Table 3.7 shows that, in July 2017, β_1 is around 10 times β_2. Thus, the percentage change in fundamental value of Bitcoin caused by investors' buying (or selling) one Bitcoin is 10 times the change caused by investors' buying (or selling) one Ethereum. At that time, the Bitcoin price was around 10 times that of Ethereum; therefore, investing one dollar in Bitcoin had a similar impact on its fundamental value to investing one dollar in Ethereum. In most months, β_1 is more than 20 times β_2, so, although Ethereum orders also contained relevant information that influenced Bitcoin orders, the influence was much smaller than that of Bitcoin orders. The results presented in Table 3.8 are similar, indicating that Bitcoin orders on Kraken had a much stronger impact than Ethereum orders on Bitcoin price.

Tables 3.9 and 3.10 summarise how Bitcoin orders influenced Ethereum price on Bitfinex and Kraken, respectively. Similarly, β_2 in the tables demonstrates that Ethereum orders had a significantly positive impact on the Bitcoin price through the price discovery channel. Therefore, information contained in Ethereum orders also determined Bitcoin price. In addition, β_2 was bigger than β_1, but by less than 10 times, so one dollar invested in Ethereum had a greater impact on Ethereum price than one dollar invested in Bitcoin. All of the cross-cryptocurrency results suggest that order flows of one cryptocurrency carry information that may influence the value of other cryptocurrencies. It is possible that some information is market-wide and influences the entire cryptocurrency market. For example, a news report on new technology or a new regulation could simultaneously affect investors' expectations of both Bitcoin and Ethereum, thus permanently changing both prices through order flows (according to Love and Payne (2008), public announcements are also impounded into prices through order flows). In addition, news related to ICOs could influence investors' expectations of the whole cryptocurrency market, thus simultaneously changing Bitcoin and Ethereum prices through orders. Meanwhile, α_2 is

TABLE 3.7: Impact of Ethereum Order Flows on Bitcoin Price – Bitfinex

This table presents estimated parameters in the following state space model:

$$p_t = m_t + s_t$$
$$m_t = m_{t-1} + \beta_1 \hat{X}_{1,t} + \beta_2 \hat{X}_{2,t} + e_t$$
$$s_t = \phi s_{t-1} + \alpha_1 X_{1,t} + \alpha_2 X_{2,t} + u_t$$

where p_t is the observed log price (cumulative log return from the beginning of the week) of BTCUSD on Bitfinex; m_t is the fundamental value; s_t is the pricing error; e_t and u_t are uncorrelated i.i.d. processes. $\hat{X}_{1,t}$ is investors' order flow innovation of BTCUSD. $\hat{X}_{2,t}$ is investors' order flow innovation of ETHUSD. $X_{1,t}$ is investors' order flow of BTCUSD. $X_{2,t}$ is investors' order flow of ETHUSD.
Daily parameters are estimated by 10-minute price and order flow of BTCUSD and ETHUSD from January 2017 to January 2018 on Bitfinex, and then averaged every month.

	β_1	t-stats	β_2	t-stats	α_1	t-stats	α_2	t-stats	ϕ	σ_e	σ_u
17-Jan	0.1361	31.8433	0.0033	2.5744	0.0328	7.1458	0.0002	0.1329	0.3928	778.0964	244.4820
17-Feb	0.1119	28.9286	0.0020	2.4376	0.0134	4.1157	-0.0018	-2.6906	0.1563	183.8617	85.3454
17-Mar	0.0983	32.1229	0.0012	3.1064	0.0274	10.9837	-0.0006	-1.7243	0.1609	574.3827	143.7115
17-Apr	0.0852	18.5230	-0.0010	-2.0467	0.0412	9.5344	0.0007	1.5462	0.5971	153.5813	111.7173
17-May	0.1930	19.6271	0.0033	4.1682	0.0680	8.3780	-0.0022	-2.7256	0.5204	962.9800	321.1883
17-Jun	0.2527	21.4875	0.0068	4.3549	0.1094	11.5653	0.0014	0.9672	0.4958	1111.3360	626.6426
17-Jul	0.1429	18.4612	0.0145	13.9663	0.0829	9.2808	-0.0061	-6.1761	0.5422	1028.8693	514.0453
17-Aug	0.1282	31.5640	0.0023	2.0030	0.0560	14.7131	0.0035	3.2243	0.6974	449.3412	404.6394
17-Sep	0.1037	37.9762	0.0061	6.4456	0.0136	4.6490	0.0053	6.4977	0.3465	633.1115	509.2772
17-Oct	0.0862	36.6356	0.0023	2.4462	0.0164	8.3598	0.0024	2.8513	0.4700	290.4000	200.5766
17-Nov	0.1210	37.8705	0.0033	3.6876	0.0238	8.5001	0.0001	0.0759	0.3057	643.6275	337.3888
17-Dec	0.2240	29.2546	0.0143	6.9272	0.1254	17.5765	-0.0003	-0.1424	0.6416	2314.8872	1345.9089
18-Jan	0.2396	29.7370	0.0081	3.8685	0.1401	19.0653	0.0095	5.5647	0.6498	1960.0380	340.2294

TABLE 3.8: Impact of Ethereum Order Flows on Bitcoin Price – Kraken

This table presents estimated parameters in the following state space model:

$$p_t = m_t + s_t$$
$$m_t = m_{t-1} + \beta_1 \hat{X}_{1,t} + \beta_2 \hat{X}_{2,t} + e_t$$
$$s_t = \phi s_{t-1} + \alpha_1 X_{1,t} + \alpha_2 X_{2,t} + u_t$$

where p_t is the observed log price (cumulative log return from the beginning of the week) of BTCUSD on Kraken; m_t is the fundamental value; s_t is pricing error; e_t and u_t are uncorrelated i.i.d. processes. $\hat{X}_{1,t}$ is investors' order flow innovation of BTCUSD. $\hat{X}_{2,t}$ is investors' order flow innovation of ETHUSD. $X_{1,t}$ is investors' order flow of BTCUSD. $X_{2,t}$ is investors' order flow of ETHUSD.
Daily parameters are estimated by 10-minute price and order flow of BTCUSD and ETHUSD from January 2017 to January 2018 on Kraken, and then averaged every month.

	β_1	t-stats	β_2	t-stats	α_1	t-stats	α_2	t-stats	ϕ	σ_e	σ_u
17-Jan	0.7486	43.8478	0.0103	3.6603	0.0708	4.3898	0.0062	2.5919	-0.0452	1756.0183	465.8755
17-Feb	0.5745	16.5663	-0.0134	-4.5256	0.0072	0.2792	0.0164	5.3153	0.5092	289.1848	1091.2037
17-Mar	0.6017	49.1177	0.0013	0.9832	0.1692	11.6612	-0.0011	-1.0461	0.0569	1104.9066	682.9322
17-Apr	0.3306	33.9917	-0.0025	-1.3439	0.0793	7.0338	-0.0024	-1.1640	0.2153	176.0017	288.2551
17-May	0.6267	41.5725	0.0170	8.4823	0.0297	2.4781	-0.0071	-3.6782	0.0491	1206.0491	461.7257
17-Jun	0.5795	54.3460	0.0270	10.9733	0.1313	10.6947	-0.0084	-3.7230	0.4849	1167.8217	404.7511
17-Jul	0.2843	42.7333	0.0157	12.8000	0.1637	22.1077	-0.0004	-0.3050	0.6004	880.3938	231.6048
17-Aug	0.4516	38.5229	0.0028	1.1366	0.1888	19.7611	0.0057	2.4636	0.6890	453.8941	463.2419
17-Sep	0.4647	37.9026	0.0202	11.2309	0.1308	9.1179	0.0041	2.4697	0.6186	576.4536	631.3309
17-Oct	0.6706	62.5212	0.0085	2.5129	-0.0124	-1.1335	0.0106	3.5189	0.3930	380.5748	201.0460
17-Nov	0.4331	39.0775	-0.0007	-0.2023	0.1252	12.2129	0.0047	1.3821	0.4014	857.0921	488.2063
17-Dec	1.2865	66.6108	0.0742	10.4818	0.2462	15.5362	-0.0244	-5.2402	0.4962	2215.6415	1296.1090
18-Jan	0.1315	7.3124	0.0398	6.7802	1.5025	54.1698	-0.0164	-2.8070	0.9553	948.0654	1243.3583

either wrongly signed or insignificant in each month. Therefore, taken together, the above results suggest information spill-over between Bitcoin and Ethereum, while liquidity spill-over is not evident and liquidity providers separately manage the inventory levels of each cryptocurrency.

TABLE 3.9: Impact of Bitcoin Order Flows on Ethereum Price – Bitfinex

This table presents estimated parameters in the following state space model:

$$p_t = m_t + s_t$$
$$m_t = m_{t-1} + \beta_1 \hat{X}_{1,t} + \beta_2 \hat{X}_{2,t} + e_t$$
$$s_t = \phi s_{t-1} + \alpha_1 X_{1,t} + \alpha_2 X_{2,t} + u_t$$

where p_t is the observed log price (cumulative log return from the beginning of the week) of ETHUSD on Bitfinex; m_t is the fundamental value; s_t is pricing error; e_t and u_t are uncorrelated i.i.d. processes. $\hat{X}_{1,t}$ is investors' order flow innovation of ETHUSD. $\hat{X}_{2,t}$ is investors' order flow innovation of BTCUSD. $X_{1,t}$ is investors' order flow of ETHUSD. $X_{2,t}$ is investors' order flow of BTCUSD.
Daily parameters are estimated by 10-minute price and order flow of BTCUSD and ETHUSD from January 2017 to January 2018 on Bitfinex, and then averaged every month.

	β_1	t-stats	β_2	t-stats	α_1	t-stats	α_2	t-stats	ϕ	σ_e	σ_u
17-Jan	0.0110	5.7515	0.0737	10.1030	-0.0015	-0.9197	0.0180	2.9072	0.1630	1202.2371	455.9228
17-Feb	0.0126	7.4147	0.0123	2.5145	0.0045	3.2173	0.0256	5.2542	0.2368	403.7284	330.2135
17-Mar	0.0175	20.8275	0.0060	0.9480	0.0019	2.6844	0.0111	2.0020	-0.0059	2983.8653	843.4557
17-Apr	0.0153	15.2348	-0.0066	-0.7446	0.0044	4.9525	-0.0122	-1.5879	0.2709	754.6034	653.4981
17-May	0.0291	19.0106	0.0927	8.0862	-0.0009	-0.6820	-0.0042	-0.4188	0.1076	2781.5575	913.5814
17-Jun	0.0526	21.8474	0.1544	12.3512	0.0077	3.2669	0.0819	6.2284	0.4328	2705.8912	1266.2274
17-Jul	0.0350	20.2728	0.2005	20.8796	0.0057	3.9434	0.0221	2.7997	0.0078	3120.7402	403.4100
17-Aug	0.0295	21.9024	0.0372	5.9136	-0.0001	-0.0419	0.0333	5.7766	0.3270	804.3946	358.9381
17-Sep	0.0173	14.7737	0.0757	17.2212	0.0071	6.5365	0.0226	5.1972	0.5249	1184.3996	541.5482
17-Oct	0.0200	20.6992	0.0152	6.5491	0.0010	1.2078	0.0152	6.7991	0.3345	561.6335	114.4575
17-Nov	0.0149	16.3176	0.0122	3.4789	0.0049	5.3549	0.0095	3.0528	0.5919	659.9713	297.3495
17-Dec	0.0237	11.5382	0.1103	14.0562	0.0115	6.5251	0.0651	8.3591	0.7958	2359.5458	1273.2965
18-Jan	0.0286	12.3767	0.0718	9.1773	0.0117	5.6470	0.1006	14.7564	0.5115	3303.3856	57.7085

Tables 3.11, 3.12, 3.13, and 3.14 demonstrate how order flows on one exchange influence the fundamental value and pricing error of Bitcoin (or Ethereum) price on the other. Table 3.11 shows that β_2 is significantly positive in each month, demonstrating that orders placed on Bitfinex reveal relevant information that can influence the fundamental value of Bitcoin price on Bitfinex. In other tables, β_2 is significant, suggesting that information contained in order flows on one exchange helps to determine the price on the other through price discovery. Thus, information on

TABLE 3.10: Impact of Bitcoin Order Flows on Ethereum Price – Kraken

This table presents estimated parameters in the following state space model:

$$p_t = m_t + s_t$$
$$m_t = m_{t-1} + \beta_1 \hat{X}_{1,t} + \beta_2 \hat{X}_{2,t} + e_t$$
$$s_t = \phi s_{t-1} + \alpha_1 X_{1,t} + \alpha_2 X_{2,t} + u_t$$

where p_t is the observed log price (cumulative log return from the beginning of the week) of ETHUSD on Kraken; m_t is the fundamental value; s_t is pricing error; e_t and u_t are uncorrelated i.i.d. processes. $\hat{X}_{1,t}$ is investors' order flow innovation of ETHUSD. $\hat{X}_{2,t}$ is investors' order flow innovation of BTCUSD. $X_{1,t}$ is investors' order flow of ETHUSD. $X_{2,t}$ is investors' order flow of BTCUSD.
Daily parameters are estimated by 10-minute price and order flow of BTCUSD and ETHUSD from January 2017 to January 2018 on Kraken, and then averaged every month.

	β_1	t-stats	β_2	t-stats	α_1	t-stats	α_2	t-stats	ϕ	σ_e	σ_u
17-Jan	0.0382	7.8187	0.2684	8.1601	-0.0029	-0.5372	-0.0070	-0.2551	0.4760	1163.2279	2075.0605
17-Feb	0.0248	7.9174	0.0715	2.6705	-0.0034	-1.0941	0.1103	3.7101	0.2058	754.7239	920.7751
17-Mar	0.0362	13.0749	0.2292	15.7780	0.0022	0.8589	0.0755	4.7526	0.1282	3662.8147	2517.3416
17-Apr	0.0440	11.8588	-0.2587	-18.0610	0.0230	6.1491	0.0932	6.1523	0.3053	751.7436	1337.3263
17-May	0.0709	20.8730	0.1637	8.6119	-0.0032	-1.0700	-0.0055	-0.2736	0.1822	2633.7950	1526.8350
17-Jun	0.0851	21.8615	0.4347	30.3471	0.0072	2.2223	-0.0334	-3.5999	0.0405	2931.1538	935.8725
17-Jul	0.0575	22.8346	0.3365	18.1428	0.0030	1.1956	-0.0036	-0.2049	0.1090	2777.8688	972.4887
17-Aug	0.0637	22.6719	0.2111	16.7999	-0.0012	-0.4051	-0.1018	-8.1810	0.3453	593.6511	683.9281
17-Sep	0.0433	19.1274	0.3551	30.5080	0.0069	3.0044	0.1201	10.6801	0.5286	1070.6274	1082.3135
17-Oct	0.0676	0.5942	0.1482	1.2319	0.0078	0.0685	0.0405	0.3374	0.0774	416.4258	120.0389
17-Nov	0.0688	18.9449	0.1265	10.2020	-0.0144	-4.8780	-0.0984	-9.6525	0.2232	596.8714	344.4566
17-Dec	0.1229	19.7001	0.0470	3.4241	0.0027	0.4704	0.4298	28.8701	0.6432	1620.4099	1708.5765
18-Jan	0.1016	15.8993	0.6122	27.4832	-0.0017	-0.2936	0.1788	6.6935	0.0669	2135.8995	766.5785

both exchanges is impounded into cryptocurrency price through order flows. This finding also confirms the significant heterogeneity in where price formation happens across exchanges, as proposed by Makarov and Schoar (2019a). The results suggest information spill-over across cryptocurrency exchanges. In addition, since cryptocurrencies traded on Bitfinex and Kraken are identical assets, the Law of One Price says the prices should be the same. Therefore, any differences should be wiped off by arbitrage opportunities, and, thus, arbitrage trading helps to transmit information among exchanges. The results confirm that order flows carry information that determines price in the price discovery process. In all four tables, the impact of orders on Kraken is larger than that on Bitfinex, suggesting worse information asymmetry on Kraken. However, my results do not indicate whether information was passed from Bitfinex to Kraken or from Kraken to Bitfinex. At the same time, α_2 in those tables is not significant, suggesting that price pressure does not spill over across exchanges. For example, the Bitcoin inventory change of liquidity providers on Bitfinex does not influence liquidity providers' willingness to provide Bitcoin liquidity on Kraken.

TABLE 3.11: Impact of Kraken Order Flows on Bitfinex Price for Bitcoin

This table presents estimated parameters in the following state space model:

$$p_t = m_t + s_t$$
$$m_t = m_{t-1} + \beta_1 \hat{X}_{1,t} + \beta_2 \hat{X}_{2,t} + e_t$$
$$s_t = \phi s_{t-1} + \alpha_1 X_{1,t} + \alpha_2 X_{2,t} + u_t$$

where p_t is the observed log price (cumulative log return from the beginning of the week) of BTCUSD on Bitfinex; m_t is the fundamental value; s_t is pricing error; e_t and u_t are uncorrelated i.i.d. processes. $\hat{X}_{1,t}$ is investors' order flow innovation on Bitfinex. $\hat{X}_{2,t}$ is investors' order flow innovation on Kraken. $X_{1,t}$ is investors' order flow on Bitfinex. $X_{2,t}$ is investors' order flow on Kraken.
Daily parameters are estimated by 10-minute price and order flow of BTCUSD from January 2017 to January 2018 on Bitfinex and Kraken, and then averaged every month.

	β_1	t-stats	β_2	t-stats	α_1	t-stats	α_2	t-stats	ϕ	σ_e	σ_u
17-Jan	0.1116	21.9304	0.2722	20.6372	0.0390	8.8196	0.0096	0.8776	0.5173	542.1018	245.3659
17-Feb	0.0999	34.5146	0.0404	4.1789	0.0135	4.6927	0.0534	6.1711	0.3721	162.8437	67.0808
17-Mar	0.0924	30.5407	0.1438	16.4434	0.0317	8.3157	-0.0045	-0.5555	0.2758	446.2483	190.9834
17-Apr	0.0814	18.6069	0.2145	23.6962	0.0432	9.6707	-0.1118	-11.5320	0.5039	160.5536	95.8521
17-May	0.1801	15.2737	0.2217	13.8573	0.0687	6.9302	-0.0783	-5.7149	0.4262	1113.9115	185.7866
17-Jun	0.2409	22.0573	0.3873	22.2526	0.1134	11.0759	-0.0923	-6.2383	0.4122	1273.1314	527.6300
17-Jul	0.1552	14.5142	0.3829	29.1480	0.0705	8.5777	-0.1733	-17.0688	0.3549	1150.3375	392.8510
17-Aug	0.1186	20.3844	0.2459	19.8753	0.0497	8.0462	-0.0190	-1.5710	0.5444	398.7473	383.1617
17-Sep	0.1156	22.7982	0.1835	18.6022	0.0172	5.3413	0.0749	7.2121	0.2308	766.0482	418.5900
17-Oct	0.0740	26.9527	0.2926	32.9424	0.0219	8.5793	-0.0492	-5.0903	0.4678	260.9236	205.6883
17-Nov	0.1134	23.9783	0.1489	11.6938	0.0283	7.6233	0.0237	1.8815	0.1881	631.7745	305.1091
17-Dec	0.2071	17.1213	0.6332	22.3385	0.1374	12.3436	-0.1731	-5.7711	0.5159	2225.9687	1413.6538
18-Jan	0.2326	24.2463	0.7466	33.5483	0.1365	10.9059	0.2090	13.0457	0.5881	1590.1095	627.2682

TABLE 3.12: Impact of Bitfinex Order Flows on Kraken Price for Bitcoin

This table presents estimated parameters in the following state space model:

$$p_t = m_t + s_t$$
$$m_t = m_{t-1} + \beta_1 \hat{X}_{1,t} + \beta_2 \hat{X}_{2,t} + e_t$$
$$s_t = \phi s_{t-1} + \alpha_1 X_{1,t} + \alpha_2 X_{2,t} + u_t$$

where p_t is the observed log price (cumulative log return from the beginning of the week) of BTCUSD on Kraken; m_t is fundamental value; s_t is pricing error; e_t and u_t are uncorrelated i.i.d. processes. $\hat{X}_{1,t}$ is investors' order flow innovation on Kraken. $\hat{X}_{2,t}$ is investors' order flow innovation on Bitfinex. $X_{1,t}$ is investors' order flow on Kraken. $X_{2,t}$ is investors' order flow on Bitfinex.
Daily parameters are estimated by 10-minute price and order flow of BTCUSD from January 2017 to January 2018 on Bitfinex and Kraken, and then averaged every month.

	β_1	t-stats	β_2	t-stats	α_1	t-stats	α_2	t-stats	ϕ	σ_e	σ_u
17-Jan	0.3626	15.5429	0.1243	18.4310	0.0679	3.9580	-0.0066	-1.1200	0.0948	587.2864	438.1723
17-Feb	0.1465	11.1787	0.1003	25.5924	0.0635	5.4147	-0.0176	-4.4359	0.1816	167.0887	249.7454
17-Mar	0.3595	30.5098	0.0899	16.3125	0.1813	16.2912	-0.0016	-0.3699	0.0662	739.0769	726.2314
17-Apr	0.2458	21.2515	0.0700	12.9836	0.0957	6.1142	-0.0019	-0.3540	0.1828	136.3737	278.6093
17-May	0.5191	33.4610	0.1376	12.3856	0.0826	6.3265	-0.0141	-1.3869	-0.0088	1291.9831	451.2010
17-Jun	0.5211	47.9807	0.1322	16.1212	0.1761	16.0412	0.0509	6.7063	0.4723	916.2978	641.3206
17-Jul	0.2697	33.2812	0.1271	18.0842	0.1959	18.9311	-0.0151	-2.7552	0.1958	1091.3341	105.6910
17-Aug	0.4897	57.9674	0.1032	16.4046	0.0202	2.6122	-0.0263	-5.6248	0.0791	617.3287	179.2955
17-Sep	0.4019	31.5279	0.0962	25.5310	0.0604	4.5590	-0.0245	-7.0187	0.0913	823.3647	229.4785
17-Oct	0.4219	47.4052	0.0654	29.4802	0.0392	3.8617	-0.0127	-5.2206	0.1500	299.3503	151.3357
17-Nov	0.3719	40.3750	0.1005	27.5144	0.0029	0.3032	-0.0295	-9.1359	-0.0780	851.9302	153.9901
17-Dec	1.3619	76.8365	0.2065	24.9655	-0.1286	-11.3544	-0.0599	-8.7852	-0.0698	2761.6725	274.9998
18-Jan	1.6303	59.1666	0.2357	33.0853	-0.2246	-12.3211	-0.0327	-4.6237	-0.0615	1822.5079	126.7439

TABLE 3.13: Impact of Kraken Order Flows on Bitfinex Price for Ethereum

This table presents estimated parameters in the following state space model:

$$p_t = m_t + s_t$$
$$m_t = m_{t-1} + \beta_1 \hat{X}_{1,t} + \beta_2 \hat{X}_{2,t} + e_t$$
$$s_t = \phi s_{t-1} + \alpha_1 X_{1,t} + \alpha_2 X_{2,t} + u_t$$

where p_t is the observed log price (cumulative log return from the beginning of the week) of ETHUSD on Bitfinex; m_t is fundamental value; s_t is pricing error; e_t and u_t are uncorrelated i.i.d. processes. $\hat{X}_{1,t}$ is investors' order flow innovation on Bitfinex. $\hat{X}_{2,t}$ is investors' order flow innovation on Kraken. $X_{1,t}$ is investors' order flow on Bitfinex. $X_{2,t}$ is investors' order flow at Kraken.
Daily parameters are estimated by 10-minute price and order flow data of ETHUSD from January 2017 to January 2018 on Bitfinex and Kraken, and then averaged every month.

	β_1	t-stats	β_2	t-stats	α_1	t-stats	α_2	t-stats	ϕ	σ_e	σ_u
17-Jan	0.0161	0.2284	0.0288	0.3847	0.0003	0.0047	-0.0051	-0.0723	0.3317	1691.0019	1206.6365
17-Feb	0.0152	7.8032	0.0151	5.5606	0.0047	2.3664	-0.0038	-1.4933	0.2699	449.9112	740.7910
17-Mar	0.0152	18.0878	0.0167	9.5983	0.0021	2.6634	-0.0004	-0.2726	-0.0352	2653.1685	865.5275
17-Apr	0.0126	13.5166	0.0246	9.3782	0.0044	4.4066	0.0054	1.9628	0.2886	598.0511	734.4656
17-May	0.0206	14.4574	0.0373	13.0540	0.0017	1.4889	-0.0019	-0.8474	0.0812	2360.8505	870.8511
17-Jun	0.0472	20.8853	0.0397	10.6219	0.0063	2.9884	0.0067	1.9613	0.2426	2554.7485	1020.2221
17-Jul	0.0273	16.3999	0.0348	14.1789	0.0090	6.9124	-0.0006	-0.3148	-0.0242	2612.9175	538.9586
17-Aug	0.0245	18.7715	0.0249	10.5449	0.0015	1.2202	0.0064	2.5872	0.3826	598.8495	493.7958
17-Sep	0.0233	19.9949	0.0171	8.1651	0.0082	6.7866	0.0066	3.4512	0.3546	1493.7084	467.7527
17-Oct	0.0175	15.8688	0.0268	9.9194	0.0026	2.8975	0.0081	3.1627	0.5104	358.0669	256.8349
17-Nov	0.0143	15.6033	0.0176	5.4659	0.0050	5.9487	0.0081	2.7793	0.6784	585.0209	350.2297
17-Dec	0.0287	13.6295	0.0441	5.8648	0.0135	6.3926	0.0124	1.6878	0.7886	1883.6661	2361.4591
18-Jan	0.0177	7.0511	0.0551	8.0123	0.0247	10.8190	0.0054	0.8661	0.8016	2408.5337	1027.0058

TABLE 3.14: Impact of Bitfinex Order Flows on Kraken Price for Ethereum

This table presents estimated parameters in the following state space model:

$$p_t = m_t + s_t$$
$$m_t = m_{t-1} + \beta_1 \hat{X}_{1,t} + \beta_2 \hat{X}_{2,t} + e_t$$
$$s_t = \phi s_{t-1} + \alpha_1 X_{1,t} + \alpha_2 X_{2,t} + u_t$$

where p_t is the observed log price (cumulative log return from the beginning of the week) of ETHUSD on Kraken; m_t is the fundamental value; s_t is pricing error; e_t and u_t are uncorrelated i.i.d. processes. $\hat{X}_{1,t}$ is investors' order flow innovation on Kraken. $\hat{X}_{2,t}$ is investors' order flow innovation on Bitfinex. $X_{1,t}$ is investors' order flow on Kraken. $X_{2,t}$ is investors' order flow on Bitfinex.
Daily parameters are estimated by 10-minute price and order flow of ETHUSD from January 2017 to January 2018 on Bitfinex and Kraken, and then averaged every month.

	β_1	t-stats	β_2	t-stats	α_1	t-stats	α_2	t-stats	ϕ	σ_e	σ_u
17-Jan	0.0355	6.9276	0.0149	4.1674	-0.0002	-0.0364	-0.0043	-1.1856	0.4134	1597.0236	1484.3379
17-Feb	0.0135	4.0979	0.0111	5.3010	0.0060	1.9048	0.0015	0.6797	0.5114	485.2349	1209.5482
17-Mar	0.0207	10.6242	0.0138	14.2090	0.0058	2.8119	-0.0003	-0.3105	0.1568	2709.9751	2733.5641
17-Apr	0.0300	11.1301	0.0106	9.3135	0.0201	7.1694	0.0009	0.8383	0.2980	589.3406	1245.1800
17-May	0.0534	19.1855	0.0142	9.7503	0.0048	1.7359	-0.0001	-0.0453	0.2521	2143.4550	1659.3837
17-Jun	0.0652	19.1288	0.0375	15.4164	0.0068	2.0114	-0.0048	-2.3881	0.1021	2170.9672	1101.3282
17-Jul	0.0481	19.6608	0.0241	13.6831	0.0042	1.7128	-0.0034	-2.1915	0.1567	2417.8517	1081.6064
17-Aug	0.0439	16.4306	0.0189	15.0978	0.0081	3.1778	-0.0049	-3.6989	0.2912	522.7086	606.0300
17-Sep	0.0370	14.2151	0.0214	16.9736	0.0064	2.8484	-0.0025	-2.2260	0.3942	1126.7628	800.8948
17-Oct	0.0510	18.0339	0.0100	10.5961	0.0105	3.9920	0.0018	1.4331	0.3630	316.1656	192.9321
17-Nov	0.0487	18.2029	0.0125	14.1696	-0.0050	-1.8678	-0.0051	-6.5184	0.1098	532.9543	311.8105
17-Dec	0.1065	20.4433	0.0030	1.8207	0.0051	1.0164	0.0160	9.8245	0.7291	1717.8272	1648.7310
18-Jan	0.0709	16.2097	-0.0019	-1.1615	0.0160	3.1815	0.0253	15.7319	0.8770	1352.0585	1586.4684

3.6 Conclusion

I conclude that order flows of Bitcoin and Ethereum have a significant positive impact on the fundamental value and pricing error components of the prices defined by my SSF for January 2017 to January 2018. This finding proves that order flows influence cryptocurrency prices through both information and liquidity providers' inventory control, thus determining the price through both price discovery and price pressure.

At the beginning of both the market boom and the market crash, the fundamental values of Bitcoin and Ethereum were more sensitive to orders. The results suggest that liquidity providers adjusted quotes more in response to the 'good news' contained in buy orders than to the 'bad news' contained in sell orders, leading to the growth of the bubble. When the market began to crash, both buy and sell orders had a greater impact on fundamental values; thus, price decreased rapidly. At the same time, the pricing error components of both cryptocurrencies were more sensitive to orders. Therefore, the bubble growth can be attributed to increased information asymmetry, while the bubble bursting is accelerated by both increased information asymmetry and tighter inventory control.

Finally, I conclude that order flows of one cryptocurrency contain relevant information that can influence the price of another; thus, there is an information spill-over between Bitcoin and Ethereum. However, both cryptocurrencies are influenced by order flows of their own. In addition, the price of one cryptocurrency on one exchange is influenced by information contained in order flows on the other exchange, which eliminates any price deviation between the exchanges. This confirms that order flows determine price through the price discovery process. Order flows have a greater impact on fundamental value on Kraken, suggesting worse information asymmetry on Kraken than on Bitfinex. However, a liquidity spill-over effect is not found across either cryptocurrencies or exchanges. Thus, I conclude that liquidity providers separately manage their inventory levels of the different cryptocurrencies on different exchanges.

Conclusion

Chapter 1 of my thesis is dedicated to explaining returns through risk factors. My within-asset-class results are consistent with the finding in the existing literature, showing that within each asset class, cross-sectional differences in returns of carry and momentum portfolios load significantly on market return risk and volatility risk factors. I also find that investors can take advantage of diversification and sort assets into value, carry, and momentum portfolios, regardless of asset classes, thereby obtaining HML portfolios with larger risk-adjusted returns than within-asset-class portfolios. However, it is difficult to justify the return cross-section of those non-segmented portfolios by volatility or liquidity risk factor, suggesting that the returns within different asset classes have different sources.

In Chapter 2, I attempt to determine the cause of the liquidity dry-up in the UK equity market during the 2008 financial crisis. My results suggest that the pricing error component of the equity price was more sensitive to orders, indicating that the liquidity providers' inventory control was the primary cause of the liquidity evaporation, though information asymmetry worsened for some small capitalisation companies. Therefore, liquidity decreased dramatically because the liquidity providers' inventory absorption capacity was constrained, or providers required greater profits to compensate for increased liquidity provision costs.

Chapter 3 applies SSF to the emerging cryptocurrency market and confirms that, as in other asset classes, cryptocurrency price is significantly influenced by order flows through price discovery and price pressure. Although the fundamental value defined here does not necessarily represent the real value of the asset, my time variation of estimates reveals that the fundamental values of both Bitcoin and Ethereum were more sensitive to information contained in orders at the beginning of the market boom and the market crash. Therefore, the bubble may have been triggered by uninformed liquidity providers reacting more to buy orders than to sell orders. Following this, the burst may have been worsened by an adverse selection problem. At the same time, the liquidity providers' inventory control also contributed to the bubble burst, as in the equity market. I find that, information flows between the two exchanges through order flows, eliminating most of the price deviations. In addition, information contained in orders of one cryptocurrency influences the fundamental values of others.

Bibliography

Albuquerque, R., Bauer, G. H., and Schneider, M. (2009). Global private information in international equity markets. *Journal of Financial Economics*, 94(1):18–46.

Ang, A., Hodrick, R. J., Xing, Y., and Zhang, X. (2006). The cross-section of volatility and expected returns. *The Journal of Finance*, 61(1):259–299.

Anshuman, R. and Viswanathan, V. (2005). Costly collateral and liquidity. *Work. Pap., Duke Univ*.

Asness, C. S., Moskowitz, T. J., and Pedersen, L. H. (2013). Value and momentum everywhere. *The Journal of Finance*, 68(3):929–985.

Balcilar, M., Bouri, E., Gupta, R., and Roubaud, D. (2017). Can volume predict bitcoin returns and volatility? a quantiles-based approach. *Economic Modelling*, 64:74–81.

Bansal, R. and Shaliastovich, I. (2012). A long-run risks explanation of predictability puzzles in bond and currency markets. *The Review of Financial Studies*, 26(1):1–33.

Bao, J., O'Hara, M., and Zhou, X. A. (2018). The volcker rule and corporate bond market making in times of stress. *Journal of Financial Economics*, 130(1):95–113.

Barclay, M. J. and Hendershott, T. (2004). Liquidity externalities and adverse selection: Evidence from trading after hours. *The Journal of Finance*, 59(2):681–710.

Bariviera, A. F., Basgall, M. J., Hasperué, W., and Naiouf, M. (2017). Some stylized facts of the bitcoin market. *Physica A: Statistical Mechanics and its Applications*, 484:82–90.

Baur, D. G. and Dimpfl, T. (2018). Asymmetric volatility in cryptocurrencies. *Economics Letters*, 173:148–151.

Baur, D. G., Dimpfl, T., and Kuck, K. (2018). Bitcoin, gold and the us dollar–a replication and extension. *Finance Research Letters*, 25:103–110.

Bekaert, G. and Harvey, C. R. (1995). Time-varying world market integration. *The Journal of Finance*, 50(2):403–444.

Ben-David, I., Franzoni, F., and Moussawi, R. (2012). Hedge fund stock trading in the financial crisis of 2007–2009. *Review of Financial Studies*, 25(1):1–54.

Biais, B., Bisiere, C., Bouvard, M., Casamatta, C., and Menkveld, A. J. (2020). Equilibrium bitcoin pricing. *Available at SSRN 3261063*.

Bolton, P., Santos, T., and Scheinkman, J. A. (2011). Outside and inside liquidity. *The Quarterly Journal of Economics*, 126(1):259–321.

Borri, N. and Shakhnov, K. (2018). Cryptomarket discounts.

Bouoiyour, J., Selmi, R., Tiwari, A. K., Olayeni, O. R., et al. (2016). What drives bitcoin price. *Economics Bulletin*, 36(2):843–850.

Brandt, M. W. and Kavajecz, K. A. (2004). Price discovery in the us treasury market: The impact of orderflow and liquidity on the yield curve. *The Journal of Finance*, 59(6):2623–2654.

Brogaard, J., Hendershott, T., and Riordan, R. (2014). High-frequency trading and price discovery. *The Review of Financial Studies*, 27(8):2267–2306.

Brunnermeier, M. K. and Pedersen, L. H. (2009). Market liquidity and funding liquidity. *Review of Financial studies*, 22(6):2201–2238.

Campbell, J. Y., Grossman, S. J., and Wang, J. (1993). Trading volume and serial correlation in stock returns. *The Quarterly Journal of Economics*, 108(4):905–939.

Cenedese, G., Payne, R., Sarno, L., and Valente, G. (2014). What do stock markets tell us about exchange rates? *Available at SSRN 2467707*.

Cheah, E.-T. and Fry, J. (2015). Speculative bubbles in bitcoin markets? an empirical investigation into the fundamental value of bitcoin. *Economics Letters*, 130:32–36.

Chordia, T., Roll, R., and Subrahmanyam, A. (2002). Order imbalance, liquidity, and market returns. *Journal of Financial economics*, 65(1):111–130.

Chordia, T., Sarkar, A., and Subrahmanyam, A. (2005). An empirical analysis of stock and bond market liquidity. *Review of Financial Studies*, 18(1):85–129.

Chung, K. H. and Chuwonganant, C. (2014). Uncertainty, market structure, and liquidity. *Journal of Financial Economics*, 113(3):476–499.

Ciaian, P., Rajcaniova, M., and Kancs, d. (2016). The economics of bitcoin price formation. *Applied Economics*, 48(19):1799–1815.

Cochrane, J. H. (2002). Stocks as money: convenience yield and the tech-stock bubble. Technical report, National bureau of economic research.

Comerton-Forde, C., Hendershott, T., Jones, C. M., Moulton, P. C., and Seasholes, M. S. (2010). Time variation in liquidity: The role of market-maker inventories and revenues. *The Journal of Finance*, 65(1):295–331.

Dang, T. V., Gorton, G., and Holmstrom, B. (2009). Opacity and the optimality of debt for liquidity provision. *Manuscript Yale University*.

Deuskar, P. (2006). Extrapolative expectations: Implications for volatility and liquidity. In *AFA 2007 Chicago Meetings Paper*.

Dimpfl, T. and Peter, F. J. (2020). Nothing but noise? price discovery across cryptocurrency exchanges. *Journal of Financial Markets*, page 100584.

Dyhrberg, A. H. (2016). Bitcoin, gold and the dollar–a garch volatility analysis. *Finance Research Letters*, 16:85–92.

Evans, M. D. and Lyons, R. K. (2002a). Informational integration and fx trading. *Journal of International Money and Finance*, 21(6):807–831.

Evans, M. D. and Lyons, R. K. (2002b). Order flow and exchange rate dynamics. *Journal of political economy*, 110(1):170–180.

Fama, E. F. and French, K. R. (2012). Size, value, and momentum in international stock returns. *Journal of financial economics*, 105(3):457–472.

Fry, J. and Cheah, E.-T. (2016). Negative bubbles and shocks in cryptocurrency markets. *International Review of Financial Analysis*, 47:343–352.

Garleanu, N. and Pedersen, L. H. (2007a). Liquidity and risk management. *American Economic Review*, 97(2):193–197.

Garleanu, N. B. and Pedersen, L. H. (2007b). Liquidity and risk management. Technical report, National Bureau of Economic Research.

Glosten, L. R. and Milgrom, P. R. (1985). Bid, ask and transaction prices in a specialist market with heterogeneously informed traders. *Journal of financial economics*, 14(1):71–100.

Gorton, G. and Metrick, A. (2012). Securitized banking and the run on repo. *Journal of Financial Economics*, 104(3):425–451.

Gorton, G. B. and Metrick, A. (2009). Haircuts. Technical report, National Bureau of Economic Research.

Griffin, J. M. (2002). Are the fama and french factors global or country specific? *The Review of Financial Studies*, 15(3):783–803.

Griffin, J. M. and Shams, A. (2018). Is bitcoin really un-tethered? *Available at SSRN 3195066*.

Gronwald, M. (2014). The economics of bitcoins–market characteristics and price jumps.

Grossman, S. J. and Miller, M. H. (1988). Liquidity and market structure. *the Journal of Finance*, 43(3):617–633.

Hameed, A., Kang, W., and Viswanathan, S. (2010). Stock market declines and liquidity. *The Journal of Finance*, 65(1):257–293.

Hansch, O., Naik, N. Y., and Viswanathan, S. (1998). Do inventories matter in dealership markets? evidence from the london stock exchange. *The Journal of Finance*, 53(5):1623–1656.

Hasbrouck, J. (1991a). Measuring the information content of stock trades. *The Journal of Finance*, 46(1):179–207.

Hasbrouck, J. (1991b). The summary informativeness of stock trades: An econometric analysis. *Review of Financial Studies*, 4(3):571–595.

Hendershott, T., Jones, C. M., and Menkveld, A. J. (2011). Does algorithmic trading improve liquidity? *The Journal of Finance*, 66(1):1–33.

Hendershott, T. and Menkveld, A. J. (2014). Price pressures. *Journal of Financial economics*, 114(3):405–423.

Hendershott, T. and Seasholes, M. S. (2007). Market maker inventories and stock prices. *The American economic review*, pages 210–214.

Hileman, G. and Rauchs, M. (2017). Global cryptocurrency benchmarking study. *Cambridge Centre for Alternative Finance*, 33.

Hubrich, S. (2017). 'know when to hodl 'em, know when to fodl 'em': An investigation of factor based investing in the cryptocurrency space.

Jegadeesh, N. and Titman, S. (2001). Profitability of momentum strategies: An evaluation of alternative explanations. *The Journal of finance*, 56(2):699–720.

Jeon, Y., Samarbakhsh, L., and Hewitt, K. (2021). Fragmentation in the bitcoin market: Evidence from multiple coexisting order books. *Finance Research Letters*, 39:101654.

Klein, T., Thu, H. P., and Walther, T. (2018). Bitcoin is not the new gold–a comparison of volatility, correlation, and portfolio performance. *International Review of Financial Analysis*, 59:105–116.

Koijen, R. S., Moskowitz, T. J., Pedersen, L. H., and Vrugt, E. B. (2013). Carry. Technical report, National Bureau of Economic Research.

Kyle, A. S. (1985a). Continuous auctions and insider trading. *Econometrica: Journal of the Econometric Society*, pages 1315–1335.

Kyle, A. S. (1985b). Continuous auctions and insider trading. *Econometrica: Journal of the Econometric Society*, pages 1315–1335.

Kyle, A. S. and Xiong, W. (2001). Contagion as a wealth effect. *The Journal of Finance*, 56(4):1401–1440.

Lettau, M., Maggiori, M., and Weber, M. (2014). Conditional risk premia in currency markets and other asset classes. *Journal of Financial Economics*, 114(2):197–225.

Levine, R. and Zervos, S. (1998). Stock markets, banks, and economic growth. *American economic review*, pages 537–558.

Li, T., Shin, D., and Wang, B. (2018). Cryptocurrency pump-and-dump schemes. *Available at SSRN 3267041*.

Liu, Y., Tsyvinski, A., and Wu, X. (2019). Common risk factors in cryptocurrency. Technical report, National Bureau of Economic Research.

Love, R. and Payne, R. (2008). Macroeconomic news, order flows, and exchange rates. *Journal of Financial and Quantitative Analysis*, 43(2):467–488.

Lustig, H., Stathopoulos, A., and Verdelhan, A. (2013). The term structure of currency carry trade risk premia. Technical report, National Bureau of Economic Research.

Makarov, I. and Schoar, A. (2018). Trading and arbitrage in cryptocurrency markets.

Makarov, I. and Schoar, A. (2019a). Price discovery in cryptocurrency markets. In *AEA Papers and Proceedings*, volume 109, pages 97–99.

Makarov, I. and Schoar, A. (2019b). Trading and arbitrage in cryptocurrency markets. *Journal of Financial Economics*.

Menkhoff, L., Sarno, L., Schmeling, M., and Schrimpf, A. (2012). Currency momentum strategies. *Journal of Financial Economics*, 106(3):660–684.

Menkhoff, L., Sarno, L., Schmeling, M., and Schrimpf, A. (2014). Carry trades and global fx volatility. Technical report.

Menkhoff, L., Sarno, L., Schmeling, M., and Schrimpf, A. (2016). Information flows in foreign exchange markets: Dissecting customer currency trades. *The Journal of Finance*, 71(2):601–634.

Mitchell, M., Pedersen, L. H., and Pulvino, T. (2007). Slow moving capital. Technical report, National Bureau of Economic Research.

Morris, S. and Shin, H. S. (2012). Contagious adverse selection. *American Economic Journal: Macroeconomics*, 4(1):1–21.

Musto, D., Nini, G., and Schwarz, K. (2018). Notes on bonds: Illiquidity feedback during the financial crisis. *The Review of Financial Studies*, 31(8):2983–3018.

Nagel, S. (2012). Evaporating liquidity. *Review of Financial Studies*, 25(7):2005–2039.

Naik, N. Y. and Yadav, P. K. (2003). Do dealer firms manage inventory on a stock-by-stock or a portfolio basis? *Journal of Financial Economics*, 69(2):325–353.

O'Hara, M. (2003). Presidential address: Liquidity and price discovery. *The Journal of Finance*, 58(4):1335–1354.

Pagano, M. and Volpin, P. (2012). Securitization, transparency, and liquidity. *The Review of Financial Studies*, 25(8):2417–2453.

Pal, D. and Mitra, S. K. (2019). Hedging bitcoin with other financial assets. *Finance Research Letters*, 30:30–36.

Pastor, L. and Stambaugh, R. F. (2001). Liquidity risk and expected stock returns. Technical report, National Bureau of Economic Research.

Pástor, L. and Stambaugh, R. F. (2003). Liquidity risk and expected stock returns. *Journal of Political economy*, 111(3):642–685.

Reiss, P. C. and Werner, I. M. (1998). Does risk sharing motivate interdealer trading? *The Journal of Finance*, 53(5):1657–1703.

Sadka, R. (2006). Momentum and post-earnings-announcement drift anomalies: The role of liquidity risk. *Journal of Financial Economics*, 80(2):309–349.

Shen, D., Urquhart, A., and Wang, P. (2020). A three-factor pricing model for cryptocurrencies. *Finance Research Letters*, 34:101248.

Shleifer, A. and Vishny, R. W. (1997). The limits of arbitrage. *The Journal of finance*, 52(1):35–55.

Sockin, M. and Xiong, W. (2020). A model of cryptocurrencies. Technical report, National Bureau of Economic Research.

Townsend, R. M. (1978). Intermediation with costly bilateral exchange. *The Review of Economic Studies*, 45(3):417–425.

Trebbi, F. and Xiao, K. (2019). Regulation and market liquidity. *Management Science*, 65(5):1949–1968.

Urquhart, A. (2017). Price clustering in bitcoin. *Economics letters*, 159:145–148.

Weill, P.-O. (2007). Leaning against the wind. *The Review of Economic Studies*, 74(4):1329–1354.

Xiong, W. (2001). Convergence trading with wealth effects: an amplification mechanism in financial markets. *Journal of Financial Economics*, 62(2):247–292.

Xu, J. and Livshits, B. (2018). The anatomy of a cryptocurrency pump-and-dump scheme. *arXiv preprint arXiv:1811.10109*.

Yermack, D. (2015). Is bitcoin a real currency? an economic appraisal. In *Handbook of digital currency*, pages 31–43. Elsevier.